NUCLEONICS

VOL. 4, NO. 2, FEBRUARY, 1949

An International Journal for Techniques and Applications of Nuclear Science

TECHNICAL CONSULTANTS

John R. Dunning, Clark Goodman, A. Kalitinsky, R. E. Lapp, W. F. Libby, C. Rogers McCullough, L. A. Ohlinger, Winfield W. Salisbury, T. I. Taylor, E. O. Wollan

With the cooperation of . . .

THE NETHERLANDS — C. J. BAKKER
DENMARK and SWEDEN — GEORGE HEVESY
GERMANY — HANS KOPFERMANN
SWITZERLAND — P. SCHERRER

CONTENTS

Future Developments in Nuclear Energy 9
CLARK GOODMAN

Uranium Hydride—II 17
A. S. NEWTON, J. C. WARF, F. H. SPEDDING, O. JOHNSON, I. B. JOHNS, R. W. NOTTORF, J. A. AYRES, R. W. FISHER, and A. KANT

A Coincidence Scintillation Counter 25
G. A. MORTON and K. W. ROBINSON

Neutron Distributions in Elementary Diffusion Theory—I ... 30
PHILIP R. WALLACE

Beta- and Gamma-ray Spectroscopy—II 56
GERALD J. HINE

Counting Rate Meters versus Scalers 67
ARTHUR G. BOUSQUET

BOOKS 76
PRODUCTS AND MATERIALS 83
NUCLEONIC EVENTS 77
ABSTRACTS 87

Keith Henney ..... Editor

Jerome D. Luntz ..... Assistant Editor
Ethel Pelzer ..... Assistant Editor

Gladys Montgomery . Washington Editor

Walter M. DeCew ... Consulting Editor
S. D. Kirkpatrick ..... Consulting Editor
P. W. Swain ..... Consulting Editor

E. J. Tangerman ..... General Manager

NUCLEONICS (with which is consolidated "Atomic Power" and "Atomic Engineering") [February, 1949, Vol. 4, No. 2. Publication Office: 212 East York St., York, Pa. Editorial and Circulation Offices: 330 W. 42nd St., New York 18, N. Y. Published monthly by McGraw-Hill Publishing Company, Inc. Entered as second class matter December 17, 1947, in the Post Office at York, Pa., under the act of March 3, 1879.

Copyright 1949 by McGraw-Hill Publishing Company, Inc. All rights reserved. James H. McGraw, Jr., President; J. A. Gerardi, Secretary; Curtis W. McGraw, Treasurer.

Allow at least ten days for change of address. All communications about subscriptions should be addressed to J. E. Blackburn, Jr., Director of Circulation, 330 W. 42nd St., New York 18, N. Y. Price per copy $1. Subscription rates: United States and U. S. Possessions $10 for 1 year, $16 for 2 years, $20 for 3 years. Canada $15 a year. Latin America $20 a year. All other countries $25 a year. Return postage guaranteed. Member A.B.C.

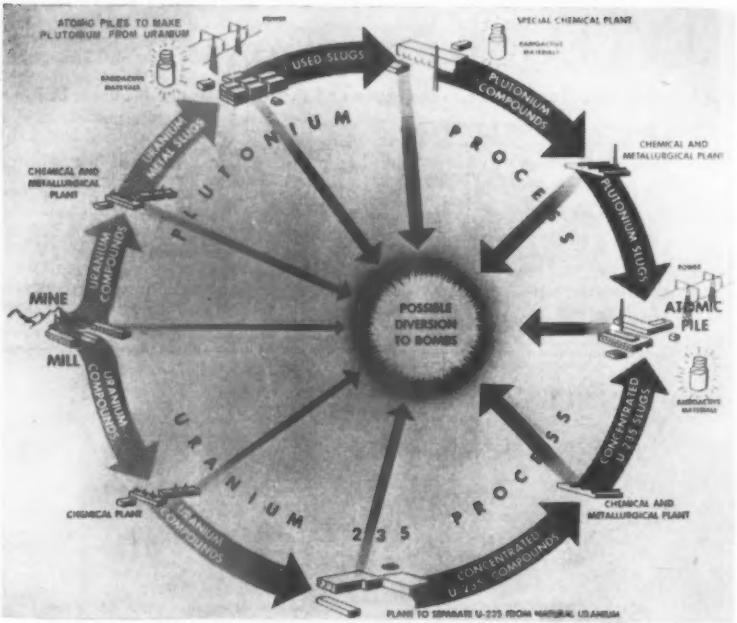

How Nuclear Energy Plants Might Be Diverted for Military Purposes

FUTURE DEVELOPMENTS IN NUCLEAR ENERGY*

By CLARK GOODMAN

Department of Physics, Massachusetts Institute of Technology
Cambridge, Massachusetts

THE MAJOR APPLICATIONS of nuclear energy have been, and in all probability will continue for some time to be, military in nature. Any type of nuclear reactor built for the generation of power is susceptible, with only relatively moderate effort, to diversion into the production of Pu^{239} and U^{233}. In concentrated form these nuclear fuels are suitable for atomic armament.

Likewise, if gaseous diffusion, electromagnetic or other methods of isotope separation are used to obtain enriched uranium for compact, nuclear power reactors, the concentrated U^{235} might be diverted to the production of bombs. This dual dilemma is illustrated schematically in the diagram above. It is seen that in the plutonium process useful power may be produced at two

* From Chapter 17, Vol. II, "The Science and Engineering of Nuclear Power." (Addison-Wesley Press, Inc., Cambridge, Mass., 1949). References to Volume I in this paper refer to the first book in this series of three.

stages, in the production of Pu^{239} from U^{238} and in the fission of the Pu^{239}. In the uranium process very sizable plants are required to separate the U^{235} from the natural uranium. The gaseous diffusion plant at Oak Ridge is the equivalent of a building one-half mile long by one-quarter mile wide and four stories high. The largest steam power plant ever constructed at one time supplies 238,000 kw of power and steam to this plant. The construction of the entire installation was about 500 million dollars. The electromagnetic plant at Oak Ridge consists of 175 buildings and cost approximately 317 millions, not including the 400 million dollars worth of pure silver bus bars on loan from the U.S. Treasury Department. This process requires large amounts of electric power, complex electrical equipment, complex mechanical equipment, and a large amount of chemical equipment.

While no production costs are available for the two uranium processes, they are obviously far more costly than the plutonium process. The endothermic nature of the isotope separation processes, the waste of large amounts of U^{238}, and the large installation and operating costs all combine to place the exothermic plutonium process in a much more favorable economic position for peacetime applications. While the gaseous diffusion plant is continuing to operate at full rate, it is highly unlikely that the enriched uranium produced will ever be used for the development of industrial power, although some of this enriched uranium may be used in experimental nuclear reactors.

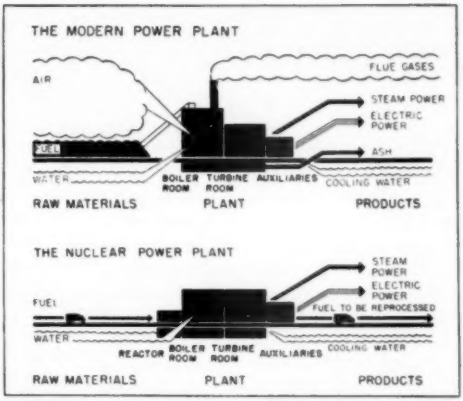

Schematic representation of advantages of nuclea energy over chemical energy

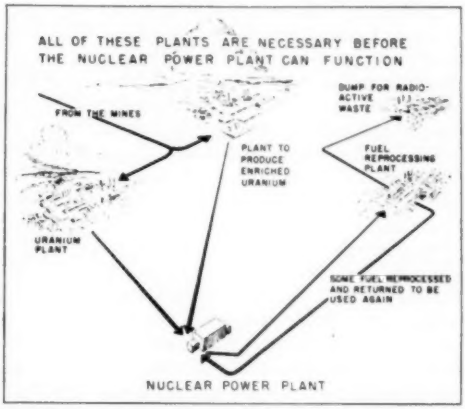
ALL OF THESE PLANTS ARE NECESSARY BEFORE THE NUCLEAR POWER PLANT CAN FUNCTION
FROM THE MINES
DUMP FOR RADIO-ACTIVE WASTE
PLANT TO PRODUCE ENRICHED URANIUM
FUEL REPROCESSING PLANT
URANIUM PLANT
SOME FUEL REPROCESSED AND RETURNED TO BE USED AGAIN
NUCLEAR POWER PLANT

Complex system upon which nuclear power plant depends for operation

Nuclear-Powered Aircraft

In its report of March 1, 1948 the Congressional Aviation Policy Board stated:

"In the event of war or in any international situation likely to lead to war, nuclear energy for the propulsion of aircraft would be comparable in significance to the atomic bomb itself. Presently

known limitations inherent in all chemical fuels make difficult the delivery by air of atomic bombs against a distant enemy. Therefore, if the United States had nuclear energy propulsion in addition to atomic bombs, it could be the dominant factor in maintaining world peace. Until these ends are attained, the United States must depend on military weapons and techniques currently available."

An inherent limitation of chemically powered aircraft is that the gross weight of the fueled plane increases rapidly with both range and speed.* These relations are shown in qualitative terms in Fig. 1. It is evident that the demand for higher speeds, in order to reduce vulnerability, requires an increase in gross weight. The greater the selected range, the more rapid is the rise in gross weight. For a given range there is an upper limit to the speed of chemically powered aircraft regardless of weight. For a working range of 11,000 miles (5,000-mile radius plus 1,000 mile margin of safety in fuel) the maximum speed sustainable with chemical fuels without refueling, lies between about 300 and 400 mph. These speeds are much too slow for any future wars.†

A nuclear-powered aircraft would be represented in Fig. 1 by a horizontal straight line. In order to fly at all and be manned, it must have a certain gross weight, made up largely of shielding material. Once it is airborne, the rate of consumption of nuclear fuel will be a negligible fraction of the gross weight of the airplane.‡

Several types of nuclear power plants have been proposed for the propulsion of aircraft. These are represented

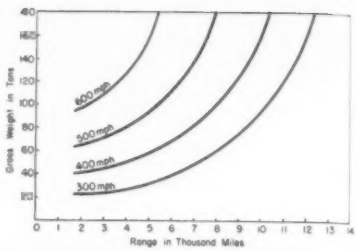

FIG. 1. Increase of gross weight with range for chemically powered aircraft

schematically in Figs. 2 to 5. In principle the simplest of these is the ram jet. Air is compressed in the diffuser by the forward speed of the plane. The air is then heated as it flows through ducts in the nuclear reactor. Thrust is provided by the large increase in velocity acquired by the air when it expands in the exhaust nozzle. The ram-jet requires a high flight speed in order to function and becomes really effective only at extreme speeds, well up in the supersonic region.

Very high air temperatures are required in the ram-jet. In a chemically powered ram-jet, the fuel is sprayed into the air stream and combustion takes place as the mixture passes through a chamber. In Fig. 2 the reactor replaces this combustion chamber. In the chemically powered ram-jet the potential energy stored in the fuel appears as the kinetic energy of the molecular combustion products, largely H_2O, CO_2, and CO, and of the unreacted O_2 and N_2. Temperatures of 2,000°C and above are reached by these gases. The walls of the combustion chamber and of the exhaust nozzle, although made of refractory materials, are cooled to prevent melting, corrosion and oxidation. In an atomic-powered ram-jet, only a small fraction of the heat energy is actually liberated in the air as it passes through the reactor. Instead, practically all of

* This section has drawn heavily upon the discussions of Andrew Kalitinsky [*The Pegasus* **12** (August, 1948) and unpublished paper presented before the Society of Automotive Engineers, June, 1948].

† W. Stuart Symington, Secretary of the Air Force, announced that on Sept. 15, 1948, Major R. L. Johnson had established a new speed record of 670.98 mph for a loaded tactical airplane when he flew an F-86 over a measured 3-km course.

‡ Assuming a thermodynamic efficiency of 20%, the rate of consumption of fissionable material will be about 1 gram per 6,000 thrust horsepower-hours (see Fig. 9-6 in Volume I).

the propulsive energy must be transferred to the working fluid by conduction and convection.* As a result the temperatures attainable are seriously limited by the refractory properties of the materials of construction. For use in nuclear ram-jets, the material should also have good thermal conductivity at high temperature. No known substance or combination of substances combines all of the properties needed for efficient operation of a nuclear ram-jet. In the development of all types of nuclear power, there is serious need for specialized materials. But in the development of a nuclear ram-jet, the materials problem is far more important than all the others combined. For this reason it is unlikely that this type of aircraft will be possible for many years to come.

In rocket propulsion a propellant must be provided. The gaseous propellant escapes at high velocity through the exhaust nozzle. The rocket is driven by the recoil momentum of the escaping propellant. Since no air is required, the rocket presumably could operate outside the earth's atmosphere. In order to escape the gravitational field of the earth, about 15,000 calories per gram of escaping material is needed. Since the energy content of fissionable material is about a million times this amount, the energy requirement is not, in itself, prohibitive, even if a relatively low thermodynamic efficiency obtains. However, E. P. Wigner† has pointed up a difficulty in this idea that has generally been overlooked. For a given efficiency there is a definite rate at which the waste heat must be removed in order to avoid vaporizing the rocket. As long as the rocket is moving through the atmosphere, heat can be removed by convection. Outside the atmosphere it can keep cool only by throwing off heated portions of the rocket or by radiation. The first alternative has definite limitations, but may be just sufficient to achieve the escape velocity. The second alternative, discarding the heat by radiation, is subject to the same difficulties involved in the transfer of heat from a reactor to a working fluid by means of radiation. As in the case of the nuclear ram-jet, the refractory properties of the materials limit the practical temperatures to undesirably low values.

In addition the nuclear rocket must carry a very large amount of propellant. Liquid hydrogen is the only substance that appears even remotely feasible. Because of its low molecular weight, the specific impulse from hydrogen is greater than that of any substance. At the same temperature, the specific impulse is about four times as great for hydrogen as for chemically fueled rockets. However, liquid hydrogen has a very low density ($\sim$ 4.5 cu ft per lb) and boiling point (-252.7°C). It has been estimated (Chapter 11) that several hundred tons of hydrogen would be required. On this basis the volume of a nuclear rocket would be about ½ million cubic feet which corresponds to a cylinder about 40 feet in diameter and 400 feet in length. This gigantic missile would dwarf a V-2. In the light of these preliminary considerations, nuclear-powered rockets seem far more remote than nuclear ram-jets.

In comparison the nuclear turbo-jet seems considerably more reasonable of attainment. In this system, as in the ram-jet, the nuclear reactor would replace the combustion chamber of the chemically fueled equivalent. As indicated in the diagram of Fig. 4, air is drawn into the compressor which forces it through the reactor. In the reactor the air is heated largely by convection. Good heat transfer requires high

* The impracticability of heat transfer by radiation has been considered briefly, but conclusively, in Chapters 9 and 10 of Volume I.

† Quoted by W. L. Laurence, *New York Times*, Sept. 16, 1948.

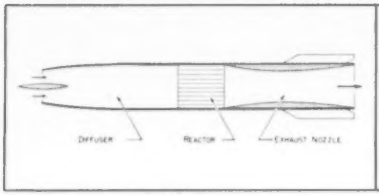

FIG. 2. Ram-jet

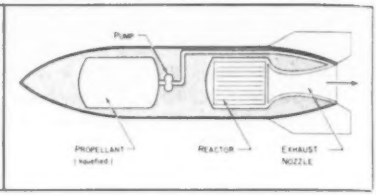

FIG. 3. Rocket

temperatures, high thermal conductivity, and a large surface of contact. Because the turbo-jet is best suited for use at high subsonic speeds, Mach number of 0.8 to 0.9+, the exhaust temperatures do not need to be as high as those required for rockets or ram-jets. Hence, there is a reasonable possibility of finding materials with a suitable combination of nuclear and refractory properties for use in turbo-jet reactors. However, for aerodynamic reasons it is desirable to have the frontal area and length of the reactor be as small as possible which in turn requires higher temperatures to effect the necessary transfer of heat energy. In a practical design, therefore, the temperature characteristics of the materials dictate the size and efficiency of the turbo-jet power plant.

Power for the compressor is provided by a partial expansion of the heated air in the turbine. The propulsive thrust is produced by expansion in the exhaust jet nozzle. In order to produce a net thrust, the velocity of the air as it leaves the jet nozzle obviously must be greater than the velocity as it enters the compressor. In order to achieve this and at the same time keep the volume of the reactor small, very high compression ratios are required of the air compressor. As Kalitinsky (op. cit.) has indicated, not only must the nuclear fuel in the reactor be protected by non-oxidizable coatings in order to prevent corrosion by the hot, high-pressure air, but also the coating must prevent the escape of any appreciable fraction of the radioactive fission products into the air stream. The latter problem is a matter of diffusion of the fission products, some of which are gaseous, through the coating. Diffusion rates generally increase with increasing temperature. This problem is particularly acute in the open-cycle turbo-jet and the closed-cycle systems since, in these, deposits of the fission products might build up in the unshielded turbine, condenser and pump.

The fourth general type of power plant might be the closed-cycle turbine, shown schematically in Fig. 5. In this case the reactor replaces the boiler of a conventional power plant. The working fluid might be high-pressure steam (or mercury in a fast reactor) which would be generated in the reactor and expanded in the turbine. Propulsion might be by a propeller driven by the turbine. This system is inherently limited to relatively low air speeds, 200 to 300 mph. While these speeds would be of interest for commercial flight, they are far too low in future military applications. Since only the latter could justify the extensive development required to achieve nuclear-powered flight, closed-cycle systems of this type do not appear to be practical.

Various combinations of these four general types immediately suggest themselves. If the condenser in the closed-cycle system were in addition

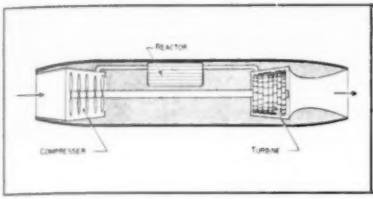

FIG. 4. Turbo-jet

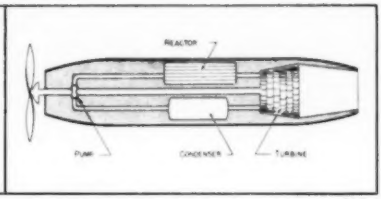

FIG. 5. Closed-cycle turbine

used to heat an air stream, the result would be a prop-jet system that might have limited usefulness. Similarly, a closed-cycle system using a liquid metal coolant or high-pressure water might be used as a closed-cycle turbo-jet. Also a combination system might use the turbo-jet principle at subsonic and ram-jet action at supersonic speeds.

Nuclear-Powered Submarines

The role of naval vessels in an atomic war is not clear. However, the advantages offered by nuclear power of unlimited range without oxygen and without refueling are much more important for submarines than for surface vessels. Consequently, in the writer's opinion, it appears probable that the first important naval application of nuclear power will be in the propulsion of submarines.

Numerous complications in such a development are immediately obvious. However, the tactical advantages to be gained might warrant a major concentration of effort in this direction. Even with the addition of *Snorkle* and major improvements in streamlining, the modern submarine is not a true *Unterseeboot*. Like its biological equivalent, the whale, the present submarine depends on oxygen for the release of the energy stored in its chemical fuel. The use of concentrated sources of oxygen, such as liquid O_2 and H_2O_2, extend underwater operations, but the range at full power is limited, and is not a great deal better than that of a hump-backed whale. The nostrils of the whale are located high on the head, so that very little of the animal need be exposed to enable it to breathe. Similarly *Snorkle* is made of minimum size for the submarine's respiration. Even with these adaptations, both the whale and the submarine are much more vulnerable to attack because of their dependence on air.

A nuclear-powered submarine could cruise practically indefinitely, since the consumption of fuel is extremely small even at full power. Furthermore it can operate underwater just as well as on the surface, since oxygen is not needed for power. The relatively small supply of oxygen required by the crew could be carried in condensed form and the carbon dioxide removed by conventional methods. In fact, the major problems of continued submergence would be psychological rather than physical in nature.

A submarine is a delicately balanced and thoroughly integrated engineering unit. Hence, the radical modifications that would be required to accommodate a nuclear power plant will probably necessitate a completely new hull design. Figures 6 and 7 are intended to illustrate in a general way some of the salient changes that might be involved. These sketches are essentially an artist's conception of how a typical World War II submarine might be adapted to nuclear power.

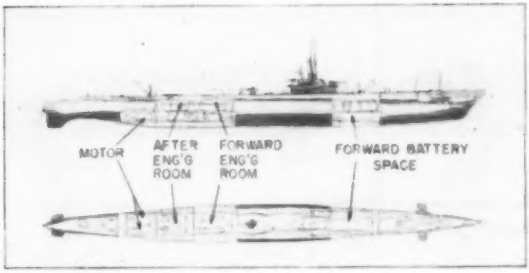

FIG. 6. Sketch of outboard profile of submarine hull and deck

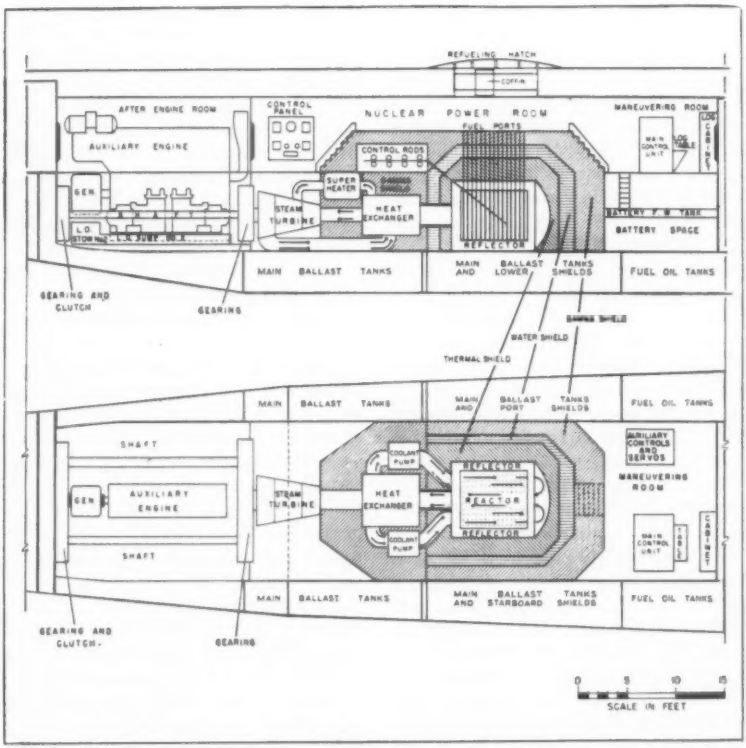

FIG. 7. Artist's conception of how a submarine might be adapted to use of nuclear power

Figure 6 is an outboard profile of the unmodified hull and deck, portions of which have been cut away to show the forward battery space and fuel tanks and the main engine compartments and ballast tanks. In the following discussion it is tacitly assumed that the trim of the vessel would be maintained

by redistribution of various components. Nearly 100 tons of batteries could be eliminated. Part of the space thus made available might be given over to a radioactivity counter room, enlarged recreational facilities and improved housing in the forward section. In the counter room, samples of air, sea water, fuel oil, lube oil and steam condensate could be monitored for induced radioactivity, and the radiation dosage received by the crew could be monitored. A recreation room and library would help offset the psychic difficulties of prolonged submergence. In the after section the main diesel engines, ancillary equipment, and electric motors have been replaced by a nuclear power plant and single auxiliary engine as shown in Fig. 7.

To minimize the amount of fissionable material required, a thermal reactor has been assumed. Under these conditions either graphite or beryllium could serve as the reflector and moderator. While it is far from clear just how such a reactor and power plant would be built, the writer has assumed: (1) the nuclear fuel and moderator could be a homogeneous mixture forming a cylindrical core that is subcritical when installed together with the reflector through the refueling hatch, (2) sufficient additional fuel for the production and maintenance of power could be added as needed through the vertical ports, (3) some of the partially expended fuel could be withdrawn into a lead coffin lowered over the fuel ports, (4) energy could be extracted from the reactor by means of a liquid metal coolant such as lead,* (5) by suitable arrangement of the flow this heavy metal coolant might also serve in part as the thermal shield and primary gamma-ray shield, and (6) a closed-cycle steam turbine would convert the heat into propulsive power.

* See Gilliland, Bareis and Feick, Chap. 10, Vol. II.

Because some induced radioactivity would probably appear in the coolant, the pumps, heat exchanger and superheater would probably need to be surrounded by some gamma-ray shielding. However, if this were the case it would not be necessary to shield the power equipment since the steam and condensate would have essentially no induced activity. Sea water has been suggested as part of the shielding. The main ballast tanks and the central portion of the main shielding tanks are assumed full of sea water during the development of power in the reactor. Under this arrangement the personnel are protected from the primary neutrons and gamma rays by at least several feet of sea water or five feet of composite thermal-water-gamma shielding. A fore and aft passageway with four-foot vertical clearance is indicated over the top of the shield. Separate controls are indicated beyond the companionway at each end. The heat exchanger, superheater and turbine, plus additional equipment not indicated, form the power unit for driving the two main propeller shafts, the generator, the compressors, pumps and other minor power-driven units. The auxiliary engine is a low-power diesel which might be included for emergency use only.

Industrial Nuclear Power

Were it not for the urgent military demands on the technical personnel and atomic resources, industrial atomic energy would be supplying electricity and comfort heating in many localities within the United States ten years from now. A power plant of 100,000 to 500,000 kw capacity,† such as is common practice in power generation, that requires no large storage of fuel, needs no air for combustion, and pro-

† At 25% efficiency, it would be able to generate 25,000 to 125,000 kw of electric power and yield about three times this amount of power for comfort heating.

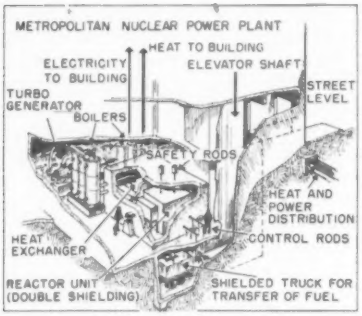

FIG. 8. What a nuclear power plant might look like in New York City

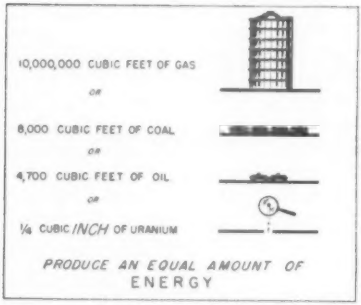

FIG. 9. Comparison between nuclear and other energy sources

duces no ash or flue gases is very attractive indeed. These advantages of nuclear energy over chemical energy are represented schematically on page 3. The appearance of such a plant in the heart of Manhattan might be something like that shown in Fig. 8. If operated at an average of 50% of capacity, this plant would consume between two and ten ounces of fuel per day. Figure 9 emphasizes the relatively small nuclear fuel consumption compared to coal, oil and gas.

The most economical plan would be to use ordinary uranium which contains only 0.71% of the fissionable isotope U^{235}. Assuming fuel replacement is necessary because of depletion and metallic corrosion, shipment of uranium would probably not be more than a few tons, which could be transported by means of a single truck as shown. The removal of an equal amount of fuel, containing extremely radioactive fission products, would demand a large amount of shielding on the single truck required for transport. It is conceivable that the reactor could be "turned off" during the late evening and early morning and still be able to supply the low-load demand with the heat from the fission product radioactivity. Refueling could take place then with slightly greater convenience than while in operation.

The heat would be transferred from the reactor to the working fluid by means of a liquid metal coolant, such as Na, Pb, or Bi, which has low absorption for thermal neutrons.* The coolant would enter the reactor at a temperature somewhat above its freezing point (204° F for Na; 520° F for Bi; 621° F for Pb) and emerge at about 1,400° F. If necessary, magnetostriction pumps could be used to circulate the liquid metal coolant at a moderate velocity. By means of counter-current flow, heat exchangers, and superheaters, the heat would be transferred to water and steam. A boiler operating at 500–600 psi would be used for flashing the water into steam. The superheated steam would drive a turbine for the generation of electricity. The condensation of exhaust steam would provide comfort heating for the surrounding buildings. Conventional methods would be used to distribute the electricity and comfort heating. The water and steam which constitute secondary coolants would not be radioactive since the primary, liquid metal coolant will emit only alpha, beta, or gamma rays which do not produce appreciable induced radioactivity.

---

* Mercury would not be satisfactory for this reason.

TABLE 1

Sources of Energy (per Annum)
(Based on 1941 Data)

Source	World			United States			% of World
	Energy in 10^{12} kwh	*Production in 10^6 tons*	*Equivalent U in lbs*	*Energy in 10^{12} kwh*	*Production in 10^6 tons*	*Equivalent U in lbs*	
Solar	1.2×10^6	—	120×10^9	18,000	—	2×10^9	1.6
Coal	17.5	2,200	175×10^4	4.4	550	44×10^4	25
Petroleum	4.4	510	44×10^4	2.7	310	27×10^4	61
Natural gas	1.0	130	10×10^4	0.88	110	8.8×10^4	88
Water power	0.42	—	4.2×10^4	0.12	—	1.2×10^4	29
Nuclear power	0.0066	—	660	0.0065	—	650	99
Total	23	2,840	2.34×10^6	8.1	970	0.82×10^6	

As illustrated, the reactor would be surrounded by about six feet of heavy concrete shielding, and the coolant lines and heat exchanger by about half this thickness. Since the unit would be subterranean, earth could be used in part for shielding. In any event, it would not be difficult to lower the outside radiation to well below the tolerance level.

World Power Requirements

A comparison of the amount and energy of the fuels used currently per year in the world and in the United States with the weight of U (or Th) required for replacement is given in Table 1. The solar energy reaching the earth is included for comparison. It is assumed that all the uranium, both U^{235} and U^{238}, and all of the thorium are completely consumed, the U^{238} being converted to Pu^{239} and the Th^{232} to U^{233}. These thermally fissionable isotopes are essentially equivalent to U^{235} for fuel purposes. One sees that almost 10^6 pounds of uranium (or thorium) would be required to furnish the total power consumed *at present* per year in this country.

It is somewhat ironic that the country which has the greatest know-how in the field of nuclear energy should be so poorly endowed with natural sources of nuclear fuels. The United States has more than its proportionate share of the world's supply of coal, oil and natural gas, but it is pathetically poor in uranium and thorium ores. The unprecedented demands for uranium made by the Manhattan Project and its successor, the Atomic Energy Commission, have been and are continuing to be met largely by imported uranium. Canada and the Belgian Congo have furnished practically every pound of uranium used in the piles at Hanford and in the isotope separators at Oak Ridge. While little has appeared in print on this subject, it is obvious that important international implications are involved. To help overcome this deficiency, the AEC is stimulating interest in prospecting for uranium ores not only by offering higher prices, but also by posting a reward of $10,000 for the discovery of a new, high-grade commercial ore deposit.

It is difficult to make accurate estimates of reserves of fissionable

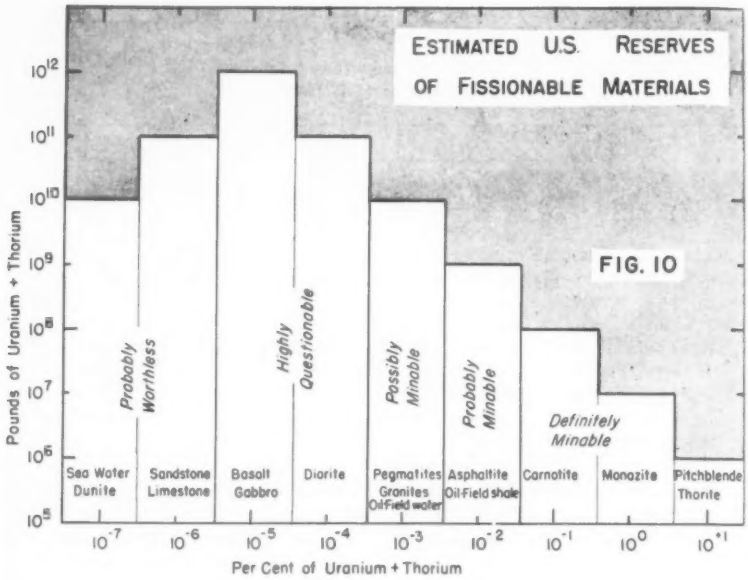

minerals. Nevertheless a crude tabulation, such as that given in Fig. 10, is of value in pointing up the problem of these strategically important mineral reserves in the United States. The uncertainty in the estimate of reserves increases as the grade, or elemental concentration, in the source material decreases. But the feasibility of mining and recovering uranium and thorium also increases in uncertainty with decrease in grade. Hence, the accuracy of the estimates for low grade materials is less important than for the high grade. The numerical values given in Fig. 10 include an increase of 100%, over estimated present reserves, as the result of new discoveries. It is unlikely that more than this increase can occur, because the most promising sections of the United States have been so thoroughly explored in the search for other heavy minerals.

A very rough estimate of the reserves of Th and U available in the United States is shown in Fig. 10. The United States is very deficient in high-grade ore deposits. The writer has estimated that by scraping very hard, we could round up about 10^6 pounds which would supply all our power by nuclear means for only one year. Since the United States as yet has not produced significant amounts of uranium from lower-grade deposits, it is clear that we have been largely dependent on high-grade imports for our nuclear developments to date.

As we have seen, energy is developed in nuclear reactors in the form of heat at temperature levels that are dictated by the properties of the materials of construction. This heat might possibly be used directly in a variety of industrial and non-industrial uses requiring both low- and high-temperature heat. It has been suggested that the waste heat from plutonium production

might be used in locations remote from sources of chemical fuel, for example in the polar regions. Another scheme proposes to supply fresh water for semi-arid regions in the southwestern United States by evaporating sea water or brakish well water. Nuclear power has been proposed as a source of electric power for the conversion of bauxite to alumina. However, the apparent advantages of the compact nuclear fuel which engender such utopian proposals are to a considerable degree offset by the complications of fuel preparation and reprocessing and the disposal of radioactive wastes.* The nuclear power plant is dependent upon a complex system, such as that pictured on page 3, in order to yield heat and electric power—both of which can be produced by conventional means using chemical fuels.

In brief, nuclear power can probably be produced at useful temperatures on an industrial scale without extraordinary engineering developments. Ignoring for the moment the limitations imposed by military applications, the breadth of its industrial use will certainly be dictated by the relative advantages measured in dollars and cents, in pounds and shillings or in rubles and kopecks.

Economics of Nuclear Power

For nuclear power to find really broad industrial applications, it must be able to compete with chemical fuels on an economic basis. In spite of the aforementioned advantages of this compact energy source, it is far from clear what will be the *cost* of nuclear power.

At the present time, electricity is produced most cheaply in large hydroelectric developments such as Norris Dam in the TVA system and Grand Coulee on the Columbia River. As a means of comparison, these installations have power ratings of about 10^5 and 10^6 kw, respectively. Water power exists only where natural conditions permit. It is not considered economical to transmit electricity beyond a radius of about 300 miles. The cost of electricity based on a fuel such as coal is generally higher than for hydroelectric power, but such fuels are very widely used because they can be transported to the power station.

The transportation of chemical fuels is costly. For example, each 200 miles of coal transportation by rail adds about 1 mill per kwh to the cost of electricity. It is clear that the cost of transporting nuclear fuels, even when shielding is necessary, is negligible compared to chemical fuels. As a result, nuclear power costs for similar plants should be fairly uniform throughout the world. For this reason, an approximate estimate of the relative attractiveness of nuclear power in various parts of the world can be based on present costs of generating electric power from coal. A comparison of this type given in Table 2 has been made by S. H. Shurr, co-director of the study, "Economic Aspects of Atomic Energy," conducted by the Cowles Commission at the University of Chicago.†

Table 2 refers to two concurrent independent estimates that have been made of the cost of nuclear power. The Thomas report was prepared by members of the Clinton Laboratories staff and of the Monsanto Chemical Company Engineering Department in 1947. They considered a number of types of nuclear power plants, but based their cost comparisons on a modified Hanford-type pile, since more design and operation information was available for this type than for any other kind. Unfortunately, the indi-

* This serious problem has not yet received much attention. The radioactive wastes at Hanford are stored for the present.

† *Bulletin of Atomic Scientists* **3**, 117 (1947).

TABLE 2

Estimated Costs of Generating Electricity in Selected Regions of the World, 1937 and 1947, Compared with Estimated Costs of Nuclear Power

	*Average Generating Costs in Mills per Kilowatt Hour**		*Cost of Nuclear Power in Mills per kwh*
	1937	*1947*	
Thomas Report			8.0–10.0†
Condliffe Report			4.0‡
Argentina			
Coastal regions	9.0	16.0	
Inland regions	10.0–11.0	17.0–18.0	
China			
Mining regions	6.5–7.0	—	
Other regions	7.0–9.0	—	
Great Britain	7.25	9.5	
Hungary	9.25	—	
India			
Mining regions	6.5–7.5	—	
Other regions	7.5–10.0	—	
Soviet Union§			
Ural region	6.5	—	
United States‖			
At mines	5.50–6.25	5.75–6.75	
Near mines or on developed waterways	6.50–7.25	7.00–8.25	
Far from mines, accessible by rail	7.50–8.75	8.50–9.50	

* In order to place all electricity costs on a comparable technological base, data on actual generating costs are not shown, since these would be influenced by the condition of the plants in operation. Instead, electric generating costs have been estimated from the cost of fuel in the various regions, assuming the same relationship between fuel costs and generating costs as would obtain in a modern 100,000 kilowatt plant operating with a 50% load factor. [Based on data in *Electrical World*, December 2, 1939, "4th Steam Station Cost Survey," and Bauer and Gold, "The Electric Power Industry," (Harper, 1939)]. All coal prices include cost at mine and transportation charges. Transport costs from mines to consuming regions estimated from representative railway, river, and ocean freight charges during year indicated.

† 75,000 kilowatt plant assumed. Lower cost based on 100% load factor; higher cost estimated for 50% load factor.

‡ 500,000 kilowatt plant and 45% load factor assumed.

§ Data on mining costs could not be found for this region, hence U. S. mine price was used.

‖ Coal plants only. Generating costs estimated on basis of standard relationship described in reference. Earlier figures relate to 1938 and are based on data on actual fuel costs for plants in operation in that year. Figures for 1947 are preliminary estimates derived from general information on coal prices and freight rates.

vidual items in their estimate are not given. Hence, a direct comparison is not possible with the more detailed, but probably less accurate, estimate by J. B. Condliffe's project of the Carnegie Endowment Committee on Atomic Energy. The Thomas group estimated that electricity could be generated at a cost of about 8 mills per kwh by a 75,000 kw power plant operating at 100% capacity. Shurr has pointed out that power stations normally operate at only about 50% capacity. This correction would increase the estimated cost to about 10 mills per kwh.

The Condliffe group estimated, on the basis given in Table 3, that a 500,000 kw plant of the same general type might produce electricity for as little as 4 mills per kwh operating at 45% capacity. The large differences in these two estimates are partly the result of the greater economy of a larger unit, but mainly are the result of the

TABLE 3

Power Station Cost Analysis*

Plant Comparisons	*Coal*	*Primary Pile*
Capacity, kw	100,000	500,000
Area, acres	10	(10,000)
Boiler room, cu ft	1,500,000	2,000,000
Turbine room, cu ft	900,000	3,500,000
Switchhouse, cu ft	500,000	2,000,000
Thermal efficiency, %	35	40
Employees, number	60	200
Capital Costs (Dollars)		
Land and improvements	600,000	(2,000,000)
Bldgs. (exclusive of piles)	3,000,000	8,500,000
Pile units and accessory facilities		(24,000,000)
Fuel handling and storage	2,000,000	200,000
Condensing supply	250,000	1,500,000
Waste handling	100,000	1,000,000
Boiler plant	1,500,000	7,500,000
Draft system	200,000	
Feedwater system	400,000	2,000,000
Piping system	500,000	2,500,000
Heat recovery apparatus	250,000	1,000,000
Turbine-generators and auxiliary equipment	2,400,000	10,000,000
Switchgear and wiring	1,200,000	6,000,000
Switching yard and equipment	800,000	2,500,000
Total	13,200,000	68,700,000
Operating Costs (Dollars)		
Fuel†	1,000,000	100,000
Wages and salaries (at $4,000)	240,000	800,000
Maintenance and supplies	120,000	1,000,000
Fixed charges (15%)	1,980,000	10,300,000
Total cost per year	3,340,000	12,200,000
Cost per kwh	7½ mills	

* This cost schedule is adapted from *Electrical World*, December 2, 1939.
† Based on coal at $6 per ton, uranium at $10 per pound.

uncertainty in the estimates of the costs of construction and operation of the two units. The two estimates may therefore be taken to suggest that the cost of generating electricity in nuclear power plants may be somewhere between 4 mills and 10 mills per kwh (1947 cost basis).

Taking a mean of 7 mills per kwh, it is seen that on this basis nuclear energy might be very attractive to certain localities on the earth, while not so economically interesting in the United States. Great Britain is reported to be building a graphite-uranium power pile at Harwell, England, after having recently put into operation an experimental, graphite-uranium pile for isotope production. The figures given in Table 2 suggest that Argentina might benefit even more than Great Britain in the development of industrial nuclear power. Thus we find ourselves in the peculiar position of having a tenuous monopoly on processes which for peaceful purposes are of considerably greater interest to other countries.

Thus far we have considered only

U^{233}, U^{235} and Pu^{239} as nuclear fuels, with Th^{232} and U^{238} as primary source materials. Among the possible developments of the future are new nuclear fuels which conceivably could possess improved nuclear, chemical or metallurgical properties. The number of neutrons per fission, η, and the fission cross section, σ_f, are the two most important nuclear properties. The transuranic elements are more similar to actinium than to their homologues in the Periodic Table. For this reason, we would not expect any major difference in the chemical and metallurgical properties of americium, curium and heavier elements, up to about atomic number 100, which may be produced in the future.

Exhaustive experiments have fairly well eliminated elements below atomic number 88 as being chain-reacting. Only a limited number of the man-made heavy isotopes have sufficiently long half-lives to be potential nuclear fuels. Most of these are alpha-ray emitters. The fission cross sections of all such isotopes have not been reported. It is to be expected that other long-lived isotopes will be found to fill in the blank spaces adjoining the general line of nuclear stability. It is only reasonable to expect that one or more of these isotopes might serve as a nuclear fuel.

At the other end of the binding energy curve, an even greater amount of energy per particle may be released in transmutation. For example, the synthesis of He^4 from hydrogen and neutrons would release about seven times as much energy per particle as in fission. Some mention has been made of these possibilities in the public press. However, one of the most thorough discussions has been given by Bethe* in his considerations of whether air or water could explode in the immediate vicinity of an atomic bomb. "The conclusion from these calculations is that there is no danger of a nuclear explosion in any substance naturally occurring on the earth with any of the atomic bombs which have been developed or which have been conceived on paper." Because of the considerable amount of inert material associated with the active portion of the bomb, the temperatures which can be produced in the air or water surrounding such an explosion are of the order of 10^6 degrees. This is much lower than the temperature prevailing at the center of ordinary stars which are of the order of 20×10^6 degrees. In normal stars, the most important nuclear reactions are believed to be between protons on one side and carbon and nitrogen nuclei on the other. The reaction is extremely slow, and it would take several million years for the carbon in the sun to be consumed (if it were not re-generated in the actual stellar reaction cycle). Another reaction, the theory of which has been developed in detail, is the combination of two protons to form a deuteron with the emission of a positron during the collision. However, it is well known that reactions involving the emission of negative or positive electrons are extremely improbable as measured by nuclear standards. However, since it involves a relatively small potential barrier, this reaction will fall off less rapidly than others when the temperature is decreased. It is therefore presumably the most likely reaction around 10^6 degrees, but since the probability of an explosion even at 20×10^6 degrees is off at least by a factor of 10^{17}, at 10^6 degrees the reaction must be negligibly slow.

In spite of these theoretical observations, it is not only possible but probable that as the nature of nuclear forces becomes understood, improved methods will be developed for releasing a larger and larger fraction of the mass energy stored in atomic nuclei.

* *Bulletin of Atomic Scientists* **1**, 2 (1946).

URANIUM HYDRIDE—II

RADIOCHEMICAL and CHEMICAL PROPERTIES*

Second of three papers discussing the studies carried out at the Ames laboratory following preparation of uranium hydride from the massive metal for the first time early in 1943

BY

A. S. Newton, J. C. Warf, F. H. Spedding, O. Johnson, I. B. Johns, R. W. Nottorf, J. A. Ayres, R. W. Fisher, and A. Kant†

Institute for Atomic Research, Iowa State College
Ames, Iowa

Radiochemical Properties

Extraction of fission products. The finely subdivided state of uranium hydride suggested leaching of the fission products and plutonium from the hydride prepared from metal from the piles. A sample of uranium, which had been subjected to slow neutron bombardment in the cyclotron (via deuteron bombardment of beryllium) and which thus contained measurable amounts of the various fission products and plutonium, was divided into two portions, and each was converted into uranium hydride. One was refluxed with hydrochloric acid alone, and the other with hydrochloric acid containing milligram amounts of Sr, Y, Zr, Mo, Te, I, Ba, La and Ce, to act as carriers for the corresponding fission products. As the boiling continued, the suspensions of uranium hydride acquired a deep green color, because of slow reaction with the acid, forming uranous chloride. Aliquots of the first were taken periodically, centrifuged, and the solutions evaporated to dryness. Total radioactivity measurements were made on the residues, which were then analyzed for uranium and plutonium. Aliquots of the second suspension were centrifuged, and the carrier elements uranium and plutonium were separated by chemical methods. This permitted determination of the radioactivity of each fission product corresponding to the carrier element employed.

The results showed that no preferential extraction of any element occurred, and that the activities of the solutions were in proportion to the amount of uranium they contained. It thus became evident that the fission products and plutonium were dissolved only when the uranium hydride in which they were held was also dissolved, and that no enrichment could be achieved.

Behavior of radioxenon. Among the fission products of uranium are two isotopes of xenon, Xe^{133} and Xe^{135}, of 5.3-day and 9.2-hour half-lives, respec-

* This paper is based on work done for the Plutonium Project of the Manhattan District in 1943–44 and was first reported in Plutonium Project Reports CC-580, CC-587, CC-705, CC-725, CC-803, CC-858, CC-1057, CC-1059, CC-1091, CC-1194, CC-1201, CC-1504 and CC-1524.

† Present addresses: A. S. Newton, Radiation Laboratory, University of California, Berkeley, Calif.; J. C. Warf, Department of Chemistry, University of Southern California, Los Angeles, Calif.; F. H. Spedding and R. W. Fisher, Institute for Atomic Research, Iowa State College, Ames, Iowa; O. Johnson, Shell Development Co.; Emeryville, Calif.; I. B. Johns, Central Research Department, Monsanto Chemical Company, Dayton, Ohio; R. W. Nottorf, Photo Products Research Laboratory, E. I. du Pont de Nemours & Co., Inc., Parlin, N. J.; J. A. Ayres, Knolls Atomic Power Laboratory, General Electric Co., Schenectady, N. Y.; A. Kant, Bureau of Mines, Pittsburgh, Pa.

tively (*2*). These are the only inert gas isotopes of reasonably long half-life which are formed in significantly high yields. A sample of neutron-bombarded uranium, in which the short-lived isotopes of krypton had decayed, and which thus contained the above isotopes of xenon as the only important inert gas constituents, was placed in a flask attached through several reaction tubes to a cylinder holding an aluminum-walled Geiger-Müller counter tube, over which the gases could be passed (see section titled *Experimental*). In this way the radioxenon could be detected and measured when it was driven from the uranium.

The uranium was converted to the hydride, and any radioxenon liberated was flushed into the cylinder holding the counter tube, where its activity was measured. A little argon or nitrogen was used as a carrier gas. Next the hydride was decomposed at 400° under reduced pressure; the gases evolved were again collected and the radioactivity measured. Finally the remaining metal was completely dissolved in phosphoric acid, and the gas was collected. This permitted determination of the total amount of radioxenon present.

The studies showed that the conversion of the massive uranium to the very finely divided hydride caused less than 1 % of the xenon to be liberated. Upon thermally decomposing the hydride at 400°, only 15 % of the xenon was given up. Complete solution of the sample was necessary to effect the complete evolution of the xenon. Uranium hydride prepared from ordinary metal (*i.e.*, not bombarded in the presence of some radioxenon) failed to adsorb the gas.

The data given above are in keeping with the retention of the fission products by the hydride upon leaching. Evidently when uranium is converted to its hydride, the small particles formed are still very large compared to atomic dimensions, and foreign atoms entrapped in the hydride lattice are held more or less firmly.

Chemical Properties

Action of air. Handling and transfer of uranium hydride. The pyrophoric nature of uranium hydride has been mentioned (*3*). Some samples, however, were found not to ignite in the air, and it was observed that exposure of preparations to small amounts of air for a period of about an hour stabilized them sufficiently to permit handling in the air (*4*, *5*). It was also noticed that specimens which had been exposed in a "dry box" filled with nitrogen or carbon dioxide could frequently be handled in air without catching fire. The air stability was probably due to the formation of a protective layer of oxide on each particle. Such preparations were not completely air stable, gradual oxidation taking place as shown by periodic weighings of a sample.

When transfer of the hydride was necessary it was done in an atmosphere of nitrogen or carbon dioxide in a dry box, but on some occasions when the boxes were not flushed sufficiently, the sample ignited and continued to burn. A box containing lumps of dry ice, and flushed with carbon dioxide from a cylinder of liquefied gas, was usually found to be safe in transferring the powder from one vessel to another, although even in this atmosphere some attack of the hydride occurred. It was found helpful to cool the hydride samples with dry ice during manipulation in the dry box; even under these conditions samples occasionally ignited, especially when agitated. It is recommended, when possible, that transfers be avoided by preparing the hydride in the vessel in which it is to be used, but that when handling it is necessary, the operator take the precaution of wearing asbestos gloves and a face shield.

Action of the common reagents. Since the investigations of the chemical properties of uranium hydride were of a survey and exploratory character, only a few reactions were studied exhaustively. The evidence showed that uranium hydride generally reacted as a powerful reducing agent, and often had an effect similar to that of the free metal in finely divided form.

Small quantities (up to 25 g) of the hydride were covered with water, usually with no visible reaction (acetylenic odors were detected). But on a larger scale a deflagration usually took place, forming uranium dioxide according to the equation

$$UH_3 + 2H_2O \rightarrow UO_2 + {}^7/_2H_2$$

The sudden red heat broke open the glass containers. When water was added dropwise to a large quantity of the hydride (400 g), a small amount of heat was generated (*6*). By maintaining a low temperature, the whole mass was thoroughly wetted without violent reaction.

The effects of several non-oxidizing acids were noted. Hydrochloric acid, dilute or concentrated, added to small quantities of the hydride, reacted only very slowly; even on boiling the reaction was relatively slow. This was in contrast to the reaction of uranium metal, even in the massive form, which was attacked by hydrochloric acid with extreme rapidity. The effects of dilute sulfuric, perchloric, or phosphoric acids on the hydride were similar to that of hydrochloric (*4*, *5*).

Concentrated sulfuric acid, when heated with the hydride, was readily reduced to sulfur dioxide, sulfur, and hydrogen sulfide. Hot concentrated phosphoric acid dissolved the hydride rapidly, forming a uranous phosphate.

There was no reaction between uranium hydride and dilute acetic acid but, on boiling under reflux, a brownish-black, apparently colloidal, suspension resulted. No reaction with glacial acetic acid occurred until a little hydrogen chloride gas was bubbled into the suspension. This caused a vigorous exothermic reaction; upon cooling, a light green precipitate was deposited, which was found to consist mostly of uranous acetate.

A number of common oxidizing agents were tested. Nitric acid attacked the hydride vigorously, especially when concentrated, and on several occasions ignition resulted. Uranyl nitrate was formed. Uranium hydride was oxidized by 30% hydrogen peroxide with the emission of sparks (*7*). In the presence of dilute nonoxidizing acids, hydrogen peroxide caused dissolution of the hydride to form the uranyl salt of the acid. These included hydrochloric, sulfuric, phosphoric, perchloric, acetic, tartaric, and citric acids. Other oxidizing agents which dissolved the hydride in acidic medium, forming uranyl salts, included ceric sulfate, potassium dichromate, permanganate, bromate, and chlorate (*8*).

Alkaline solutions, including sodium, potassium, and ammonium hydroxides, and sodium cyanide, failed to react with uranium hydride.

Action of heavy metal salt solutions (*9*, *10*, *11*). A number of heavy metal salts, particularly silver salts, were found to react with uranium hydride. Silver nitrate in aqueous solution was reduced readily, liberating silver and hydrogen and forming uranyl nitrate. The principal reaction may be represented as follows:

$$2UH_3 + 12AgNO_3 + 2H_2O \rightarrow 12Ag + 2UO_2(NO_3)_2 + 8HNO_3 + 3H_2$$

which indicates that 6 mols of silver were liberated per mol of uranium hydride consumed. The silver from a known amount of the hydride was filtered off and weighed; calculations showed that the Ag/UH_3 ratio was 5.8. This ratio of slightly less than 6 was partly attributed to the oxidation of some of the uranium hydride by the

nitric acid formed by the primary reaction.

The less soluble silver salts, including the acetate, and tartrate, were much more sluggish in their reactions with uranium hydride. Silver sulfate reacted moderately rapidly. Silver fluoride, which is exceedingly soluble in water, was reduced vigorously and exothermally, the uranium being oxidized only to the tetravalent state owing to the insolubility of the tetrafluoride:

$$2UH_3 + 8AgF \rightarrow 2UF_4 + 8Ag + 3H_2$$

Silver perchlorate solutions reacted with the hydride particularly rapidly. Contrary to expectations, it was found that some of the perchlorate ion itself was reduced and precipitated as silver chloride, the silver-silver chloride mixture separating as a gray, spongy mass. The two simultaneous reactions can probably be represented as follows:

$$2UH_3 + 12AgClO_4 + 4H_2O \rightarrow 12Ag + 2UO_2(ClO_4)_2 + 8HClO_4 + 3H_2$$

$$2UH_3 + 5AgClO_4 \rightarrow 4Ag + AgCl + 2UO_2(ClO_4)_2 + 3H_2$$

Silver perchlorate is also abundantly soluble in toluene (*12*). It was observed that in this nonaqueous medium a rapid, exothermic reaction with the hydride ensued. Both silver and silver chloride were found in the reaction products.

The reactions of the salts of a few other heavy metals were briefly investigated. Cupric sulfate solutions failed to react with the hydride at room temperature but, upon boiling, a slow reaction occurred, as evidenced by the formation of copper. A solution of cupric ammonium chloride, which dissolves metallic iron without formation of a precipitate (*13*), was found to oxidize uranium hydride quickly, causing complete solution.

Mercuric chloride solution caused a rapid reaction, yielding mercury, mercurous, uranous, and uranyl chlorides. Mercuric nitrate was also reduced. Arsenic and antimony trichlorides were reduced, the latter rapidly. Ferric sulfate solution containing a little sulfuric acid dissolved the hydride smoothly at 100°.

Reactions with various gases (*14, 15*). **Preparation of tri- and tetravalent uranium compounds.** It was found possible to prepare a number of tri- and tetravalent uranium compounds conveniently by passing certain gases over the hydride at temperatures varying from room temperature to 500°, depending on the specific reaction. A dry state may be maintained by this means. In no case was it necessary to exceed the melting point of the product. The result was an anhydrous, fine and easily handled product rather than a fused mass.

In the reactions at elevated temperatures, there may be some doubt as to whether uranium hydride or the finely divided metal resulting from the decomposition of the hydride is the actual reactant. Those occurring above about 350° or 400° are undoubtedly reactions with the free metal, but at 250°, where the dissociation pressure of the hydride is 4.8 mm, the reactant could be the metal or the hydride or both. The product is the same in either case.

The reactions of uranium hydride with various gases and vapors are outlined in Table 1. The composition of each product was established, when possible, by the weight gain caused by reaction with uranium hydride prepared from a known amount of uranium; usually this was supplemented with analytical data. Notes on the reactions are presented below; analyses are given in the *Experimental* section.

(a) Copper and nickel apparatus was employed in the reactions with hydrogen fluoride. It was found that under the proper conditions it was not necessary to convert all of the uranium to the hydride before admitting the hydrogen fluoride, since the hydrogen released by the reaction served to con-

TABLE 1

Reactions of Uranium Hydride with Various Gases and Vapors

Gas or vapor	*Temperature*	*Product*	*Appearance*	*Notes*
HF	20–400°	UF_4	Pale green powder	a
HCl	250–300°	UCl_3	Reddish-brown powder when hot; fine olive-green when cooled	b
Cl_2	250°	UCl_4	Light green powder	c
$COCl_2$	250°	UCl_4	Green powder	d
CCl_4	250°	UCl_4	Green powder	d
HBr	300°	UBr_3	Fine reddish-brown powder	
Br_2	300–350°	UBr_4	Light brown powder	e
HI	250–400°		Brown powder	f
I_2	400°		Brown powder	f
CH_3I	275–300°		Brown powder	f
H_2O	350°	UO_2	Brown powder	
H_2S	400°	US_2	Fine black powder	
NH_3	250°	U_2N_3–UN_2	Gray powder	g
N_2	250°	U_2N_3–UN_2	Gray powder	g
PH_3	400°	U_3P_3	Dark gray powder	
CO	400°			h
CO_2	300°	UO_2	Dark powder	i
HCN	400°		Dark gray powder	j
C_2H_4	500°		Black powder	k
CH_4	550°	UC	Dark powder	l

vert the remaining metal to the intermediate hydride. With agitation, 92% of an 1160 g lump of uranium was converted to the tetrafluoride within two hours (*16*).

(b) On a few occasions during the preparation of uranium trichloride, a trace of white crystalline sublimate condensed in the cooler parts of the glass reaction tube. This was identified as ammonium chloride, and was traced to nitride impurities in the uranium. The halides of uranium, except UF_4, were hygroscopic.

(c) When pure chlorine was passed over the hydride, a violent and uncontrollable reaction took place. This was remedied by diluting the chlorine with 10 volumes of helium. The recommended technique of preparing the tetrachloride is to chlorinate the trichloride, prepared in turn by the action of hydrogen chloride on uranium hydride:

$$UH_3 + 3HCl \rightarrow UCl_3 + 3H_2$$
$$2UCl_3 + Cl_2 \rightarrow 2UCl_4$$

(d) The uranium tetrachloride formed by the action of carbonyl chloride or carbon tetrachloride on the hydride was contaminated in each case by carbon or a carbide, and was of heterogeneous appearance.

(e) Helium was used as a carrier gas and diluent for bromine vapor (*17*). The preferred procedure for preparation of uranium tetrabromide is to brominate the tribromide.

(f) The uranium iodides were thermally unstable, and were attacked by the atmosphere. Satisfactory analyses were not made. The products were probably uranium tri- or tetraiodide, or mixtures of these. The iodine vapor was carried by helium into the reaction tube (*18*). The product from methyl iodide contained some carbonaceous material.

(g) The composition of the product

obtained by the reaction of ammonia or nitrogen with uranium hydride was slightly variable because of the existence of a single phase in the uranium-nitrogen system between U_2N_3 and UN_2 (*19*).

(**h**) No reaction of the hydride with carbon monoxide occurred up to 400°; the hydride was decomposed to the metal.

(**i**) The reaction of carbon dioxide with the hydride was quite rapid above 300° and carbon monoxide was formed. There was a very slow but appreciable reaction at room temperature.

(**j**) The reaction at 400° with hydrogen cyanide gave a mixture of uranium carbide and nitride.

(**k**) The reaction with ethylene at 500° was slow and yielded a black powder, evidently a mixture of a uranium carbide and uranium metal.

(**l**) Methane reacted at 550° giving a dark mixture, whose principal component was identified as uranium monocarbide by X-ray analysis (*19*).

Certain of these compounds readily prepared from uranium hydride may be employed in the purification of laboratory gases (*20*); these include the purification of hydrogen chloride over uranium trichloride and of nitrogen over uranium nitride.

Action of solvents. When samples of uranium hydride were covered with a series of solvents, the only visible effect was the evolution of very small bubbles for a few hours. The solvents included benzene, toluene, hexane, mineral oil, ether, ethanol, dioxane, ethyl and amyl acetates, carbon disulfide, glacial acetic acid, and acetone (*4, 5*).

When a fresh preparation of uranium hydride was treated with carbon tetrachloride (*21*), an explosive reaction occurred. Other chlorinated solvents, such as chloroform and chlorobenzene, reacted weakly with some evolution of heat but did not cause explosions.

Reduction of organic compounds (*4, 5, 22*). Cursory experiments on the reduction of organic compounds with the aid of uranium hydride were conducted using naphthalene, maleic anhydride, and nitrobenzene. In the first case, naphthalene was mixed with a relatively small quantity of uranium and the pressure increased to 104 atmospheres with hydrogen in a hydrogenation bomb. The temperature was maintained at 250°. After cooling, it was found that the uranium had been converted to the hydride, but the melting point of the hydrocarbon was identical with that of the original naphthalene. As a matter of fact, calculations showed that the reverse of the above attempted reaction is thermodynamically favored (*3*), namely, the dehydrogenation of tetralin and decalin by uranium to form naphthalene and uranium hydride. It is quite possible that uranium, prepared by the decomposition of the hydride, could serve as a dehydrogenating agent useful in synthetic organic work.

The reduction of maleic anhydride was attempted at atmospheric pressure by melting and refluxing the pure compound (b.p. 200°) with uranium hydride. A viscous dark brown liquid resulted from which no crystals could be isolated. The material gave a strong unsaturation test. Similar attempts were made to reduce nitrobenzene by heating mixtures of various compositions to 180–185° with uranium hydride. A definite reaction occurred, but no positive tests for aniline were obtained. It is realized that the experiments above are inconclusive, but more pressing work prevented further study. If certain reductions of organic compounds can be made employing uranium hydride, the use of uranium deuteride may prove valuable for introducing deuterium into organic molecules.

Uses of uranium hydride and the hydride reaction. It is of interest to

note some of the applications of uranium hydride and the reaction by which it is formed. Use of the compound as a laboratory source and reservoir of pure hydrogen or deuterium has been discussed (*3*), as well as its decomposition to furnish powdered uranium. The reactions of the hydride with a number of gases affords preparative methods for certain compounds otherwise quite difficult to make in a pure anhydrous state. Conversion of uranium alloys to a powder by hydride formation permits sieving out crystals of the intermetallic compounds of uranium present (*23*). Short treatment of metallographic specimens of uranium alloys with hydrogen at 250° causes etching, which improves the clarity of the micro-structure (*24*). Imperfections in the coating of uranium ingots may be detected by heating in hydrogen; wherever a hole or crack exists, the uranium is attacked, and a swelling is formed. A number of other minor applications have been discovered.

Experimental

Extraction of fission products. The bombarded samples of uranium were converted to uranium hydride by first heating to 250° in hydrogen and then cooling. Vycor vessels were employed to minimize adsorption of the traces of fission products. The first sample was refluxed with 0.5 *N* hydrochloric acid, and the second with 5 *N* hydrochloric acid containing milligram quantities of KI and Na_2MoO_4 and the chlorides of the following metals: Sr, Y, Zr, Te, Ba, La, and Ce. Radioactivity measurements on the aliquots were made using a Lauritsen electroscope. The carrier elements were separated by ordinary chemical methods; the plutonium was carried down by precipitating lanthanum fluoride and determined by an alpha counter. Uranium analyses were made titrimetrically.

Behavior of radioxenon. The apparatus consisted of a reaction flask (in which the uranium hydride was prepared) connected to a bead tube containing saturated sodium bisulfite to absorb any radioiodine liberated. The bead tube was joined through a trap to a heated cupric oxide-packed tube, which served to convert excess hydrogen to water. The next member of the train was the cylinder holding a Geiger-Müller counter tube whose walls were of thin aluminum. In some of the work an eudiometer was interposed just before the counter tube; it supported a leveling bulb holding potassium hydroxide solution. After each step a small quantity of argon or nitrogen was admitted to act as a carrier for the trace of radioxenon present; this was flushed through the apparatus with carbon dioxide, which was absorbed by the alkali. The gases caught in the eudiometer were then transferred to the cylinder holding the counter tube, and the activity measurement was made.

Reactions of uranium hydride with liquid reagents. In most cases in which qualitative data on the reactions were sought, small amounts of the hydride were transferred to the reaction vessel in a carbon-dioxide-filled dry box, covered with water or other liquid, and removed to the air when the reagent was added. In a few cases, the hydride was prepared in a flask and cooled, and the reagent was introduced through a dropping funnel.

Reactions of various gases with uranium hydride. The work involving anhydrous hydrogen fluoride was conducted in nickel or copper reaction bombs equipped with copper leads. The apparatus for the remainder of the work was very simple. Through a 3-way stopcock, a Pyrex reaction tube heated by a resistance furnace was connected to a purified hydrogen supply and the source of the second reacting gas or vapor. A weighed amount of

uranium in a boat was converted at 250° to the hydride which, after adjusting the temperature, was treated with the second gas or vapor directly.

Analysis. Calc. for UF_4: U, 75.8; F, 24.2. Found: U, 75.5; F, 23.9. Calc. for UCl_3: U, 69.0; Cl, 31.0. Found: U, 69.2; Cl, 29.4. Calc. for UCl_4: U, 62.6; Cl, 37.4. Found: (product from Cl_2 and UH_3) U, 63.6; Cl, 37.5; (product from Cl_2 and UCl_3) U, 63.6; Cl, 36.4. Calc. for UBr_3: U, 49.9; Br, 50.1. Found: U, 50.1; Br, 49.9. Calc. for UBr_4: U, 42.7; Br, 57.3. Found: (product from Br_2 and UH_3) U, 42.7; Br, 57.2; (product from Br_2 and UBr_3) U, 42.4; Br, 56.9. Calc. for UI_3: U, 38.5. Found: (product from CH_3I and UH_3) U, 39.0. Calc. for US_2: U, 78.8; S, 21.2. Found: U, 79.5; S, 20.5. Calc. for U_2P_3: U, 83.7; P, 16.3. Found: U, 83.0; P, 17.0.

Reduction of organic compounds. Naphthalene (50 g) and uranium turnings (5 g) in a hydrogenation bomb were heated to 250° for an hour under 104 atmospheres of hydrogen. The bomb was shaken constantly, and was cooled before opening. In the reaction with maleic anhydride, uranium hydride was prepared from uranium (3.5 g), and the anhydride (2.0 g) was dropped in through an air condenser; a hydrogen atmosphere was maintained at all times. The organic compound was melted and refluxed for 4.5 hours. Unsuccessful attempts were made to isolate crystals from both water and dioxane. In the first attempt to reduce nitrobenzene, uranium (15 g) was converted to its hydride, and a small amount (3.5 g) of nitrobenzene was added under hydrogen atmosphere. The mixture was heated for 16 hours at 180°–185° using a salt bath. After cooling, the paste was ether extracted. The second experiment was similar and employed the same amount of uranium hydride but with more nitrobenzene (8.0 g). The mixture was heated for 3 hours, and worked up as before. Tests for aniline were made by attempted formation of an azo dye, but all results were negative.

Summary

The radiochemical properties of uranium hydride involving leaching of the fission products and the behavior of radioxenon were investigated. A general survey of the chemical properties of the hydride was made. This included its reactions with air, water, acids, oxidizing agents, heavy metal salt solutions, halogen-bearing gases, ammonia, phosphine, and other gases, the effects of solvents, and attempted reductions of organic compounds. A few of the reactions afforded excellent preparative methods for certain anhydrous uranium compounds, otherwise somewhat difficult to prepare. Some of the applications of uranium hydride and the hydride reaction were briefly listed.

* * *

In some of the chemical work with uranium hydride the authors wish to acknowledge the aid of Messrs. T. Butler, M. Goldblatt, J. Powell, and A. Tevebaugh.

BIBLIOGRAPHY

1. F. H. Spedding, *et al.*, NUCLEONICS **4**, No. 1, 2 (1949)
2. Nuclei Formed in Fission, *J. Am. Chem. Soc.* **68**, 2411 (1946)
3. A. S. Newton, O. Johnson, A. Daane, R. W. Nottorf, J. C. Warf, "The Preparation and Physical Properties of Uranium Hydride," NNES (MPTS) Division VIII
4. J. C. Warf, A. S. Newton, T. A. Butler, I. B. Johns, J. A. Ayres, "Plutonium Project Report," CC-580 (April 15, 1943)
5. J. C. Warf, A. S. Newton, T. A. Butler, I. B. Johns, J. A. Ayres, *ibid.*, CC-587 (April 19, 1943)
6. A. Tevebaugh, *ibid.*, CC-1194 (December 9, 1943)
7. M. Goldblatt, *ibid.*, CC-682, p. 1 (May 15, 1943)
8. A. S. Newton, *ibid.*, CC-1201 (January 1, 1944)
9. J. A. Ayres, *ibid.*, CN-852 (August 8, 1943)
10. J. A. Ayres, *ibid.*, CC-858 (August 7, 1943)
11. J. A. Ayres, *ibid.*, CN-925 (September 8, 1943)

12. A. E. Hill, F. W. Miller, Jr., *J. Am. Chem. Soc.* **47**, 2702 (1925)
13. F. Willems, *Z. anorg. u. allgem. Chem.* **246**, 46 (1941)
14. A. S. Newton, O. Johnson, A. Kant, R. Nottorf, "Plutonium Project Report," CC-705 (June 7, 1943)
15. A. S. Newton, O. Johnson, A. Kant, R. Nottorf, *ibid.*, CC-725 (June 15, 1943)
16. A. D. Tevebaugh, K. Walsh, J. Iliff, I. B. Johns, *ibid.*, CN-1199 (December 10, 1943)
17. R. Nottorf and J. Powell, *ibid.*, CC-1974 (September 15, 1944)
18. A. Kant, *ibid.*, CC-803 (July 15, 1943)
19. R. E. Rundle, N. C. Baenziger, A. S. Wilson, R. A. McDonald, *J. Am. Chem. Soc.* **70**, 99 (1948)
20. A. S. Newton, "The Use of Uranium and Uranium Compounds in Purifying Gases," NNES (MPTS) Division VIII
21. A. Daane, R. W. Nottorf, O. Johnson, "Plutonium Project Report," CC-1059 (October 9, 1943)
22. H. D. Brown, J. M. Wright, J. C. Warf, *ibid.*, CC-1524 (March 10, 1944)
23. I. B. Johns, T. Butler, A. D. Tevebaugh, F. J. Wolter, A. F. Voigt, *ibid.*, CN-727 (June 15, 1943)
24. T. Butler, *ibid.*, CC-725 (June 15, 1943)

A Coincidence Scintillation Counter*

Coincidence circuits eliminate many of the disadvantages in scintillation counters caused by background of photomultipliers. A crystal diode differential coincidence circuit, using anthracene as the detector, is described. It gave good performance in counting beta rays and fast neutrons

By J. A. MORTON and K. W. ROBINSON
Radio Corporation of America, RCA Laboratories Division
Princeton, New Jersey

THE SCINTILLATION COUNTER is proving to be an extremely useful tool for the detection and measurement of nuclear particle radiation. Basically, this form of detector consists of a transparent phosphor crystal, a photoelectric converter, a pulse-height discriminator, and some form of count-rate meter. The crystal phosphor is so chosen that when it is struck by a photon or particle of nuclear radiation, it produces a flash or scintillation of light. This scintillation of light is converted by the photoelectric device, usually a secondary emission multiplier, into an electrical pulse. The pulses generated in this way, after passing through a suitable selector circuit, are counted on one or another form of count-rate meter.

Crystals suitable for this purpose must produce radiation in the spectral range to which the photoelectric device is sensitive, must be transparent to this radiation, and must be efficient in converting the energy of the particle into visible radiation. A number of crystals have been found satisfactory for this purpose. Among these, thallium-activated alkali iodides and double-bonded carbon organic crystals, such as anthracene, have achieved notable success. A good crystal of sodium iodide will produce as many as 20,000 photons of visible light in converting a one Mev gamma ray.

The conversion of a gamma ray into visible light is a complicated process taking place in several steps. The gamma ray gives up some or all of its energy to an electron in the crystal,

* Work done as part of Bureau of Ships Contract NObsr-42460.

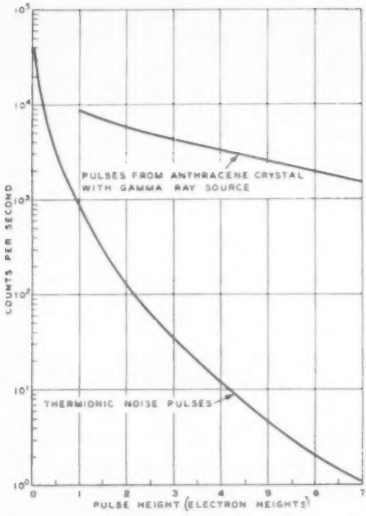
PULSES FROM ANTHRACENE CRYSTAL WITH GAMMA RAY SOURCE
THERMIONIC NOISE PULSES
COUNTS PER SECOND
PULSE HEIGHT (ELECTRON HEIGHTS)

FIG. 1. Noise and gamma-ray pulses from photomultiplier

through photoelectric conversion, Compton collisions, etc. The high-energy electrons thus formed in the crystal excite fluorescent centers in the lattice. In view of the nature of this process of conversion, a wide variation in the number of photons produced per scintillation is not unexpected. Consequently, while bright flashes may consist of several tens of thousands of photons, a large number of flashes will be smaller.

The 931-A type multiplier (i.e., RCA 931-A, 1P21 and 1P28) is frequently employed as the photoelectric converter in scintillation counters. The spectral response of these tubes is well suited to the fluorescent characteristics of both NaI:Tl and anthracene since the response has a maximum in the neighborhood of 4,000 A.U. At this wavelength the quantum efficiency of the photocathode is in the neighborhood of 5 to 10%. The gain of this type of multiplier, when operated at the normal voltage of 100 volts per stage, is, on the average, about a million. Hence, 1 photoelectron released at the photocathode will represent a charge of 1.6×10^{-13} coulombs at the output. If the capacitance of the collector and associated circuit is limited to 10 micromicrofarads, the voltage pulse produced by one electron from the photocathode is about 15 millivolts. However, by operating the multiplier at a higher voltage, the gain can be increased to 10^7 or more for some multipliers. Under these circumstances the output pulse for a single electron will be nearly 0.2 volt. For this type of operation it is necessary to select the multiplier. Furthermore, it is advisable to operate the tube with lower voltages on the first few stages than on the final stages rather than to distribute the voltage in equal voltage steps between all stages.

Even when the multiplier is in complete darkness, current pulses appear in the output of a size corresponding to one electron released from the photocathode or larger. Figure 1 is a curve showing the number of dark current pulses as a function of pulse size. The abscissa of this curve is the pulse size in units corresponding to one electron times the gain of the multiplier (Ge), while the ordinate gives the number of pulses per second of size equal to or greater than the pulse height indicated by the value on the abscissa. It will be noticed that several hundred pulses per second occur in the output with a pulse height equal to unity or greater. In order to reduce the background counting rate to less than 1 per second, it is necessary to use some form of pulse height discriminator which eliminates all pulses with heights less than about 7 electrons from the photocathode. Tests show that for suitable multipliers the dark pulse distribution curve in the units used on the above curve is relatively independent of

voltage up to the point of instability of the multiplier.

It will be apparent that the background pulses of the secondary emission multiplier put a serious constraint on the scintillation detector. In fact, where a single multiplier is used, the device will only be useful where one or more of the following conditions can be met: (1) the radiation intensity sufficient so that the large background count of the multiplier does not interfere; (2) the individual scintillations large enough so that a pulse height selector can be used to reduce the background count; (3) the multiplier cooled in order to lower the thermionic current from the photocathode and dynodes; this thermionic current is responsible in large measure for the background pulses.

Two multipliers used in coincidence overcome most of these limitations. Where two multipliers are used in this way, the effect of the background can be reduced to a very low value without the necessity of cooling the multiplier even if the scintillation is so small as to cause the release of only one electron.

When used in this way, the multipliers are so located that the flash from the crystal phosphor strikes the photocathode of each, thus producing simultaneous pulses at the outputs of both multipliers. The circuit following the multipliers can be so arranged that the pulse rate indicator responds only to simultaneous pulses from the two photomultipliers. Obviously, occasionally the random background pulses from the two multipliers will coincide. The number of these spurious coincidences will be equal to the product of the background pulses from each multiplier times the resolving time of the circuit. Resolving times of a few tenths of a microsecond can be obtained with almost no difficulty, and consequently, since the background pulse rate of the multipliers is of the order of a thousand counts per second, the expected number of accidental coincidences will be of the order of 10 to 30 pulses per minute.

The advantage of the coincidence method becomes more apparent upon further examination of Fig. 1. In addition to the noise curve, this figure shows the response of the system for a particular crystal to a γ-ray source. It should be pointed out that pulse rate for a given size indicated by this curve depends upon the intensity of the source. The decrease of counting rate with increasing pulse height depends upon the kind, size and clarity of the crystal, upon the nature of the γ-radiation, and to some extent upon the multiplier. With a single tube under the conditions exemplified in Fig. 1, if a background rate of 1 pulse per sec is desired, the pulse height selector must be biased to correspond to 7 *Ge*. The γ-ray counting rate will, therefore, be 1,500 cps. On the other hand, with a coincidence circuit with a resolving time of 10^{-6} sec, the multiplier background pulse output can be 1,000 counts per sec for a net background counting rate of 1 per second. The pulse height selector can be biased to accept pulses down to 1 *Ge*; therefore, the counting rate for the particular γ-ray source will be 9,000 counts per sec. This represents a 6-fold gain in sensitivity.

A number of different types of coincidence circuits may be used in conjunction with the multipliers. Most of these fall into one of the three following classifications:

1. Symmetric gating
2. Limiter-discriminator
3. Differential

The first two, in which vacuum tube coincidence circuits are generally used, have the disadvantage of requiring a high-gain, wide-band amplifier between the coincidence elements and each multiplier, since they will not operate with less than a few volts input if the pulses are random in height.

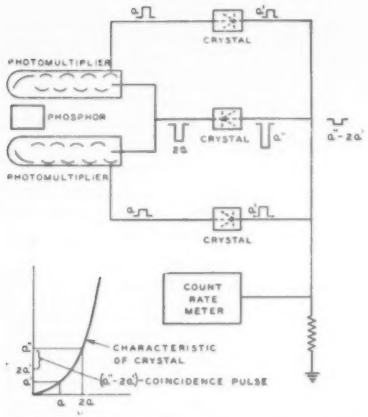

FIG. 2. Coincidence circuit using crystal diodes

A differential coincidence circuit can be devised that does not have this requirement. Figure 2 shows schematically a circuit arrangement which can be applied directly to the multiplier if the signal output is of the order of a tenth of a volt. This coincidence circuit uses crystal diodes of the 1N34 type instead of vacuum tubes. As can be seen from the schematic diagram, two of the crystals are connected to the last dynodes of the multipliers, while the two collectors are connected together and to the third crystal. If a pulse of height a occurs at one multiplier only, a pulse height of a' determined by the curvature of the crystal will appear in the output of the crystal connected to the last dynode, and one of the opposite sign at the crystal common to the two collectors. These two pulses add to cancel so that nothing is counted by the rate meter. On the other hand, if pulses of height a occur in both multipliers, the pulses from the two crystals connected to the last dynodes will simply add, giving a pulse of height equal to $2a'$, while the third crystal will receive a pulse $2a$ and consequently give an output of a'' (as can be seen from inset curve of the crystal characteristic). This pulse will be greater than $2a'$ by a residual which is the coincidence pulse counted by the count-rate meter.

To obtain an estimate of the quantitative values that might be expected from this circuit, reference is made to the simple equivalent circuit given in Fig. 3.

Here, it is assumed that the coupling resistor R is large compared with the resistances of the crystals. The current through any of the crystals in terms of the voltage across it is

$$i = K(e^{\gamma V} - 1)$$
$$K \approx 3 \times 10^{-5} \text{ amps}$$
$$\gamma = 10.75/\text{volt}$$

If pulses appear in both multipliers and are assumed to be equal in size, voltages V and $-2V$ are developed at the three circuit terminals. Since the net current at a must be zero, the output voltage V_a at this point will be given by the relation

$$2K[e^{\gamma(V+V_a)} - 1] - [Ke^{\gamma(2V-V_a)} - 1] = 0$$
$$2e^{\gamma(V+V_a)} - e^{\gamma(2V-V_a)} - 1 = 0$$
$$2e^{2\gamma V}e^{\gamma V_a} - e^{\gamma V}e^{\gamma V_a} - e^{2\gamma V} = 0$$
$$e^{\gamma V_a} = \frac{1 + \sqrt{1 + 8e^{3\gamma V}}}{4e^{\gamma V}}$$
$$V_a = \frac{1}{\gamma}[\ln (1 + \sqrt{1 + 8e^{3\gamma V}}) - \ln 4 - \gamma V]$$

The output voltage V_a, as a function of the input signal V, is also shown in Fig. 3. From this it is seen that if the signal from the multiplier corresponds to 0.2 volt the coincidence pulse will be approximately 0.1 volt. At this amplitude, the coincidence pulses can be counted with a relatively simple 3- or 4-tube count-rate meter.

This coincidence arrangement has been tested with a variety of phosphor crystals, including anthracene and the thallium-activated alkali iodides.

With a sodium iodide crystal aggregate for the phosphor crystal, it is found to have a counting rate of about

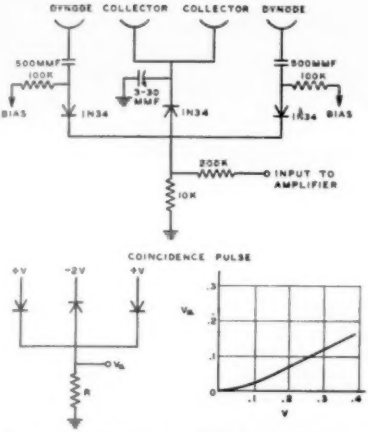

FIG. 3. Diagram of crystal coincidence circuit

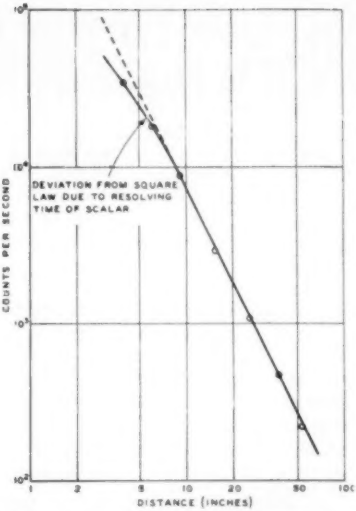

FIG. 4. Square law performance of coincidence circuit

300 counts per minute due to the natural background of the location. A Geiger counter indicates a background counting rate of about 40 counts per minute at the same site. The multipliers and circuit under these conditions are so adjusted that the background count without the crystal, is about 1 count per second.

Calibrated with a radiocobalt standard, the efficiency of the sodium iodide measured in terms of the solid angle which it subtends at the source, was found to be about 10%. In other words, about 1 in every 10 gamma-ray photons passing through the crystal produced a countable scintillation. An anthracene crystal about 1 centimeter thick showed an efficiency of approximately 5 to 8%. In order to determine the linearity and range of intensity over which this device would function as a gamma-ray detector, the rate of counting was determined as a function of the distance between the gamma-ray source and the crystal. A curve showing the result is given in Fig. 4. It will be seen that the square law is strictly obeyed up to a counting rate of 1,000,000 counts per minute. At higher counting rates, the rise is less rapid than inverse square requires indicating that there is an appreciable loss of count due to self-coincidences. Under the conditions of the tests, the electronic register with a 6 microsecond resolving time limited the rate of counting.

Using an anthracene crystal, the counter was tested as a detector of beta rays and fast neutrons. It was found to give good performance both with fast beta rays from uranium and slow beta rays from radiosulfur. It also gave good results as a fast neutron counter. The components of this system are small and simple enough so that the device can be used very satisfactorily as a radiation monitoring instrument. Even with the relatively small crystal used, the device is significantly more sensitive than an ordinary Geiger counter. With a large clear crystal, its superiority would be even more marked.

Neutron Distributions in Elementary Diffusion Theory—I

By PHILIP R. WALLACE
McGill University, Montreal, Canada

INTRODUCTION

Outline

SET DOWN HERE in systematic form are solutions to a selection of standard problems of neutron diffusion in a single medium obtained on the basis of elementary theory. The purpose underlying their presentation is to make them readily available to engineers and physicists concerned with the wide range of reactor problems in which the elementary diffusion theory gives results of practical usefulness.

The solutions are classified in terms of *a*) geometry of the medium and the distribution of sources, and *b*) kind of diffusion problem under consideration.

The various forms of medium and the types of sources which are considered are listed below. The numbers in this listing are used to designate the solutions in the following tables.

1. Infinite medium, planar distributions
2. Infinite medium, spherical distributions
3. Semi-infinite medium
4. Slab of finite thickness and infinite extent
5. Sphere
6. Sphere with a concentric cavity*
7. Infinite "pile" of rectangular cross-section*
8. Finite "pile" (parallelepiped)*
9. Cylinder*

In general, in the cases (**1**, **3**, and **4**) involving plane distributions, we shall treat *a*) a discrete plane source, *b*) a distribution of sources depending on the linear coordinate z. In the spherical problems (**2**, **5**, and **6**), we shall treat *a*) a point source at the center of the medium, *b*) a concentric shell source, *c*) a spherical distribution as a function of the radial coordinate r. In the pile problems we shall treat *a*) a point source, *b*) a distributed source in a cross-sectional plane, *c*) a general source distribution. In the cylindrical case, we shall consider only a general source distribution in a cross-sectional plane.

In several pile problems we shall give distributions resulting from a given neutron flux over the ends of the pile.

The types of diffusion problem considered are the following:

1. The thermal neutron distribution arising from given thermal neutron sources.
2. The distribution of fast neutrons, as a function of position and energy (or alternatively, "age" as defined below). In particular this gives the spatial distribution of thermal neutron sources. (We consider neutrons

* Will be contained in Part II of this paper to be published next month. An index to notations used in the solutions in both parts of the paper will appear also at that time.

EDITOR'S NOTE: This paper, which is a condensation of a report written for the National Research Council of Canada, is presented here with the thought of encouraging engineers to become familiar with the principles of reactor design.

The design of nuclear reactors has been generally regarded as requiring advanced training in nuclear physics and mathematics. For this reason, the study of such reactors for industrial applications has been left largely to experts who are specially qualified by experience on the Manhattan Project. Although the theory of nuclear reactor design has been developed by theoretical physicists to a considerable degree of complexity, the concepts involved are relatively simple, and it is possible to do creative engineering development without a thorough mastery of the more specialized extensions of the subject.

In working out the design of a new type of reactor, a normal procedure is to choose materials of construction and relative proportions and to make a trial solution for critical size, breeding ratio, and other interesting quantities. When an approximate design basis has been arrived at in this manner, the next step is to make a more detailed design of the actual pile lattice structure. The neutron density at various positions in the lattice is then found by means of diffusion theory. This involves solution of the appropriate diffusion equation with boundary conditions dictated by the geometry of the reactor. Some of the work of solving these boundary value problems is eliminated by this paper, and results in concise form are given for a variety of cases.

The size of the original report and the data and graphs presented in this condensation may appear rather forbidding to a reader unfamiliar with the subject, but it is not necessary to go through the whole paper in detail. After reading the general introduction and the preface to a particular section, it is possible to go directly to the problem of interest and find the solution. A number of analytical results are also given in graphical form as an aid in visualizing and for rough calculations; in fact this paper could be regarded as a convenient summary of analytical results to be used in the same manner as one uses a table of integrals.

There are special problems in neutron diffusion in which the simple diffusion theory is not valid, for example, diffusion in strongly absorbing media. Also the design of so-called resonance or fast piles, in which appreciable neutron absorption takes place at energies greater than thermal, requires somewhat more advanced methods of calculation. However, the results given here are adequate for practically all situations arising in the design of thermal reactors, which are of interest in power generation.

as "thermal" and of effectively uniform energy after they pass below a certain threshold energy).

3. The thermal neutron distribution resulting from a given distribution of fast neutrons. (This involves combining solutions from *1* and *2*.)

The above refer to neutron diffusion in non-multiplying media; in addition we shall treat

4. Thermal and fast neutron distributions in multiplying media.

The equations will be numbered for reference according to the above classifications: e.g., (6.3b) *will give the distribution of thermal neutrons in a spherical medium with a cavity due to a concentric shell source of fast neutrons. In general, the first number designates the shape of medium, the second the type of diffusion problem, while the letter following designates the type of source.*

Mathematical Formulation of Diffusion Problems

I. The equation for the diffusion of thermal neutrons is obtained from the continuity principle:

Rate of change of the number of thermal neutrons per unit volume ($\partial\rho/\partial t$) equals the number which flow in over the boundary ($-$ div $\mathbf{j}$), plus the number produced by sources q minus the number captured ρ/τ, all per unit time, where:

$\rho\, dV$ is the number of thermal neutrons in a volume element dV,

t is the time,

$\mathbf{j} \cdot \mathbf{n}$ is the flux of neutrons per unit area across a surface normal to the unit vector $\mathbf{n}$,

$q\, dV$ is the number of thermal neutrons produced per unit time in a volume element dV, and

τ is the mean lifetime of thermal neutrons, or the inverse of the probability of capture of a neutron per unit time.

The above equation becomes an equation in the thermal neutron density ρ by virtue of the characteristic assumption of the elementary diffusion theory:

$$\mathbf{j} = -D \text{ grad } \rho$$

where D is the "diffusion constant." D is given by

$$D = \frac{lv}{3\left(1 - \frac{l}{l_s} b\right)}$$

where l = total mean free path of thermal neutrons

l_s = scattering mean free path

v = mean velocity of thermal neutrons

b = mean cosine of the scattering angle.

This may be shown from the transport theory.

The resulting equation for ρ is, for steady neutron distributions [*i.e.*, $(\partial\rho/\partial t) = 0$]

$$D\nabla^2\rho - (\rho/\tau) = -q,$$

or, putting $D\tau = L^2$, L being the "diffusion length,"

$$\nabla^2\rho - \frac{\rho}{L^2} = -\frac{\tau}{L^2} q \qquad \text{(I.1)}$$

For most purposes, the boundary condition to be imposed is that ρ shall vanish on the boundary of the medium. A refinement may be introduced; it is known that, in a semi-infinite medium, the extrapolated density vanishes at a distance equal to 0.710 times the mean free path, outside the boundary. For media whose dimensions are large relative to the mean free path (only in this case is the application of elementary diffusion theory valid), it is valid to apply this boundary condition generally. This amounts to increasing the effective dimensions of the medium by 0.71 of the mean free path.

The true value of the density at the boundary may be shown from the transport theory to be given by

$$\rho_t = \frac{\sqrt{3}}{1 + \epsilon} \frac{j_0}{v} \qquad \text{(I.2)}$$

where j_0 is the current at the boundary as given by the elementary diffusion theory, and ϵ is a small constant which depends on the scattering law and vanishes for the case of isotropic scattering. For this reason, we shall in a number of cases quote formulas for j_0.

II. We now turn to the elementary theory of the slowing down of neutrons.

The accurate theory of the slowing down of neutrons is very complicated; we shall, however, be content here with an elementary approximate treatment, which is sufficiently accurate for many purposes. This treatment is based on the assumption of a unique functional relationship between the "age" of a neutron (the time elapsed since its birth at a primary source) and its energy, during the slowing-down process. We shall suppose that all neutrons are emitted from the primary sources with

a single energy. Because of the statistical nature of the slowing-down process, there will be a distribution of energies corresponding to each age. We shall, however, replace the actual slowing-down mechanism, in which the loss of energy takes place in jumps of different magnitude occurring at different times, by an idealized one, in which the loss of energy occurs continuously in time so that to each age corresponds a single velocity and vice versa.

We may deduce an approximate relation between velocity v and age t as follows: The fractional energy loss $-\frac{dE}{E} = -\frac{2dv}{v}$ in a time interval dt is equal to the probable number of collisions in time dt, multiplied by $a(v)$, the mean fractional energy loss per collision. The probable number of collisions in time dt is $\frac{v}{l(v)}\,dt$, where $l(v)$ is the mean free path at velocity v. Therefore

$$-\frac{2dv}{v} = \frac{va}{l(v)}\,dt$$

and

$$dt = -\frac{2l(v)dv}{a(v)v^2} \qquad \text{(II.1)}$$

This argument is obviously only valid when the interval dt (or dv) chosen is sufficiently large to contain many collisions, while $a(v)$ and $l(v)$ must have only a slight variation over such intervals.

Now let $s(\mathbf{r})$ describe the primary sources of neutrons in a medium, so that $s(\mathbf{r})dV$ is the production per unit time of neutrons of initial energy in dV. Suppose that we are interested in finding $X(\mathbf{r},t)$, which may be defined for a steady neutron distribution by either of the following equivalent statements:

$X(\mathbf{r},t)$ is the density of neutrons per unit age interval, or

$X(\mathbf{r},t)$ is the number of neutrons passing the age mark t, *or its equivalent energy mark*, per unit time.

Let us now consider at any time neutrons in the age interval $(t,t+dt)$. These are simply the neutrons which were emitted in the time interval $(0,dt)$, t seconds earlier. The density Xdt of such neutrons is precisely the density at time t due to a pulse of duration dt and strength sdt at time $t = 0$. If we denote by γdt the current of these neutrons (γ being then the current per unit age interval), and if we treat the pulse as effectively instantaneous, we have the continuity equation

$$\frac{\partial X}{\partial t} + \operatorname{div} \boldsymbol{\gamma} = s\delta(t), \qquad \text{(II.2)}$$

where we have divided by dt throughout. $\delta(t)$ is the Dirac δ-function, defined by $\delta(t) = 0$ for $t \neq 0$ and $\int \delta(t)dt = 1$ if the range of integration includes zero. In this equation, "t" is time elapsed since the emission of the neutrons, or in other words, neutron age. The term on the right-hand side is equivalent to the initial condition $X(\mathbf{r},0) = s(\mathbf{r})$.

$X(\mathbf{r},t)$ may also be defined as the number of neutrons passing a given energy mark per unit time. However, by virtue of the age-velocity relation (II.1),

$$\rho(\mathbf{r},v)dv = X(\mathbf{r},t)\,\frac{2l(v)}{a(v)v^2}\,dv \qquad \text{(II.3)}$$

is the density of neutrons in the velocity interval dv.

Let us now introduce into (II.2) the usual assumption of diffusion theory that

$$\boldsymbol{\gamma} = -D\nabla X \qquad \text{(II.4)}$$

where D has a form analogous to that of the thermal diffusion theory:

$$D = \frac{*(v)v}{3|1 - b(v)|}, \qquad \text{(II.5)}$$

$b(v)$ being the mean cosine of the scattering angle at velocity v. The diffusion coefficient now varies with velocity (and therefore with age), and (II.2) becomes:

$$\frac{\partial X}{\partial t} = D\nabla^2 X + s\delta(t) \qquad \text{(II.6)}$$

Let us introduce now the "symbolic age" θ defined by relation:

$$\theta = \int_0^t D dt = \frac{2}{3} \int_v^{v_0} \frac{l^2(v)}{a(v)[1 - b(v)]} \frac{dv}{v}, \quad \text{(II.7)}$$

v_0 being the initial velocity. The functional relationship (II.7) between θ and v implies also one between θ and t. In fact, θ is a form of measure of the energy during the slowing-down process. $X(\mathbf{r},t)$ may then be written as a function of $\mathbf{r}$ and θ, which we will designate $X(\mathbf{r},\theta)$ for simplicity of notation.

The equation (II.6) then takes the form

$$\frac{\partial X}{\partial \theta} = \nabla^2 X + s\delta(\theta) \quad \text{(II.8)}$$

This we take as the basic equation of the slowing-down process. It has the form of an ordinary time-dependent diffusion equation (heat conduction equation). The dimensions of the "symbolic age" θ are length^2; $\sqrt{\theta}$ is simply the characteristic length (slowing-down length) for neutrons of symbolic age θ in the slowing-down process.

III. The results of the two previous types of problems can now be combined to determine the thermal neutron distribution arising from known sources of fast neutrons. If we designate by $\theta_0 = L_s^2$ (where L_s is the "slowing-down length") the "symbolic age" at which neutrons cross the "thermal threshold," we need only solve the slowing-down equation

$$\frac{\partial X}{\partial \theta} = \nabla^2 X + s\delta(\theta) \quad \text{(II.8)}$$

to obtain the distribution $X(\mathbf{r},\theta_0)$ of neutrons passing this threshold, that is to say, to determine the distribution of sources of thermal neutrons. This may then be substituted in the thermal neutron equation

$$\nabla^2 \rho - \frac{\rho}{L^2} = -\frac{\tau}{L^2} X(\mathbf{r},\theta_0) \quad \text{(I.1)}$$

where we have substituted the source distribution $q = X(\mathbf{r},\theta_0)$.

IV. In the case in which the medium is a multiplying one, the "multiplication constant" k is defined as the mean number of fast (fission) neutrons released per thermal neutron captured in the medium. In this case there is a source of fast neutrons proportional to the thermal neutron density at any point. In the elementary theory it is usual to assume the fission neutrons to have a uniform energy (and thus symbolic age). This may be assumed to be the same as that for the neutrons from the primary sources if the latter are due to spontaneous fission or fission stimulated by stray neutrons. Thus we need only add to s in the equation (II.8) above a term $\frac{\rho k}{\tau}$, representing the number of fast neutrons produced per unit time due to fission arising from thermal neutron capture.

The investigation of the convergence of solutions of the resulting pair of simultaneous equations leads to the determination of the "critical conditions" for a chain-reacting system.

We neglect throughout the "resonance capture" of "fast" (*i.e.*, non-thermal) neutrons.

Two Useful Relations

If $\psi_{pt}(r)$ is a distribution due to a point source at $r = 0$, and $\psi_{pl}(z)$ is that due to a plane source at $z = 0$, these two solutions are related by the equation

$$\psi_{pt}(r) = -\frac{1}{2\pi r} \left(\frac{d\psi_{pl}}{dz}\right)_{z=r} \quad \text{(R.1)}$$

This is proved by treating a plane source as a uniform distribution of point sources on a plane.

If $\psi_s(r,r')$ is a distribution as a function of r due to a shell source at $r = r'$, then it may also be proved easily that this is given in terms of the plane source solution ψ_{pl} by the relation

$$\psi_s(r,r') = \frac{1}{4\pi r r'} [\psi_{pl}(|r - r'|) - \psi_{pl}(r + r')] \quad \text{(R.2)}$$

1. INFINITE MEDIUM, PLANE DISTRIBUTIONS

1. Thermal Neutrons

For a uniform plane source of thermal neutrons at $z = 0$

$$\rho = \frac{Q\tau}{2L} e^{-|z|/L} \tag{1.1a}$$

where ρ = thermal neutron density
Q = number of thermal neutrons from the source per unit area per unit time
τ = mean lifetime of thermal neutrons
L = diffusion length
z = distance from the source

It follows from (1.1a) that

$$\langle z^2 \rangle_{av} = \frac{\int_0^\infty z^2 \rho dz}{\int_0^\infty \rho dz} = 2L^2$$

so that the (diffusion length)^2 is one-half the mean square distance of thermal neutrons from the source.

If there is a plane source distribution $q(z)$ such that $q(z)dz$ is the number of thermal neutrons produced per unit area in thickness dz, we have

$$\rho(z) = \frac{\tau}{2L} \int_{-\infty}^{\infty} e^{-|z-z'|/L} q(z')dz' \tag{1.1b}$$

2. Fast Neutrons

The density of fast neutrons of symbolic age θ (see II.7) arising from a plane source of neutrons of symbolic age zero at $z = 0$ is

$$X = \frac{S}{\sqrt{4\pi\theta}} e^{-\frac{z^2}{4\theta}} \tag{1.2a}$$

where S is the number of neutrons emitted per unit area per unit time. It follows that

$$\langle z^2 \rangle_{av} = 2\theta = 2L_s^2$$

(L_s being the slowing-down length to age θ).

For a distributed source $s(z)$ (we shall in general use s for fast neutron source strengths and q for thermal)

$$X = \frac{1}{\sqrt{4\pi\theta}} \int_{-\infty}^{\infty} e^{-\frac{(z-z')^2}{4\theta}} s(z')dz' \tag{1.2b}$$

3. General Diffusion Problem Without Multiplication

The density of thermal neutrons due to a plane source of fast neutrons is obtained by substituting for q in (1.1b) $X(z,\theta_0)$ obtained from (1.2a). On integration this yields

$$\rho = \frac{\tau S e^{\theta_0/L^2}}{4L} \left[e^{-z/L} \left\{ 1 - \operatorname{erf}\left(\frac{\sqrt{\theta_0}}{L} - \frac{z}{2\sqrt{\theta_0}} \right) \right\} + e^{z/L} \left\{ 1 - \operatorname{erf}\left(\frac{\sqrt{\theta_0}}{L} + \frac{z}{2\sqrt{\theta_0}} \right) \right\} \right] \tag{1.3a}$$

where the notations are as in the previous sections and, in addition, $\theta_0 = L_s^2$ = the (slowing-down length)^2 to thermal energy. Erf x is the error function defined by $\text{erf } x = \frac{2}{\sqrt{\pi}} \int_0^x e^{-y^2} dy$. From (1.3a) it may be shown that

$$<z^2>_{av} = 2(L_s^2 + L^2) = 2L_0^2$$

if we introduce the "migration length" L_0 by

$$L_0^2 = L_s^2 + L^2.$$

Graphs (1.3a) and (1.3b) show (z) plotted for various values of L_s, L. By taking $S_T = 1$, ρ has been normalized; that is, the total number of thermal neutrons in the system is normalized to unity. The unit of length is chosen to be the migration length L_0. Putting $L_s/L = \gamma$, we may write

$$\rho(z,\gamma) = \frac{\sqrt{1+\gamma^2}}{4} e^{\gamma^2} \left[e^{-z\sqrt{1+\gamma^2}} \left\{ 1 - \text{erf}\left(\gamma - \frac{z\sqrt{1+\gamma^2}}{2\gamma} \right) \right\} + e^{z\sqrt{1+\gamma^2}} \left\{ 1 - \text{erf}\left(\gamma + \frac{z\sqrt{1+\gamma^2}}{2\gamma} \right) \right\} \right]$$

4. Multiplying Medium

The density of thermal neutrons from a plane source of fast neutrons is

$$\rho = \frac{S_T}{2} \sum_{n=-\infty}^{\infty} \frac{e^{\alpha_n^2 \theta_0} e^{-\alpha_n |z|}}{\alpha_n [L^2 + (1 - \alpha_n^2 L^2)\theta_0]} \tag{1.4a}$$

where L is the multiplication factor and α_n are the complex roots of

$$(1 - \alpha_n^2 L^2) e^{-\alpha_n^2 L_s^2} = k.$$

For sufficiently large z, the $n = 0$ term predominates. For $k < 1$, α_0 may be expressed in terms of k:

$$\alpha_0 = \frac{\sqrt{1-k}}{L_0} \left\{ 1 + \frac{\gamma^2(2+\gamma^2)}{(1+\gamma^2)^2} \frac{(1-k)}{4} + \frac{\gamma^4(60 + 52\gamma^2 + 13\gamma^4)}{(1+\gamma^2)^4} \frac{(1-k)^2}{96} + \cdots \right\}.$$

For k near unity

$$\alpha_0 = \frac{1-k}{L_0} = \frac{1}{c}$$

where c is designated the "multiplication length."

The remaining quantities α_n may be obtained from graph (A.1) of solutions to the equation

$$x + iy = \lambda e^{-(x+iy)}$$

For, putting

$$\gamma^2(1 - \alpha_n^2 L^2) = p = x + iy$$

in the transcendental equation for α_n, we may write it

$$p = \lambda e^{-p}$$

where $\lambda = k\gamma^2 e^{\gamma^2}$. As in the last section, γ is, of course, the ratio L_s/L. Knowing $p = x + iy$, α is obtained from

$$\alpha = \frac{1}{L_s} (\gamma^2 - p)^{1/2}$$

$$\alpha = \frac{1}{L_s} \left\{ \left(\frac{\sqrt{(\gamma^2 - x)^2 + y^2} + (\gamma^2 - x)}{2} \right)^{1/2} + i \left(\frac{\sqrt{(\gamma^2 - x)^2 + y^2} - (\gamma^2 - x)}{2} \right)^{1/2} \right\}.$$

Graph 1.3a—Infinite medium, plane source

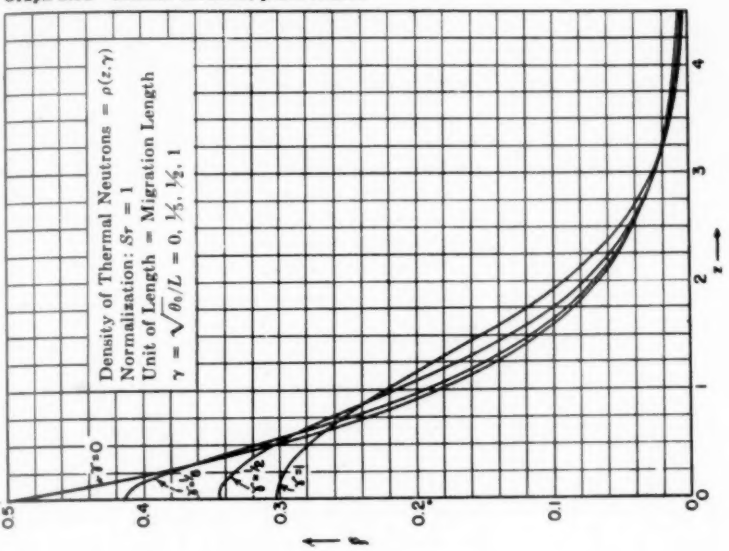

Graph 1.3b—Infinite medium, plane source

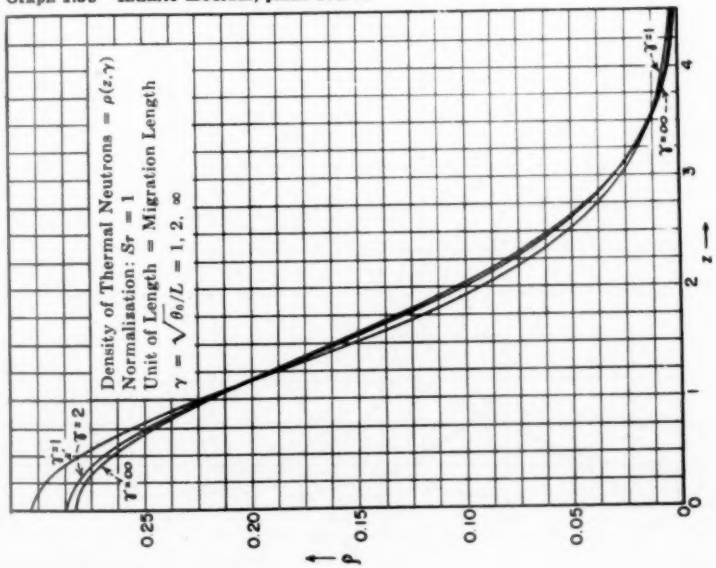

Graph A.1—Solutions of the transcendental equation $x + iy = \lambda e^{-(x+iy)}$

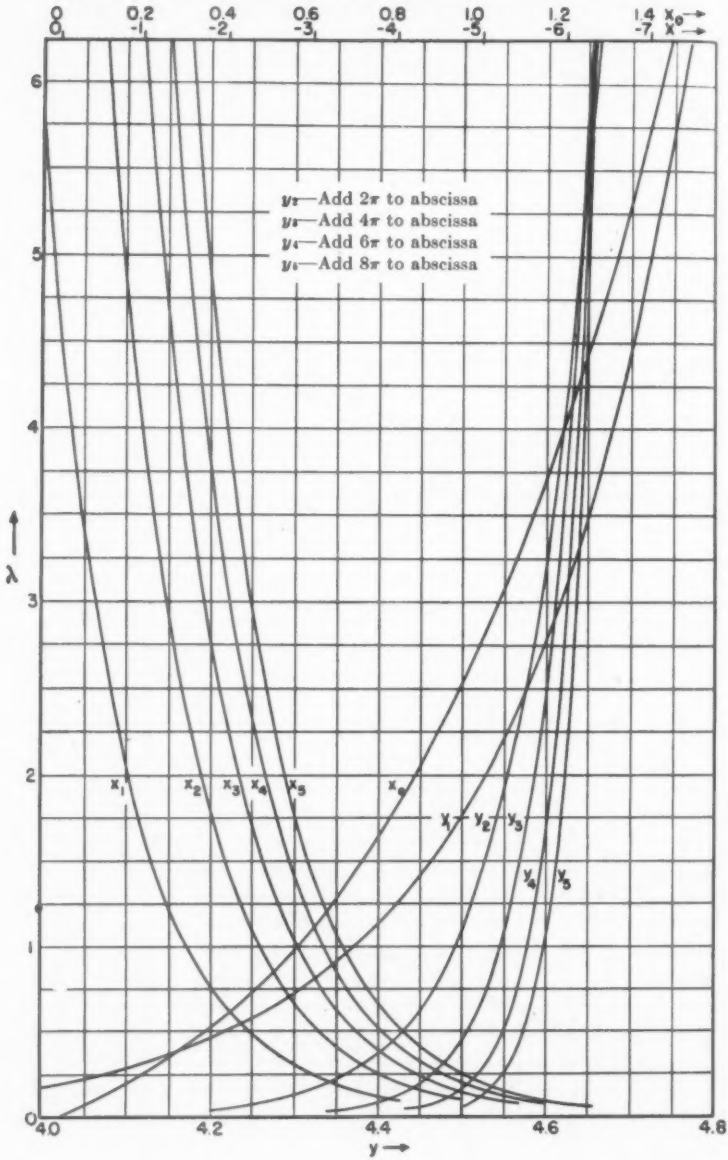
0 0.2 0.4 0.6 0.8 1.0 1.2 1.4 x_0
0 -1 -2 -3 -4 -5 -6 -7 x_0
y_2—Add 2π to abscissa
y_3—Add 4π to abscissa
y_4—Add 6π to abscissa
y_5—Add 8π to abscissa
x_1 x_2 x_3 x_4 x_5 x_6
y_1 y_2 y_3 y_4 y_5
λ
y
0 1 2 3 4 5 6
4.0 4.2 4.4 4.6 4.8

2. INFINITE MEDIUM, SPHERICAL DISTRIBUTIONS

1. Thermal Neutrons

From (R.1) and (1.1a) we get for the density due to a point source

$$\rho = \frac{Q\tau}{4\pi L^2 r} e^{-r/L} \tag{2.1a}$$

where r is the distance from the source. It follows from this that $<r^2>_{av} = 6L^2$. It is in fact true in *all* cases that $<r^2>_{av} = 3<z^2>_{av}$, where $<r^2>_{av}$ is calculated for a point source and $<z^2>_{av}$ for a plane source of corresponding strength.

For a shell source at $r = r'$, from (R.2)

$$\rho = \frac{Q\tau}{8\pi r' L} \left\{ e^{-|r-r'|/L} - e^{-|r+r'|/L} \right\} \frac{1}{r} \tag{2.1b}$$

and for a spherically symmetrical source distribution $q(r)$

$$\rho = \frac{\tau}{2Lr} \int_0^\infty r' q(r') \left[e^{-|r-r'|/L} - e^{-|r+r'|/L} \right] dr'. \tag{2.1c}$$

2. Fast Neutrons

For a fast neutron point source of strength S

$$X = \frac{S e^{-\frac{r^2}{4\theta}}}{(4\pi\theta)^{3/2}}. \tag{2.2a}$$

For a shell source, if S is the number of neutrons per unit time from the shell,

$$rX = \frac{S}{8r'\sqrt{\pi^3\theta}} \left[e^{-\frac{(r-r')^2}{4\theta}} - e^{-\frac{(r+r')^2}{4\theta}} \right]$$

$$= \frac{S}{4r'\sqrt{\pi^3\theta}} e^{-\frac{(r^2+r'^2)}{4\theta}} \sinh \frac{rr'}{2\theta}. \tag{2.2b}$$

For a spherically symmetrical source distribution $S(r')$

$$rX = \frac{1}{2\sqrt{\pi\theta}} \int_{-\infty}^{\infty} \left[e^{-\frac{(r-r')^2}{4\theta}} - e^{-\frac{(r+r')^2}{4\theta}} \right] r' s(r') dr' \tag{2.2c}$$

3. General Problem Without Multiplication

Thermal neutron distribution due to a fast neutron point source of strength S is

$$\rho(r) = \frac{\tau S e^{\theta_0/L^2}}{8\pi L^2 r} \left[e^{-r/L} \left\{ 1 - \operatorname{erf}\left(\frac{\sqrt{\theta_0}}{L} - \frac{r}{2\sqrt{\theta_0}} \right) \right\} \right.$$

$$\left. - e^{r/L} \left\{ 1 - \operatorname{erf}\left(\frac{\sqrt{\theta_0}}{L} + \frac{r}{2\sqrt{\theta_0}} \right) \right\} \right] \tag{2.3a}$$

or, in the notation of (1.3)

$$\rho(r,\gamma) = \frac{e^{\gamma^2}}{8\pi r} (1+\gamma^2) \left[e^{-r\sqrt{1+\gamma^2}} \left\{ 1 - \operatorname{erf}\left(\gamma - \frac{r\sqrt{1+\gamma^2}}{2\gamma} \right) \right\} \right.$$

$$\left. - e^{r\sqrt{1+\gamma^2}} \left\{ 1 - \operatorname{erf}\left(\gamma + \frac{r\sqrt{1+\gamma^2}}{2\gamma} \right) \right\} \right].$$

This distribution is illustrated in graphs (2.3a–d). In graph (2.3e) we plot the total number of thermal neutrons inside a given radius.

UNIVERSITY OF MICHIGAN LIBRARIES

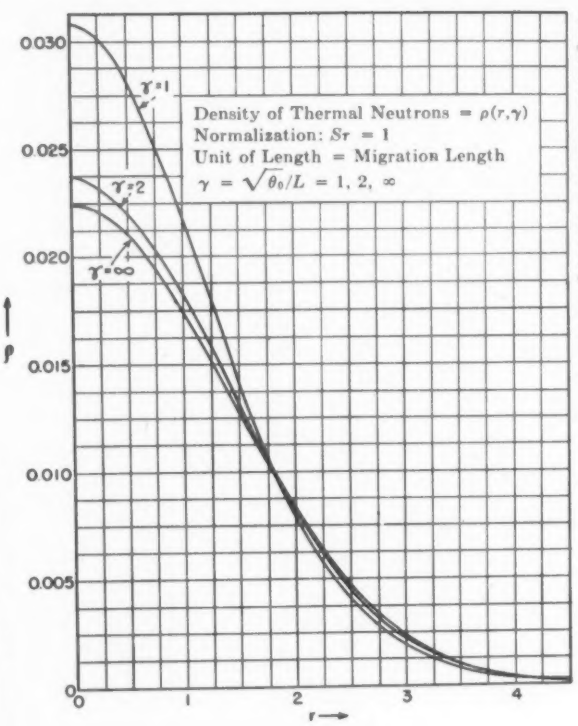

Graph 2.3b—Infinite medium, point source

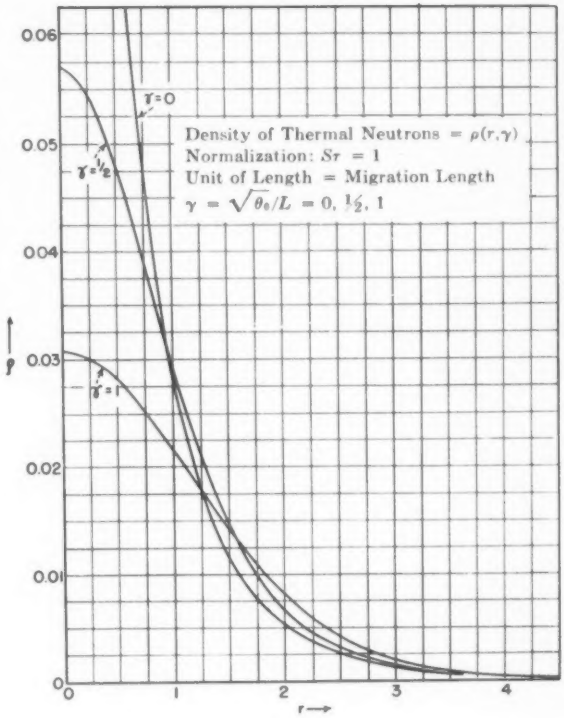

Graph 2.3a—Infinite medium, point source

Graph 2.3c—Infinite medium, point source

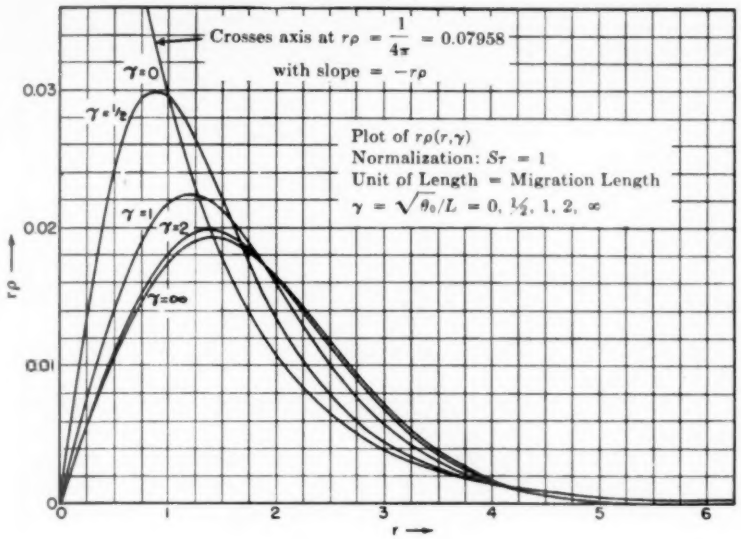

Graph 2.3d—Infinite medium, point source

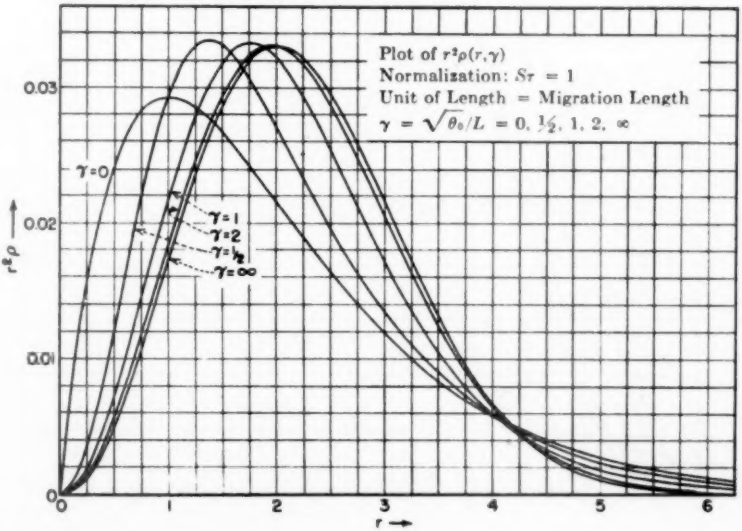

Graph 2.3e—Infinite medium, point source

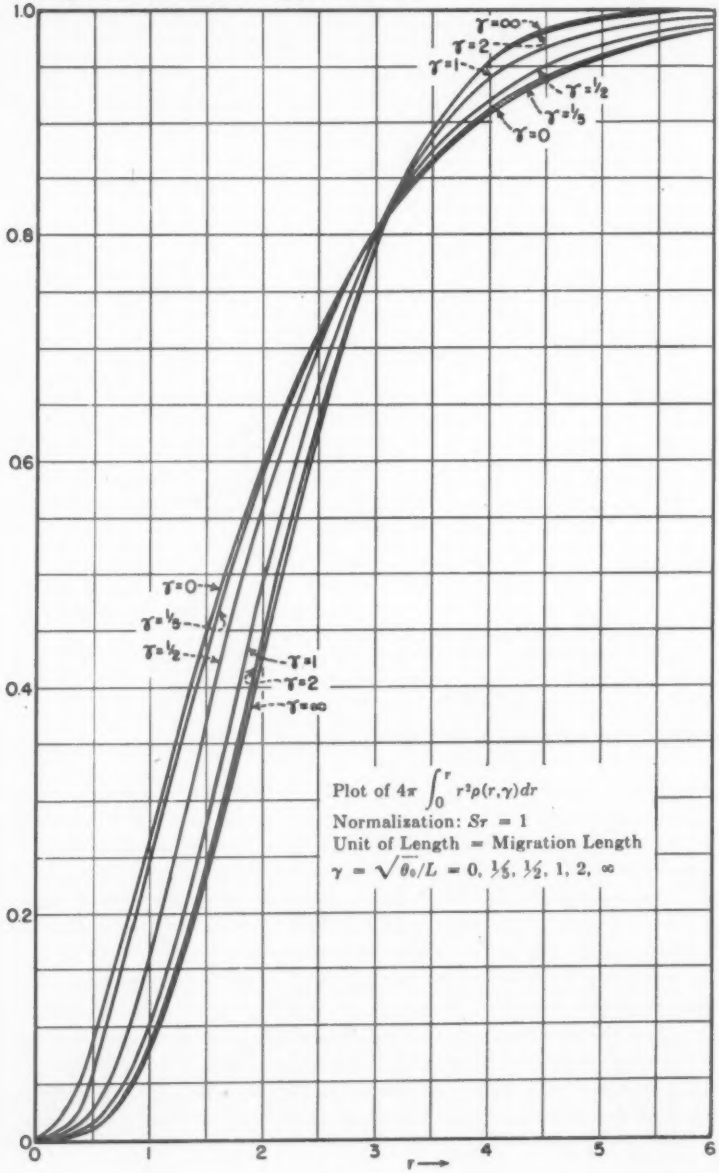

CONFIDENTIAL UNCLASSIFIED

4. Multiplying Medium

In the notation of (1.4), the thermal neutron distribution arising from a point source of fast neutrons of strength S in a medium in which the multiplication factor is k is

$$\rho = \frac{S\tau}{4\pi r}\left\{\sum_{n=-\infty}^{\infty} \frac{e^{\alpha_n^2\theta_0}e^{-\alpha_n r}}{L^2 + (1-\alpha_n^2L^2)\theta_0}\right. \tag{2.4a}$$

3. SEMI-INFINITE MEDIUM

The boundary of the medium is taken to be the plane $z = 0$.

1. Thermal Neutrons

If there is a source of strength Q at $z = z'$

$$\rho = \frac{Q\tau}{2L}\left[e^{-|z-z'|/L} - e^{-|z+z'|/L}\right]. \tag{3.1a}$$

For a distributed source $q(z')$

$$\rho = \frac{\tau}{2L}\int_0^\infty \left[e^{-|z-z'|/L} - e^{-|z+z'|/L}\right]q(z')dz'. \tag{3.1b}$$

Using (I.2), we may obtain the density at the boundary:

$$\rho_{bt}(0) = \frac{\sqrt{3}}{1+\epsilon}\cdot\frac{1}{v}\int_0^\infty e^{-z'/L}q(z')dz'.$$

The ratio of this to its value at $z = 0$ in an infinite medium (with the same source) is

$$\frac{\rho_{inf}(0)}{\rho_{bt}(0)} = \frac{1}{2}\sqrt{N}$$

where N is the average number of collisions a neutron experiences before capture.

We shall not consider any further results for a semi-infinite medium. They may, if required, be obtained from the results for an *infinite* medium by the method of images; the solution for a semi-infinite medium with source at z' is the difference of the solution in an infinite medium with source at z' and that due to an identical source at $-z'$. All further results, therefore, follow immediately from those of (*2. Infinite Medium*) above.

4. SLAB OF FINITE THICKNESS and INFINITE EXTENT

1. Thermal Neutrons

Let us take the slab as lying between $z = -a$ and $z = a$, so that its thickness is $2a$. We consider a source of strength Q at $z = z'$. Then the thermal neutron density is

$$\rho = \frac{Q\tau}{L}\frac{\sinh\dfrac{a+z'}{L}}{\sinh\dfrac{2a}{L}}\sinh\frac{a-z}{L}, \qquad (z > z') \tag{4.1a}$$

$$\rho = \frac{Q\tau}{L}\frac{\sinh\dfrac{a-z'}{L}}{\sinh\dfrac{2a}{L}}\sinh\frac{a+z}{L}, \qquad (z < z').$$

If there is a distributed laminar source $q(z')$ we have

$$\rho = \frac{\tau}{L \sinh \frac{2a}{L}} \left\{ \sinh \frac{a - z}{L} \int_{-a}^{z} \sinh \frac{a + z'}{L} q(z')dz' + \sinh \frac{a + z}{L} \int_{z}^{a} \sinh \frac{a - z'}{L} q(z')dz' \right\}. \quad (4.1b)$$

2. Fast Neutrons

The density $X(\theta,z)$ from a fast neutron source of strength S may be written in either of two forms

$$X(\theta,z) = \frac{S}{a} \sum_{m=1}^{\infty} \left\{ \cos \frac{(2m-1)\pi z'}{2a} \cos \frac{(2m-1)\pi z}{2a} e^{-\frac{(2m-1)^2\pi^2}{4a^2}\theta} + \sin \frac{m\pi z'}{a} \sin \frac{m\pi z}{a} e^{-\frac{m^2\pi^2}{a^2}\theta} \right\} \quad (4.2a)$$

or

$$X(\theta,z) = \frac{S}{\sqrt{4\pi\theta}} \left[e^{-(z-z')^2/4\theta} + \sum_{m=1}^{\infty} \left\{ e^{-(z-z'+4am)^2/4\theta} + e^{-(z-z'-4am)^2/4\theta} - e^{-[z+z'+(2m-1)2a]^2/4\theta} - e^{-[z+z'-(2m-1)2a]^2/4\theta} \right\} \right] \quad (4.2a')$$

The first form is most rapidly convergent for small "a," the second for large "a." It may be seen that the form (4.2a') is derivable from the solution for an infinite medium by the method of images. The form (4.2a), on the other hand, follows directly if we attempt to represent the solution by a Fourier series.

3. General Problem Without Multiplication

Combining the results of the previous sections, we find the thermal neutron distribution from a fast neutron source of strength S:

$$\rho = 4aS\tau \sum_{m=1}^{\infty} \frac{e^{-\frac{(2m-1)^2\pi^2\theta_0}{4a^2}}}{4a^2 + (2m-1)^2\pi^2L^2} \cos \frac{(2m-1)\pi z}{2a} \quad (4.3a)$$

or alternatively

$$\rho = \frac{\tau S}{4L} e^{\frac{\theta_0}{L^2}} \sum_{m=-\infty}^{\infty} (-1)^m \left[e^{-\frac{z+2am}{L}} \left\{ 1 - \operatorname{erf} \left(\frac{\sqrt{\theta_0}}{L} - \frac{z+2am}{2\sqrt{\theta_0}} \right) \right\} + e^{\frac{z+2am}{L}} \left\{ 1 - \operatorname{erf} \left(\frac{\sqrt{\theta_0}}{L} + \frac{z+2am}{2\sqrt{\theta_0}} \right) \right\} \right]. \quad (4.3a')$$

The current of thermal neutrons over the boundary may be written

$$j = 2L^2S \sum_{m=1}^{\infty} (-1)^{m+1} \frac{(2m-1)\pi e^{-\frac{(2m-1)^2\pi^2\theta_0}{4a^2}}}{4a^2 + (2m-1)^2\pi^2L^2}.$$

4. Multiplication

The thermal neutron distribution is

$$\rho(z) = \frac{S\tau}{a} \sum_{n=0}^{\infty} \frac{e^{-\frac{(2n+1)^2\pi^2}{4a^2}\theta_0}}{1 + \frac{(2n+1)^2\pi^2}{4a^2}L^2 - k\,e^{-\frac{(2n+1)^2\pi^2}{4a^2}\theta_0}} \cos\frac{(2n+1)\pi z}{2a} \qquad (4.4a)$$

or alternatively

$$\rho = \frac{S\tau}{2} \sum_{n=-\infty}^{\infty} \frac{e^{\alpha_n^2\theta_0}\sinh\alpha_n(a - |z|)}{\alpha_n[L^2 + (1 - \alpha_n^2L^2)\theta_0]\cosh\alpha_n a}. \qquad (4.4a')$$

In the latter form, the quantities α_n are the same as those defined in section 1.4, and may be obtained from formula (for α_0) and graph (for the others) as outlined there.

If $k > 1$, both solutions remain valid. *Critical conditions* are determined by

$$k = \left(1 + \frac{\pi^2L^2}{4a^2}\right) e^{\frac{\pi^2}{4a^2}\theta_0}.$$

This may be solved for the critical thickness

$$2a_{crit} = \frac{\pi L_0}{\sqrt{k-1}}\{1 + \eta(\gamma, k-1)\},$$

where

$$\eta(\gamma, k-1) = \frac{\gamma^2(2+\gamma^2)}{(1+\gamma^2)^2}\frac{(k-1)}{4} - \frac{\gamma^4(36 + 28\gamma^2 + 7\gamma^4)}{(1+\gamma^2)^4}\frac{(k-1)^2}{96} + \cdots$$

5. SPHERICAL MEDIUM

1. Thermal Neutrons

For a point source of thermal neutrons of strength Q

$$\rho = \frac{Q\tau}{4\pi L^2 \sinh\frac{a}{L}} \frac{\sinh\frac{a-r}{L}}{r} \qquad (5.1a)$$

where a is the radius of the sphere.

The current over the boundary is

$$j(a) = \frac{Q}{4\pi aL\sinh\frac{a}{L}}.$$

The total number of thermal neutrons in the system is

$$A(a) = Q\tau\left(1 - \frac{a}{L\sinh\frac{a}{L}}\right).$$

For a shell source of strength Q at $r = r'$

$$\rho = \frac{Q\tau\sinh\frac{a-r'}{L}}{4\pi Lr'\sinh\frac{a}{L}} \frac{1}{r}\sinh\frac{r}{L} \qquad (r < r')$$

$$\rho = \frac{Qr \sinh \frac{r'}{L}}{4\pi L r' \sinh \frac{a}{L}} \frac{1}{r} \sinh \frac{a-r}{L} \qquad (r > r') \tag{5.1b}$$

and in this case the current over the surface is

$$j(a) = \frac{Q \sinh \frac{r'}{L}}{4\pi a r' \sinh \frac{a}{L}}.$$

For a spherically symmetrical source distribution $q(r)$, it follows from equation (5.1b) that

$$\rho = \frac{\tau}{L \sinh \frac{a}{L} \cdot r} \left\{ \sinh \frac{a-r}{L} \int_0^r r' \sinh \frac{r'}{L} q(r') dr' + \sinh \frac{r}{L} \int_r^a r' \sinh \frac{a-r'}{L} q(r') dr' \right\} \tag{5.1c}$$

2. Fast Neutrons

The fast neutron density from a point source of fast neutrons is

$$X(\theta, r) = \frac{S}{2a^2 r} \sum_{m=1}^{\infty} m \sin \frac{m\pi r}{a} e^{-\frac{m^2\pi^2}{a^2}\theta} \tag{5.2a}$$

or alternatively

$$X(\theta, r) = \frac{S}{(4\pi\theta)^{3/2}} e^{-\frac{r^2}{4\theta}} \left[1 + 2 \sum_{m=1}^{\infty} \left(\cosh \frac{amr}{\theta} - \frac{2am}{r} \sinh \frac{amr}{\theta} \right) e^{-\frac{a^2 m^2}{\theta}} \right] \tag{5.2a'}$$

If the number of neutrons in the system passing symbolic age θ per unit time is designated $A_\theta(a)$, we get

$$A_\theta(a) = \int_0^a 4\pi r^2 X(\theta, r) dr = 2S \sum_{m=1}^{\infty} (-1)^{m+1} e^{-\frac{m^2\pi^2}{a^2}\theta};$$

or

$$A_\theta(a) = S \left\{ 1 - \frac{2a}{\sqrt{\pi\theta}} \sum_{n=1}^{\infty} e^{\frac{-(2n-1)^2 a^2}{4\theta}} \right\}$$

The remainder, $S - A_\theta(a)$, is the number which escapes over the surface at symbolic age θ.

3. General Problem

The density of thermal neutrons arising from a fast neutron point source of strength S is

$$\rho = \frac{S\tau}{2r} \sum_{m=1}^{\infty} \frac{m}{a^2 + m^2\pi^2 L^2} e^{-\frac{m^2\pi^2}{a^2}\theta_0} \sin \frac{m\pi r}{a}. \tag{5.3a}$$

or

$$\rho(r) = \frac{\tau S e^{\frac{\theta_0}{L^2}}}{8\pi L^2 r} \sum_{m=-\infty}^{\infty} \left[e^{-\frac{r+2am}{L}} \left\{ 1 - \operatorname{erf}\left(\frac{\sqrt{\theta_0}}{L} - \frac{r+2am}{2\sqrt{\theta_0}} \right) \right\} \right.$$

$$\left. - e^{\frac{r+2am}{L}} \left\{ 1 - \operatorname{erf}\left(\frac{\sqrt{\theta_0}}{L} + \frac{r+2am}{2\sqrt{\theta_0}} \right) \right\} \right] \quad (5.3a')$$

The total number of thermal neutrons escaping from the system per unit time is given by either

$$4\pi a^2 j(a) = 2SL^2 \sum_{m=1}^{\infty} \frac{(-1)^{m+1} \frac{m^2\pi^2}{a^2}}{1 + \frac{m^2\pi^2}{a^2} L^2} e^{-\frac{m^2\pi^2}{a^2}\theta_0}$$

or

$$4\pi a^2 j(a) = \frac{Sa}{L} \sum_{m=0}^{\infty} \left[e^{-\frac{(2m+1)a}{L}} \left\{ 1 - \operatorname{erf}\left(\frac{\sqrt{\theta_0}}{L} - \frac{(2m+1)a}{2\sqrt{\theta_0}} \right) \right\} \right.$$

$$\left. + e^{\frac{(2m+1)a}{L}} \left\{ 1 - \operatorname{erf}\left(\frac{\sqrt{\theta_0}}{L} + \frac{(2m+1)a}{2\sqrt{\theta_0}} \right) \right\} \right] - \frac{2Sa}{\sqrt{\pi\theta_0}} \sum_{m=0}^{\infty} e^{-\frac{(2m+1)^2 a^2}{4\theta_0}}$$

The total number of thermal neutrons in the system is

$$A = 2S\tau a^2 \sum_{m=1}^{\infty} (-1)^{m+1} \frac{e^{-\frac{m^2\pi^2}{a^2}\theta_0}}{a^2 + m^2\pi^2 L^2}$$

or

$$A = S\tau \left[1 - \frac{a}{L} e^{\frac{\theta_0}{L^2}} \sum_{n=0}^{\infty} \left\{ e^{-\frac{(2n+1)a}{L}} \left[1 - \operatorname{erf}\left(\frac{\sqrt{\theta_0}}{L} - \frac{(2n+1)a}{2\sqrt{\theta_0}} \right) \right] \right.\right.$$

$$\left.\left. + e^{\frac{(2n+1)a}{L}} \left[1 - \operatorname{erf}\left(\frac{\sqrt{\theta_0}}{L} + \frac{(2n+1)a}{2\sqrt{\theta_0}} \right) \right] \right\} \right]$$

Graph (5.3a) shows plots of $A(a,\gamma)$ with the usual conventions: $S\tau = 1$, the unit of length is the migration length, $\gamma = L_s/L$. The fact that $S\tau = 1$ implies that the graph gives the proportion of thermal neutrons in the system to that in an infinite system with the same source.

The plot for $\gamma = \infty$ gives the number of *fast* neutrons in the system.

Graph (5.3b) gives the flux of thermal neutrons over the boundary of the system.

Graphs (5.3c–e) give the density of thermal neutrons for $a = 1$, 2 and 3 migration lengths, respectively.

Graphs (5.3f–h) give $r^2\rho$ (where $4\pi r^2\rho$ is the number of neutrons at a given distance from the source) for $a = 1$, 2, and 3 respectively.

Graphs (5.3i–m) give plots of $r^2\rho$ as functions of r for various values of a, corresponding to $\gamma = 0$, $\frac{1}{2}$, 1, 2, and ∞, respectively.

UNIVERSITY OF MICHIGAN LIBRARIES

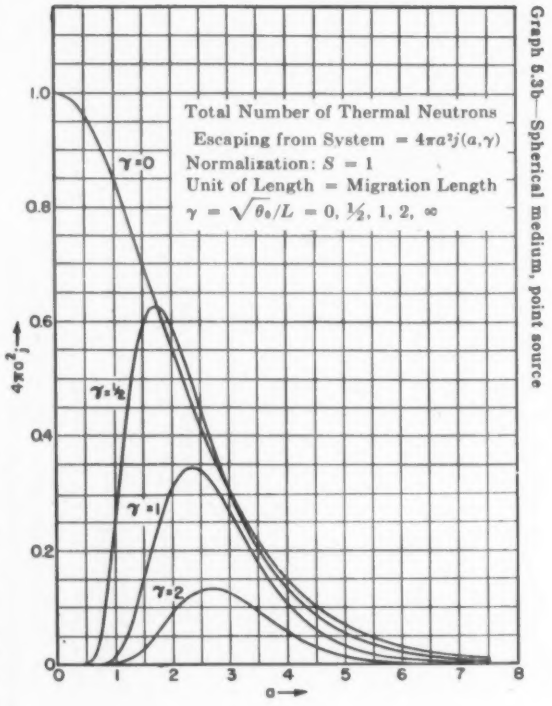

Graph 5.3b—Spherical medium, point source

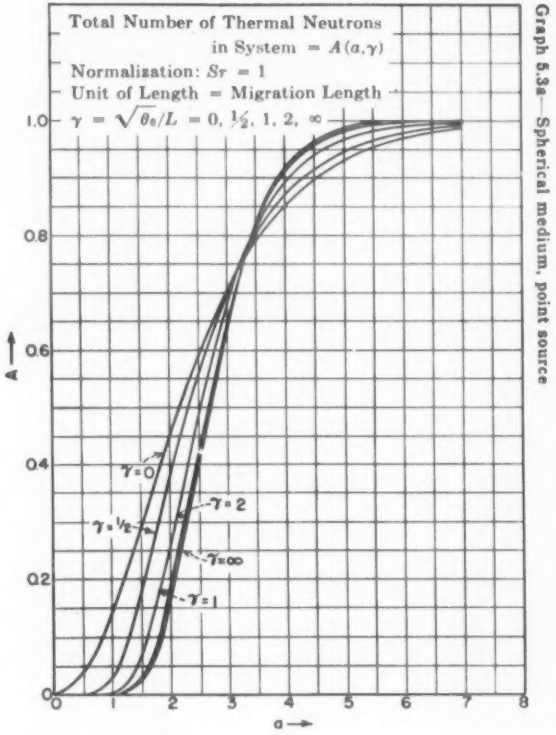

Graph 5.3a—Spherical medium, point source

Graph 5.3c—Spherical medium, point source at center

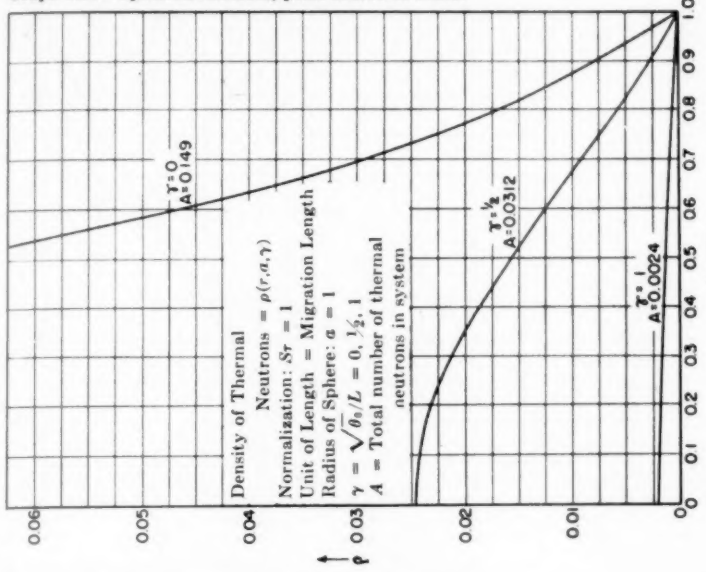
Density of Thermal Neutrons = $\rho(r,a,\gamma)$
Normalization: $Sr = 1$
Unit of Length = Migration Length
Radius of Sphere: $a = 1$
$\gamma = \sqrt{\theta_0}/L = 0, \frac{1}{2}, 1$
A = Total number of thermal neutrons in system
γ=0 A=0.149
γ=½ A=0.0312
γ=1 A=0.0024
ρ
r

Graph 5.3d—Spherical medium, point source at center

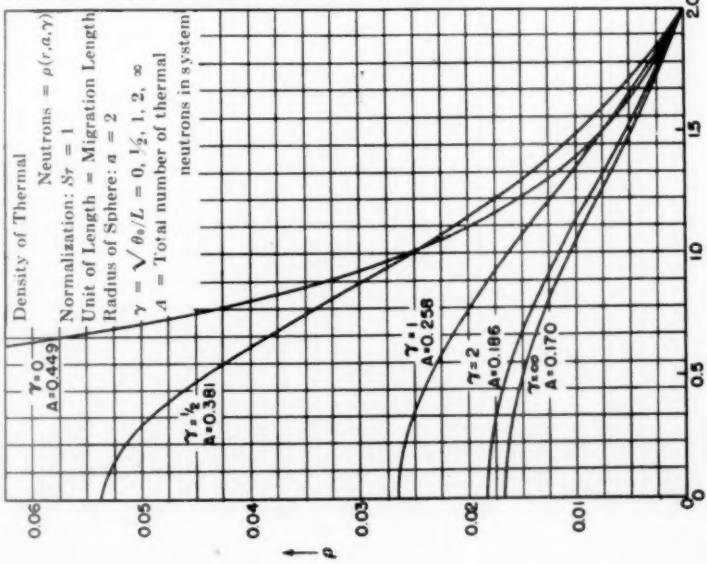
Density of Thermal Neutrons = $\rho(r,a,\gamma)$
Normalization: $Sr = 1$
Unit of Length = Migration Length
Radius of Sphere: $a = 2$
$\gamma = \sqrt{\theta_0}/L = 0, \frac{1}{2}, 1, 2, \infty$
A = Total number of thermal neutrons in system
γ=0 A=0.449
γ=½ A=0.381
γ=1 A=0.258
γ=2 A=0.186
γ=∞ A=0.170
ρ
r

Graph 5.3e—Spherical medium, point source at center

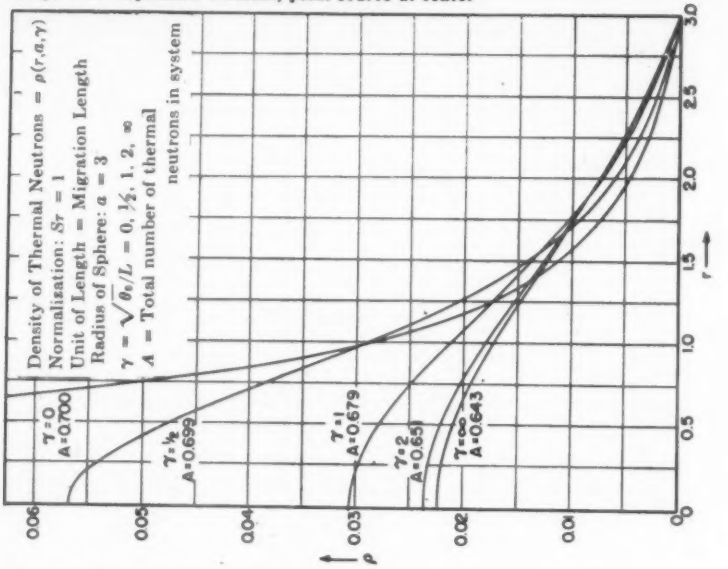

Graph 5.3f—Spherical medium, point source at center

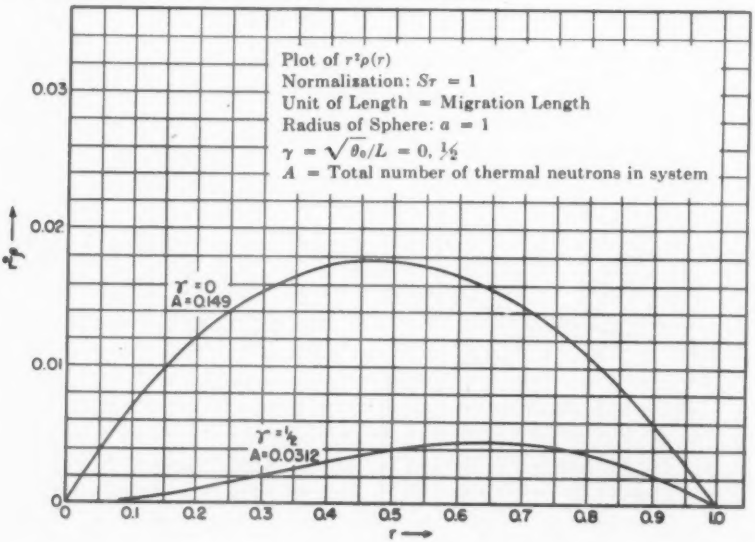

Graph 5.3g—Spherical medium, point source at center

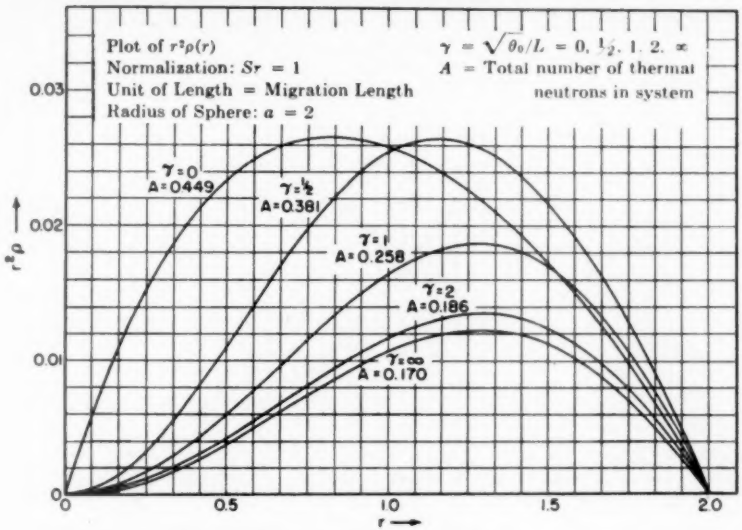

Graph 5.3h—Spherical medium, point source at center

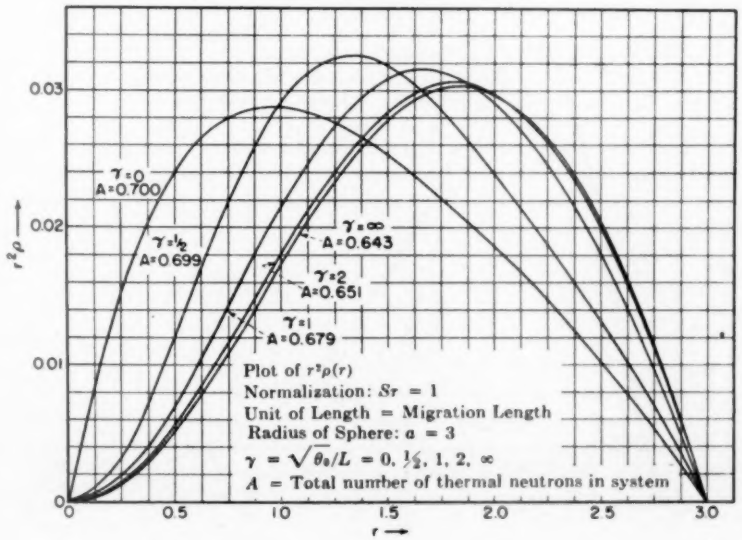

Graph 5.3i—Spherical medium, point source at center

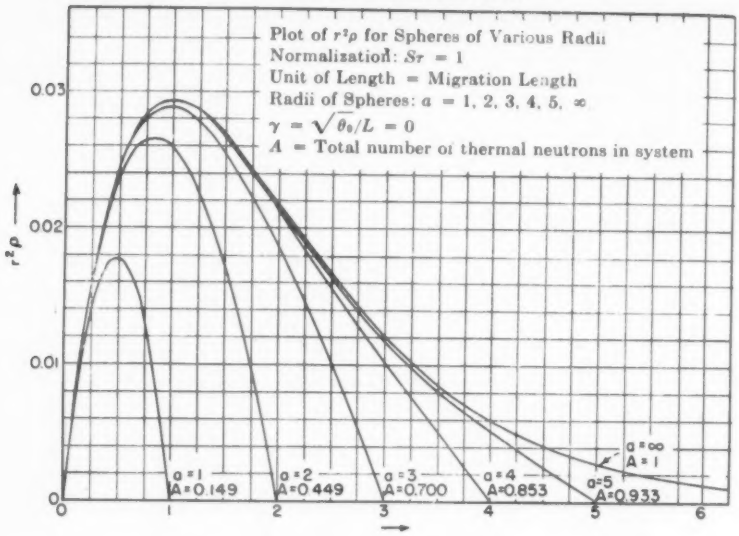

Graph 5.3j—Spherical medium, point source at center

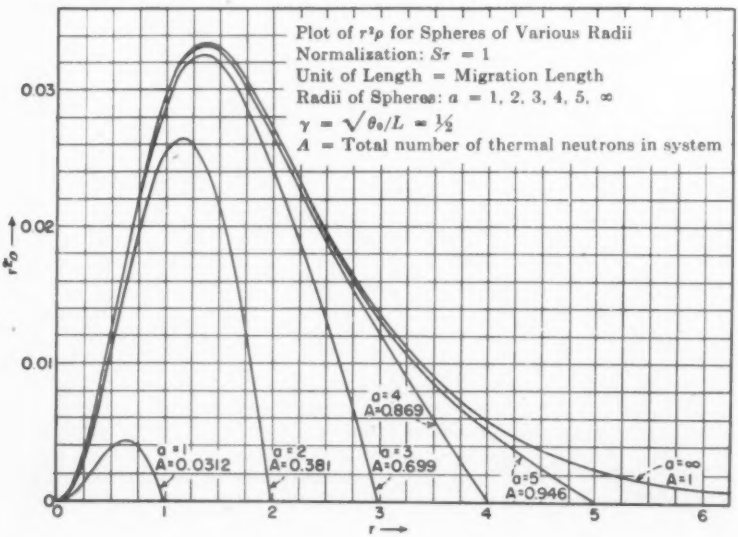

Graph 5.3k—Spherical medium, point source at center

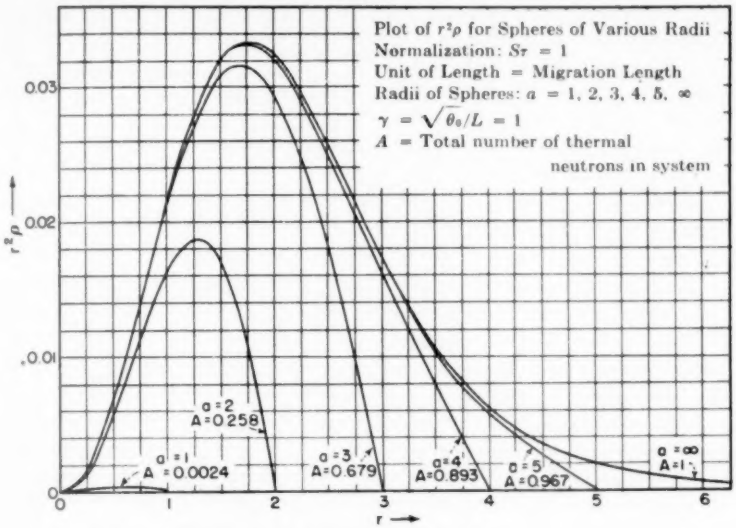

Graph 5.3l—Spherical medium, point source at center

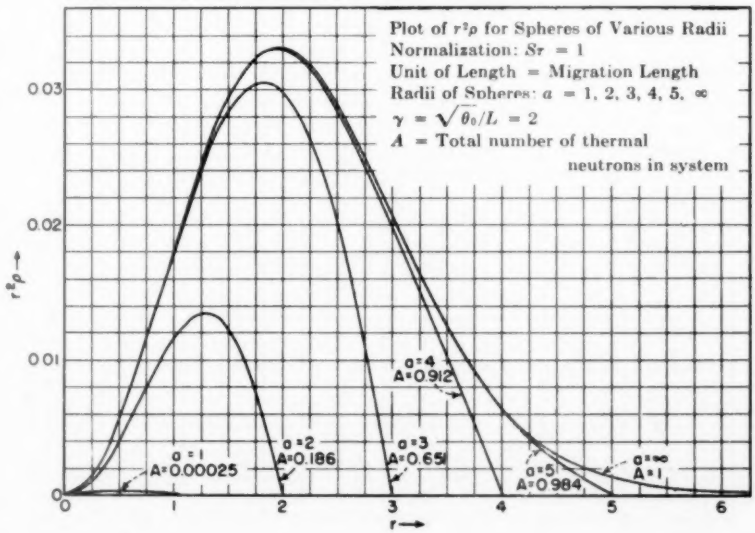

Graph 5.3m—Spherical medium, point source at center

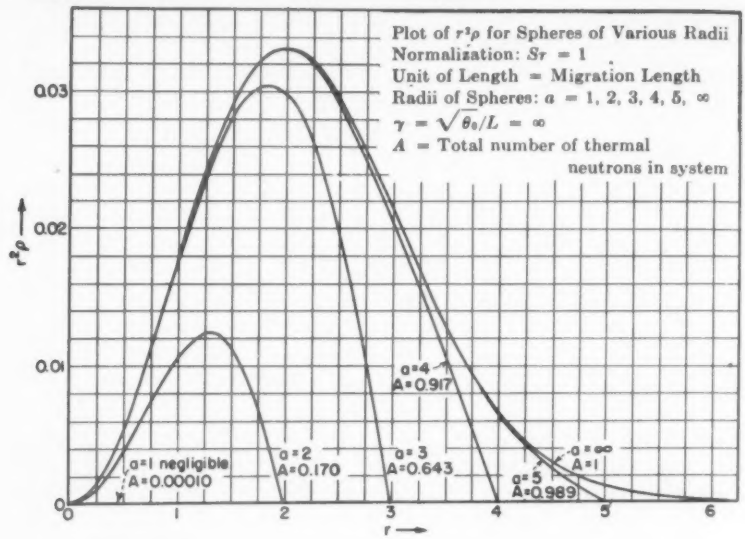

Graph 5.4a—Sphere, no source

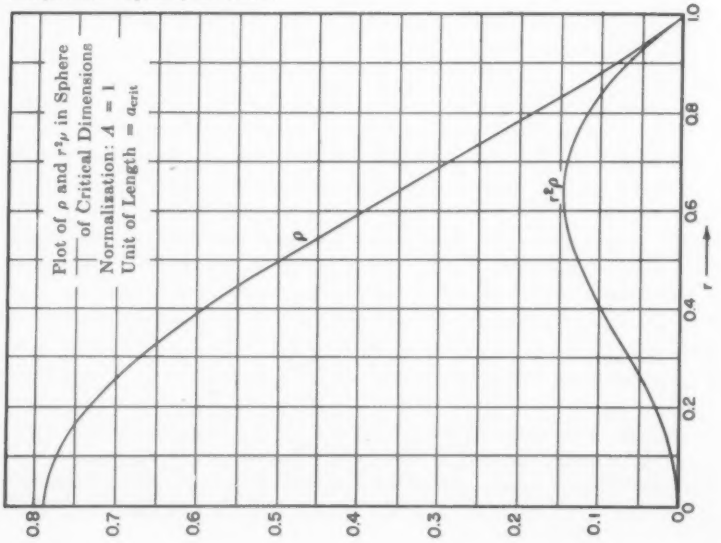

In the case of a shell source of strength at $r = r'$ the two forms of solution are

$$\rho = \frac{S\tau a}{2\pi r r'} \sum_{m=1}^{\infty} \frac{e^{-\frac{m^2\pi^2}{a^2}\theta_0}}{a^2 + m^2\pi^2 L^2} \sin\frac{m\pi r'}{a} \sin\frac{m\pi r}{a} \tag{5.3b}$$

and

$$\begin{aligned}\rho = \frac{\tau s e^{\frac{\theta_0}{L^2}}}{16\pi r r' L} \sum_{m=-\infty}^{\infty} \Bigg[& e^{-\frac{|r-r'-2ma|}{L}} \left\{1 - \operatorname{erf}\left(\frac{\sqrt{\theta_0}}{L} - \frac{|r-r'-2ma|}{2\sqrt{\theta_0}}\right)\right\} \\ & + e^{\frac{|r-r'-2ma|}{L}} \left\{1 - \operatorname{erf}\left(\frac{\sqrt{\theta_0}}{L} + \frac{|r-r'-2ma|}{L}\right)\right\} \\ & - e^{-\frac{|r+r'-2ma|}{L}} \left\{1 - \operatorname{erf}\left(\frac{\sqrt{\theta_0}}{L} - \frac{|r+r'-2ma|}{2\sqrt{\theta_0}}\right)\right\} \\ & - e^{\frac{|r+r'-2ma|}{L}} \left\{1 - \operatorname{erf}\left(\frac{\sqrt{\theta_0}}{L} + \frac{|r+r'-2ma|}{L}\right)\right\} \Bigg]\end{aligned} \tag{5.3b'}$$

4. Multiplication

The density of thermal neutrons is given by

$$r\rho = \frac{S\tau}{2a^2} \sum_{n=1}^{\infty} \frac{n\epsilon^{-\frac{n^2\pi^2}{a^2}\theta_0}}{1 + \frac{n^2\pi^2}{a^2} L^2 - k e^{-\frac{n^2\pi^2}{a^2}\theta_0}} \sin\frac{n\pi r}{a} \tag{5.4a}$$

or

$$\rho = \frac{S\tau}{4\pi r} \sum_{n=-\infty}^{\infty} \frac{e^{\alpha_n^2\theta_0} \sinh \alpha_n(a-r)}{[L^2 + (1 - \alpha_n^2 L^2)\theta_0] \sinh \alpha_n a} \tag{5.4a'}$$

where the α_n's are as defined in (1.4) and (4.4). Critical conditions are given by

$$k = \left(1 + \frac{\pi^2 L^2}{a^2}\right) e^{\frac{\pi^2}{a^2}\theta_0}$$

or, expressed as a condition for the critical radius

$$a_{\text{crit}} = \frac{\pi L_0}{\sqrt{k-1}} \{1 + \eta(\gamma, k-1)\}$$

where $\eta(\gamma, k-1)$ is as defined in (4.4).

Graph (5.4a) shows a plot of ρ and $r^2\rho$ in a sphere of critical dimensions with no source.

The foregoing paper, together with Part II to be published next month, constitutes a summary of the main results of the Canadian National Research Council Report 1480 by P. R. Wallace and J. LeCaine, somewhat rearranged for easier reference. This condensation was prepared by P. R. Wallace. The complete report is available for $1 from the Plans and Publications Branch, National Research Council, Ottawa, Canada.

BETA- and GAMMA-RAY SPECTROSCOPY—II

Discussed in this second of two papers is the Fermi diagram which directly compares measured and theoretical energy distributions and allows precise determination of maximum beta-ray energy and resolution of complex spectra. Use of the spectrometer to find gamma-ray energies and intensities by internal and external conversion is also described

By GERALD J. HINE

Department of Physics, Sloan-Kettering Institute for Cancer Research
New York, New York

WITHOUT GIVING the complete picture, some of the fundamental aspects of Fermi's theory of allowed beta-ray transitions were outlined in Part I of this paper.* The experimental beta-ray energy spectrum of some isotopes, determined by different investigators, will be compared with the results of Fermi's theory in the following paragraphs.

The Kurie Plot or Fermi Diagram

A simple method, introduced by Kurie *et al.* (*1*), offers the possibility of comparing both the observed and the calculated beta-ray energy distribution. This comparison has the advantage of being independent of the knowledge of the upper limit of the beta-ray spectrum.

For an allowed transition of an isotope with the atomic number Z, the emission probability of a beta particle per unit time, with an energy in the interval ϵ to $\epsilon + d\epsilon$, is given by Fermi as (compare Eq. 16 in Part I):

$$P(\epsilon)d\epsilon = \text{const}\, F(Z,\epsilon)\epsilon\eta(\epsilon_0 - \epsilon)^2 d\epsilon \quad (1)$$

The energy ϵ and the maximum energy ϵ_0 are in units of m_0c^2 and the momentum $\eta = (\epsilon^2 - 1)^{1/2}$ in units of m_0c. $F(Z,\epsilon)$ is the Fermi function. If the observed energy distribution $N(\epsilon)$ equals the theoretical emission probability $P(\epsilon)$, it follows from Eq. 1 that

$$\left(\frac{N(\epsilon)}{\epsilon\eta F(Z,\epsilon)}\right)^{1/2} \sim \epsilon_0 - \epsilon \quad (2)$$

Therefore a "Kurie plot" is obtained by plotting the square root of the experimentally measured energy spectrum $N(\epsilon)$ divided by the product of beta-ray energy ϵ, momentum η, and Fermi function $F(Z,\epsilon)$ versus the energy ϵ. Thus the Kurie plot, also called Fermi diagram, is expected to be a straight line with a negative slope intercepting the energy axis at a value $\epsilon = \epsilon_0$. A deviation from linearity would indicate an experimental beta-ray energy distribution different from that calculated for an allowed Fermi transition.

Most experimental results indicate a linear Fermi diagram, except for some deviation from the straight line occurring at low energies of the beta-ray spectrum (see Fig. 1) to be discussed later. A Fermi diagram is, therefore, not only a simple means of comparing the observed with the calculated energy distribution, but is also the most precise method for determining the *upper limit* ϵ_0 of the beta-ray spectrum. The maximum beta-ray energy ϵ_0 (kinetic plus rest energy) is obtained by a straight line extrapolation from a spec-

* NUCLEONICS 3, No. 6, 32 (1948).

tral region of considerable intensity to the immediate neighborhood of the upper limit, a region of vanishing intensity.

With the magnetic beta-ray spectrometer, the width of the registered momentum interval $\Delta H\rho$ increases in proportion to $H\rho$, the magnetic field times the radius of curvature. Consequently, in order to correct for constant sensitivity of the instrument, the original number of counts per unit time and momentum interval $\Delta H\rho$ has to be divided by the corresponding $H\rho$-values. The resulting $N(H\rho)$-values plotted as a function of $H\rho$, give the *momentum distribution* curve of the beta particles.

By plotting

$$\left(\frac{N(\eta)}{\eta^2 F(Z,\epsilon)}\right)^{1/2} \qquad (3)$$

versus $\sqrt{1+\eta^2} = \epsilon$, the same Fermi diagram as discussed above will be obtained. $N(\eta)$ is the same momentum distribution as $N(H\rho)$, except that the momentum of the beta particles is given in relativistic units of m_0c (Part I).

Finally the experimental energy distribution $N(\epsilon)$ is obtained from the momentum spectrum $N(\eta)$ by multi-

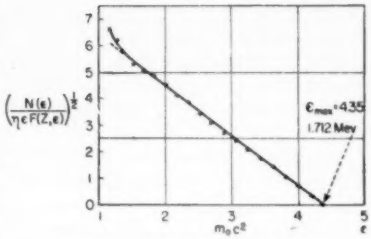

FIG. 1. Fermi diagram for P^{32} [Siegbahn (9)]

plying the $N(\eta)$-values by ϵ/η. Since $\eta^2 = \epsilon^2 - 1$ and therefore $\eta d\eta = \epsilon d\epsilon$, it follows that $N(\eta)d\eta = \epsilon/\eta N(\eta)d\epsilon = N(\epsilon)d\epsilon$.

Allowed Simple Beta-ray Spectra

Only *allowed* transitions can be expected to show an energy distribution of the emitted beta particles in accordance with the theoretical emission probability expressed in Eq. 1. Furthermore, the transition has to be a *simple* one, *i.e.*, only *one* beta-ray spectrum should be present—not a number of partial spectra. This is certainly the case if the isotope emits no gamma rays, or if the emitted gamma radiation follows each beta particle

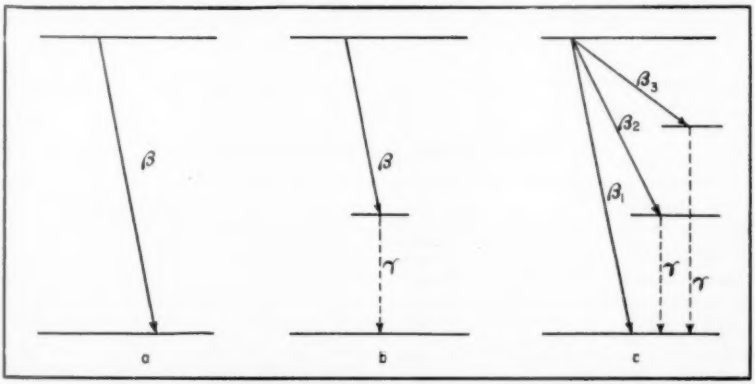

FIG. 2. Disintegration schemes
a) Single beta transition
b) Simple beta decay followed by one gamma ray
c) Complex beta decay (three partial spectra)

(Fig. 2a and 2b). In the latter case, the number of beta-gamma coincidences has to be independent of the energy of the beta rays; otherwise two or more partial spectra would be indicated (Fig. 2c).

In Table 1, those allowed simple beta-ray spectra are listed which have been recently investigated. Some isotopes are electron emitters, the others are positron emitters, as indicated in the second column, but none of these isotopes emit nuclear gamma rays. The half-lives and the maximum beta-ray energies of the isotopes are given together with those energies where the Kurie plot of the present measurements shows a distinct deviation from linearity. For all energies greater than the indicated ones, the Kurie plots of all beta-ray spectra are perfectly straight lines; at lower energies, all measurements show an excess of low-energy particles compared with the predictions of Fermi's theory.

Finally, the weight per cm² of the radioactive sources used for these investigations are given in the fifth column of Table 1. With the exception of the S^{35} measurements, most source backings consist of a Zapon film of about 0.02 mg/cm². The S^{35} beta-ray spectrum was investigated by Cook, Langer and Price (*5*) with a 0.5 mg/cm² Nylon backing and a 0.04 mg/cm² sample weight, a 0.03 mg/cm² Zapon backing and a 0.14 mg/cm² sample weight, and, finally, a 0.5 mg/cm² Nylon backing and a 0.17 mg/cm² sample weight. The results with all three sources show no significant difference; the deviation from the straight line starts at about 80 kev. Albert and Wu (*4*) succeeded in preparing collodion films of only 3 μg/cm². Their backings are about ten times thinner than all those previously used. Furthermore from a carrier-free S^{35} solution, they could prepare sources of about 1, 2 and 5 micrograms in addition to the backing film. Their total source weight is, therefore, about forty times smaller than that used by Cook, Langer and Price (*5*). Fig. 3 shows the results obtained with the three lightest sources ever used in beta-ray spectroscopy. The Fermi diagrams of the 1 and 2 μg/cm² source spectra are perfectly linear down to about 15 kev (curve A and B); that of the 5 μg/cm² source, however, shows a remarkable deviation at 80 kev (curve C).

The fact that a source as thin as 5 μg/cm² causes such a large deviation

TABLE 1

Some Allowed Simple Beta-ray Spectra

Isotope	*Emitter*	*Half-life*	*Maximum beta-ray energy* (Mev)	*Weight of radioactive source plus support* (mg/cm²)	*Deviation of the Kurie plot from straight line begins at* (kev)	*Reference*
C^{11}	β^+	20 min	0.97	Unknown	200	(*2*)
N^{13}	β^+	10 min	1.25	0.8	150	(*3*)
S^{35}	β^-	88 days	0.166	0.004	15	(*4*)
Cu^{61}	β^+	3.3 hr	1.205	0.1	500	(*6*)
Cu^{64}	β^+	12.8 hr	0.657	0.1	270	(*7*)
Cu^{64}	β^-	12.8 hr	0.571	0.1	190	(*7*)
In^{114}	β^-	72 sec	1.98	Unknown	400	(*8*)

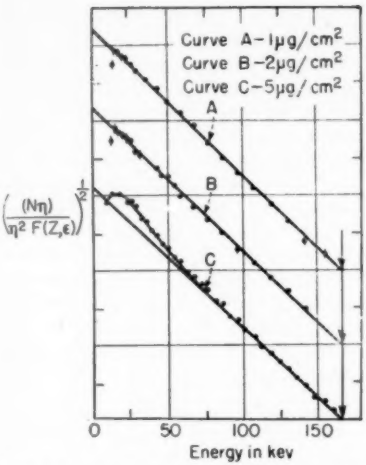

FIG. 3. Fermi diagram for S^{35} with three sources of different sample weight [Albert and Wu (4)]

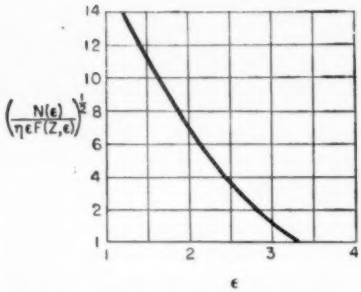

FIG. 4. Fermi diagram for RaE according to measurements of Flammersfeld (12)

from the linear Fermi plot of S^{35} is a very significant one. The source weights used for the investigation of the other isotopes given in Table 1 along with S^{35} are all more than ten times larger than 5 $\mu g/cm^2$. Therefore, it is quite possible that all discrepancies between the experimental results and the predictions of Fermi's theory in the low-energy part of the beta-ray spectra (in Table 1) result from experimental limitations.* This would indicate that Fermi's theory of beta decay is adequate for the description of the mechanism of allowed transitions.

Forbidden Simple Beta-ray Spectra

The two electron emitters P^{32} and RaE are the isotopes with the most frequently investigated beta-ray spectra. Since neither one emits nuclear gamma radiation, their spectra are certainly *simple* spectra. In addition, the long half-lives of 14.5 and 5.0 days and the high maximum energies of 1.71 and 1.17 Mev are favorable for convenient and accurate measurements.

The P^{32}-electron spectrum was observed by Siegbahn (9) by means of a radioactive source, of ~0.1 mg total weight, mounted on a Zapon film 0.1 μ thick. The Fermi diagram is linear from the maximum energy down to about 0.1 Mev (Fig. 1). Two previous measurements by Siegbahn (10) and Lawson (11), with less advanced techniques for preparing the filament, showed deviations from a straight-line Kurie plot below 0.5 Mev and 0.8 Mev, respectively. Therefore it might be possible that, under "ideal" conditions, the P^{32} Fermi diagram is also linear for its entire energy spectrum.

The RaE beta-ray spectrum has been investigated under favorable conditions (see Part I) by Flammersfeld (12), Neary (13) and others; their results are in agreement within experimental limits. The RaE Kurie plot given in Fig. 4 is *not* linear for any portion of its length. The deviation of the RaE energy spectrum from the shape of an allowed Fermi distribution is furthermore illustrated by the following fact. The *average* kinetic energy of the electrons follows from the experimental beta-

* Braden, Owen, Townsend, Cook and Shull [*Phys. Rev.* **74**, 1539 (1948)] observed recently that sources which were supported on non-conducting backing-foils, such as Zapon, Nylon or Cellophane, can establish a considerable potential difference between source and vacuum chamber. This effect might have strongly affected the results in the low-energy region of some of the beta-ray spectra listed in Table 1.

ray spectrum as $E_{av} = 330 \pm 10$ kev. The same value was obtained by calorimetric measurements (Part I). However, an allowed Fermi spectrum of an isotope of the same atomic number and maximum energy as RaE would have an average energy of about 430 kev (*14*).

From the half-lives and maximum energies of the P^{32} and RaE beta-ray spectra, it follows that *both* transitions must be regarded as *highly forbidden* ones (*15*). The Fermi diagrams of Fig. 1 and Fig. 4 indicate that the shape of the RaE electron spectrum deviates markedly from that of an allowed Fermi distribution but that the opposite is true of the P^{32} spectrum. The reasons for this behavior are connected with several unsettled questions such as the different types of selection rules and various forms of interaction between the heavy particles in the nucleus and the electron-neutrino field.

Complex Beta-ray Spectra

Fermi's theory has also proved very useful for those isotopes which emit not a simple but a complex beta-ray spectrum consisting of two or more partial spectra with different maximum energies (Fig. 2*c*). Assuming that each partial spectrum has the shape of an allowed simple Fermi spectrum, the Fermi diagram permits the resolution of the measured complex spectrum into simple partial spectra. The relative intensities of the gamma-ray lines, which follow the different partial spectra, must be coordinated with the disintegration probabilities of the competing transitions. The number of radioisotopes with complex disintegration schemes is very large. In most cases their investigation is extremely difficult and the disintegration scheme of only about a dozen isotopes with a complex beta-ray spectrum has been well established so far.

Zn^{63} with a half-life of 38.3 min is definitely an allowed transition (*15*). As an example of a complex spectrum, part of the investigation of its disintegration scheme will be discussed here. For this isotope 93% of the decay is by positron emission and 7% by *K*-capture (*16*). The transition of Zn^{63} to Cu^{63} is accompanied by the emission of essentially two nuclear gamma rays of 1.89 and 0.96 Mev. The absorption of a positron in matter results in annihilation radiation consisting of two 0.511-Mev gamma rays. The ratio of the intensities of the different Zn^{63} gamma rays has been determined (*16*) as:

$$I_{(\gamma 0.51\ \text{Mev})} : I_{(\gamma 0.96\ \text{Mev})} : I_{(\gamma 1.89\ \text{Mev})} = 100 : 4.5 : 2 \quad (4)$$

The Zn^{63} positron spectrum is given in Fig. 5. It was investigated with a semicircular spectrograph of $\rho = 10$ cm and a counter window of 0.3 μ Zapon film. The complexity of the total positron spectrum (solid curve) is not immediately indicated by its shape. The corresponding Fermi diagram is linear for energies greater than 1.4 Mev (Fig. 6, curve 1). The upper limit of the positron spectrum, determined directly from the measurements of Fig. 5, has the same value of $E_1 = 2.36$ Mev, which follows from the straight line extrapolation of the Fermi diagram (Fig. 6).

The following is the detailed procedure for the resolution of the complex spectrum into partial spectra. Since the Fermi diagram starts to deviate from a straight line at about 1.4 Mev, it is reasonable to suppose that the weak 0.96 Mev gamma radiation is connected with the emission of a *second* partial spectrum. A more accurate value for its upper limit follows from the energy difference between the maximum energy of the first transition and the energy of the gamma ray: $E_2 = (2.36 - 0.96) = 1.40$ Mev. The agreement of both values suggests a Fermi distribution for partial spectrum 1 also at energies

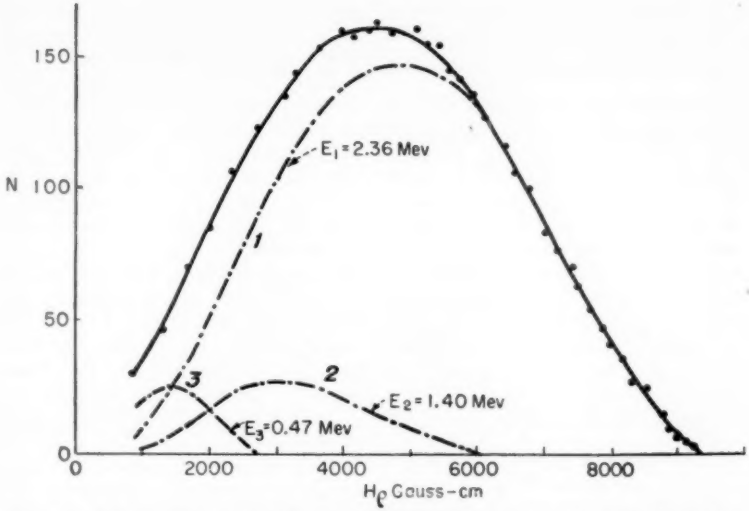

FIG. 5. Positron spectrum of Zn^{63}. Resolution into three partial spectra indicated by the broken lines *(16)*

lower than 1.4 Mev. The complete partial spectrum 1 follows from a straight-line extrapolation into the low-energy region.

The Fermi diagram of the remaining positrons is given in Fig. 6, curve 2. In the high-energy region it is again linear, indicating also an extrapolated upper energy $E_2 = 1.40$ Mev. Finally, if the 1.89-Mev gamma radiation is connected with a *third* partial spectrum, its maximum energy will be: $E_3 = (2.36 - 1.89) = 0.47$ Mev. In that energy range, the Fermi diagram of the second partial spectrum shows a deviation from linearity. The excess positrons will be assigned to the third partial spectrum, again by a straight-line extrapolation into the low-energy region of curve 2 of Fig. 6. The Fermi diagram of the third partial spectrum curve 3 of Fig. 6, is hardly significant. A small deviation of the first two, more intense partial spectra, from their extrapolated shape will strongly influence the shape of the last one. Furthermore, the absorption and backscattering of the positrons in the source will reflect mostly on the intensity of the least energetic partial spectrum.

In Fig. 5 the three partial spectra are indicated along with the measured com-

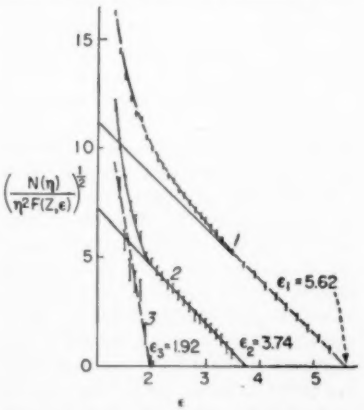

FIG. 6. Fermi diagram for the total Zn^{63}-positron spectrum and the three partial spectra *(16)*

plex positron spectrum (solid curve). Their relative intensities follow as:

$$I_{(\beta_1)} : I_{(\beta_2)} : I_{(\beta_3)} = 100 : 10 : 5 \qquad (5)$$

Neglecting the possibility that the two nuclear gamma rays might follow not only positron emission but also *K*-capture (*16*), this ratio of the intensities of the partial spectra can be compared directly with that of the gamma rays. Remembering that the annihilation radiation consists of *two* 0.511-Mev quanta per positron, both ratios (Eqs. 4 and 5), each determined by an independent method, are in good agreement. The disintegration of Zn^{65} by positron emission therefore follows the scheme indicated in Fig. 2c.

Line Spectra by Internal Conversion of Gamma Rays

The magnetic beta-ray spectrometers used for the investigation of the continuous beta-ray spectrum are also the most suitable instruments for determing gamma-ray energies and intensities. Absorption measurements of gamma rays, or of the secondary electrons produced by the gamma radiation, are simpler in many cases, but the accuracy of their results cannot be compared with those of the spectrometer measurements. Therefore, only the latter will be considered here.

In his recent paper on interaction of isotopic radiation with matter, Fluharty (*17*) summarized the different processes by which a gamma ray can be converted into an electron by losing all or part of its total energy. The emission of an orbital electron instead of a gamma ray, a phenomenon caused by an internal photoelectric effect in the atomic shell, is called *internal conversion*. The energy of the emitted electron differs from that of the converted gamma ray by the binding energy of the electron in the atomic shell from which it is ejected. Therefore, the energy difference of the electron lines resulting from the conversion of the same gamma rays, *e.g.*, in the *K*- and *L*-shell of an atom, is equal to the difference in binding energy of the orbital electrons in the corresponding shell of this element. With the precision now available in beta-ray spectroscopy, the differences of the *K-L*, or *L-M* conversion lines can be obtained with sufficient accuracy to identify the atomic number of the radiating isotope. By this method it has been proved that the gamma rays are not emitted by the initial radioactive isotope but by the newly formed element after the first one has disintegrated by the emission or absorption (*K*-capture) of a charged particle (α-particle, electron or positron).

From the internal conversion of the same gamma ray, the intensity of the *K*-line is in general much greater than that of the *L*, *M* and *N*-lines. The probability for the internal photoelectric conversion of a gamma ray in a particular atomic shell depends on the energy and the character of the gamma ray and also on the atomic number of the emitting isotope. Further details, which are mostly of theoretical interest, will not be discussed. From the large number of investigated conversion lines, those of two indium isotopes (*8*) will be presented here (Fig. 7) as an extremely interesting and instructive example.

In^{114} with a half-life of 50 days is isomeric with In^{114} of a half-life of 72 sec. The first one transforms into the second by the emission of a 192-kev gamma ray; the short-life In^{114} disintegrates by beta decay directly to the ground state of Sn^{114}. Therefore the gamma radiation emitted by In^{114} is due only to the isomeric transition.

In their investigation, Lawson and Cork (*8*) determined the conversion coefficient for the 192-kev gamma ray by comparing the number of internal conversion electrons with the number of

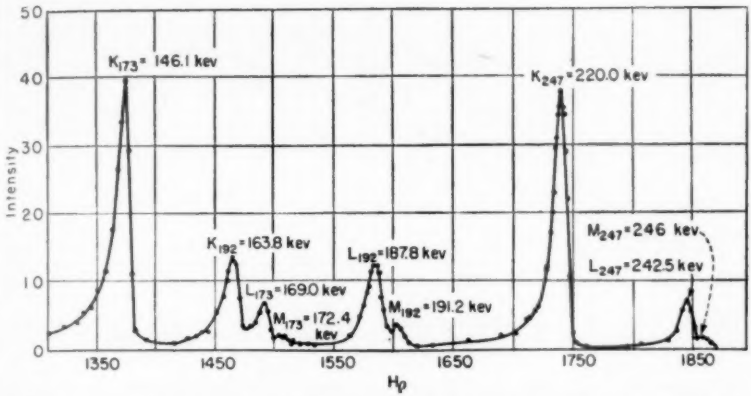

FIG. 7. Conversion electron spectrum of two indium isotopes showing *K*-, *L*-, and *M*-conversion electrons of three gamma rays of energies 173 kev, 192 kev and 247 kev respectively [Lawson and Cork (*8*)]

decay electrons emitted in the subsequent beta transition. The integration of both the In^{114} beta-ray spectrum and the conversion electron-lines obtained with the magnetic beta-ray spectrometer gave about the same value. Therefore, the total conversion coefficient of the 50-day half-life gamma ray turned out to be 105 ± 15%. This observation is in agreement with the fact that very little external gamma radiation is present; nearly all gamma rays are internally converted to conversion electrons.

Since the In^{114} gamma ray does not follow a beta transition, but is due to an isomeric transition, the gamma ray will convert in the atomic shell of indium itself instead of in a neighboring element. This is in agreement with results given in Fig. 7. The binding energy of the *K*-electron of indium added to the measured value of 164 kev and the binding energy of the *L*-electron added to 188 kev both give the gamma energy as 191.7 ± 1 kev.

If the In^{114} isotope is obtained by bombarding the neighboring element cadmium with deuterons, a great many other radioactive indium isotopes are produced since cadmium has eight stable isotopes. In addition to 50-day In^{114}, a half-life of 2.7 days is observed, after the shorter periods have decayed. This half-life, originally assigned to In^{112}, was recently proved to belong to In^{111} (*18*).

In^{111} decays by *K*-capture followed by two gamma rays in cascade, with energies of 173 and 247 kev. The *K*-, *L*-, and *M*-conversion lines of these two gamma rays have been measured along with those of the In^{114} 192-kev gamma ray (Fig. 7). In order to find out the half-lives to which the different gamma rays belong, Lawson and Cork (*8*) determined intensities of the various internal conversion lines of Fig. 7 with the same sample at different times over a period of several weeks. The 164 and 188-kev electron lines decay slowly (half-life 50 days), while the others show a half-life of 2.7 days.

Finally, In^{111} disintegrates by *K*-capture to Cd^{111}. The two gamma rays following *K*-capture can, therefore, convert only in the atom shell of cadmium and not in that of indium.

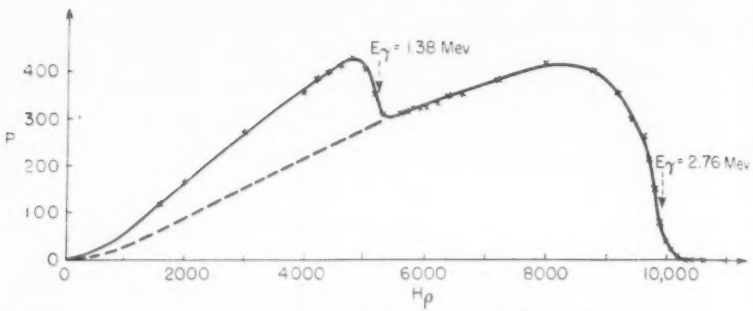

FIG. 8. Distribution of Compton electrons expelled from a copper radiator by the two gamma rays of Na^{24}. The curve is in the undivided form [Siegbahn (9)]

In agreement with this, the *K-L-M*-differences of both 2.7-day conversion lines are found to be characteristic of cadmium. From the energies of the different electron lines in Fig. 7, and the known binding energies of the electrons in the different cadmium shells, one obtains the energies of the two In^{111} gamma rays as 172.8 ± 1 kev and 246.7 ± 1 kev.

Secondary Electrons by External Conversion of Gamma Rays

Investigation of gamma-ray energies with the magnetic spectrometer is not restricted to internal conversion lines. As a matter of fact, for light and medium elements, the conversion coefficient of most gamma rays is so small that the detection of internal conversion lines is very rare. Therefore, two methods will be described here for determing energies and intensities of gamma rays even in the absence of any internal photoelectric effect.

Secondary electrons are produced by gamma rays passing through matter by external photoelectric process, Compton effect, or pair production (*17*). The last process will not be considered here, since an appreciable number of electron-positron pairs can be produced only by the most energetic gamma rays in materials of high atomic number. In an element of medium atomic number such as *copper*, almost all secondary electrons are produced by the Compton effect; only for gamma rays with energies smaller than about 0.5 Mev does the photoelectric effect in copper make a small contribution to the secondary radiation. In *lead*, however, photoelectrons are produced by gamma rays up to several Mev energy (*17*). But even for lead the photoelectric absorption coefficient for gamma rays with energies greater than about one Mev is smaller than the Compton absorption coefficient. Below one Mev the probability for production of a photoelectron increases rapidly; 0.5-Mev gamma rays produce three times more photoelectrons in lead than Compton electrons.

To investigate the *secondary electron spectrum*, Siegbahn (*9*) pressed the active sample into a small copper cylinder, the walls of which were thick enough to absorb the continuous beta-ray spectrum of the decay electrons. Figure 8 shows the distribution of the Compton electrons from the copper radiator produced by the two well-known gamma rays of Na^{24}. This isotope decays by electron emission followed by two gamma rays in cascade, with energies of 1.38 and 2.76 Mev. In Fig. 8, the ordinate is the number of

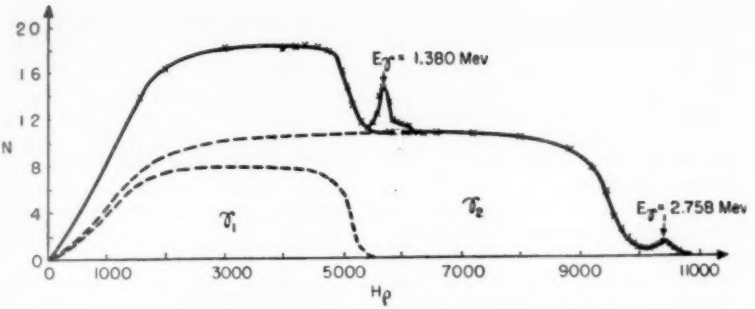

FIG. 9. Secondary electron spectrum expelled from a copper radiator covered with a 0.02 mm lead-foil by the two gamma rays of Na^{24}

impulses P counted per unit time and is not, as is more usual, the intensities over constant $H\rho$ intervals. In order to correct for constant sensitivity, the number of counts P have not been divided by the corresponding $H\rho$ value.

By this method, gamma-ray energies and intensities can be determined with moderate accuracy. The *inflection points* at the edges of the undivided Compton electron distribution (indicated by the two arrows in Fig. 8) correspond to the maximum energies of the Compton electrons (*19*). For a gamma ray with energy $h\nu$ in Mev, the maximum Compton electron energy E_c in Mev is given by

$$E_c = \frac{h\nu}{1 + \frac{0.51}{2h\nu}} \qquad (6)$$

From this expression the gamma-ray energy $h\nu$ is obtained if E_c is the energy of the inflection point

$$h\nu = \frac{E_c}{2}\left(1 + \sqrt{1 + \frac{1.02}{E_c}}\right) \qquad (7)$$

The Compton electrons registered with energies larger than E_c are due to the finite resolving power of the spectrometer.

The energy distribution of the Compton electrons, plotted in the undivided form, can easily be extrapolated to zero energy for each gamma ray separately. The broken line in Fig. 8 indicates this extrapolation. By this procedure the Compton distribution for each gamma ray can now be plotted *separately* in the usual form, *i.e.*, corrected for constant sensitivity of the spectrometer. The area of the Compton distribution for each gamma ray can be determined by graphical integration. Since both the Compton coefficient and the absorption of the secondary electrons vary with the energy of the gamma radiation, the areas of the Compton distributions are not directly proportional to the gamma-ray intensities. They must be multiplied by a factor for the efficiency of the radiator, depending on the energy of the gamma rays. Siegbahn (*19*) gives such an efficiency curve for a copper radiator, based on experimental values, from isotopes emitting gamma rays of different energies with known relative intensities.

The method described above has proved to be very useful for investigating gamma-ray energies and intensities, without being a precision tool. By using the *photoelectric process* instead of the Compton effect, the gamma-ray energies (of not too high energetic gamma rays) can be determined with the same high accuracy obtained by measurements of internal

conversion electrons. Both photoelectric effects give well-defined lines; the gamma ray converts into an electron in the atomic shell of either the disintegrated nucleus (internal conversion) or a nucleus of the absorber foil (external photoelectric effect).

Since the efficiency for the production of photoelectrons increases with increasing atomic number of the absorber, thin *lead* foils are mostly used for measurements of photoelectron lines. Figure 9 shows secondary electrons expelled by the Na^{24} gamma rays from a copper radiator covered with a 0.02-mm lead foil (*9*). Experimental values have been corrected here for constant sensitivity of the spectrometer. Distribution of the Compton electrons is essentially the same as from the copper radiator without the lead foil. But in addition to the Compton electrons, two well-marked photoelectron lines are visible in Fig. 9. The energy of the gamma rays is obtained from the energy of the photoelectrons by adding the binding energy of the *K*-shell electrons in lead, which is 88 kev.

For *high-energy* gamma rays, it is often difficult to distinguish between the contribution of the photoelectric process and the Compton effect. First, even in lead the efficiency of the production of photoelectrons by high-energy gamma rays is very small. Secondly the energy difference between the photoelectrons and maximum energy of the Compton electrons decreases with increasing gamma-ray energy. Therefore, in some cases the gamma-ray energy can be determined more accurately by using Compton effect alone.

BIBLIOGRAPHY

1. F. Kurie, J. Richardson, H. Paxton, *Phys. Rev.* **49**, 368 (1936)
2. K. Siegbahn, E. Bohr., *Arkiv Mat. Astron. Fysik* **30B**, No. 3 (1944)
3. C. S. Cook, L. M. Langer, H. C. Price, M. B. Sampson, *Phys. Rev.* **74**, 502 (1948)
4. R. D. Albert C. S. Wu, *Phys. Rev.* **74**, 847 (1948)
5. C. S. Cook, L. M. Langer, H. C. Price, *Phys. Rev.* **74**, 548 (1948)
6. C. S. Cook, L. M. Langer, *Phys. Rev.* **74**, 227 (1948)
7. C. S. Cook, L. M. Langer, *Phys. Rev.* **73**, 601 (1948)
8. J. L. Lawson, J. M. Cork, *Phys. Rev.* **57**, 982 (1940)
9. K. Siegbahn, *Phys. Rev.* **70**, 127 (1946)
10. K. Siegbahn, *Arkiv Mat. Astron. Fysik* **30A**, No. 20 (1944)
11. J. L. Lawson, *Phys. Rev.* **56**, 131 (1939)
12. A. Flammersfeld, *Z. Physik* **112**, 727 (1939)
13. G. J. Neary, *Proc. Roy. Soc. London* **175**, 71 (1940)
14. L. D. Marinelli R. F. Brinckerhoff, G. J. Hine, *Revs. Mod. Phys.* **19**, 25 (1947)
15. E. J. Konopinski, *Revs. Mod. Phys.* **15**, 209 (1943)
16. O. Huber, H. Medicus, P. Preiswerk, R. Steffen, *Helv. Phys. Acta* **20**, 495 (1947)
17. R. G. Fluharty, NUCLEONICS **2**, No. 5, 28 (1948); **3**, No. 1, 46 (1948)
18. D. J. Tendam, H. L. Bradt, *Phys. Rev.* **72**, 1118 (1947)
19. K. Siegbahn, *Phil. Mag.* **37**, 162 (1946)

WHAT CAN THE SCIENTIST DO (in the field of human affairs)? Each must act according to his judgment, as he would in his own field, listening to all sides, attempting to evaluate and criticize such evidence as is presented, opposing authoritarian dogma as he would in science. He must be humble, recognizing the limitations of his own knowledge and that of others. He must be restrained and infinitely patient. He must think imaginatively but not emotionally. He must be willing to alter his ideas to meet changing conditions. All these processes are part of his training and have proved themselves as powerful tools.

—*H. D. Smyth*, American Scientist, p. 500, Oct., 1947

COUNTING RATE METERS versus SCALERS

Comparison of the advantages and disadvantages of two general types of instruments widely used to determine counting rates of pulses produced by radiation detectors

By ARTHUR G. BOUSQUET

General Radio Company, Cambridge, Massachusetts

NUMEROUS MEANS of detecting radioactivity are now in use—Geiger tube, ionization chamber, scintillation counter, etc. Whatever the method the result is the same: electrical pulses are ultimately produced after the radiation impinges upon the particular detector employed.

It is the function of the accessory equipment to translate the electrical impulses into useful data, to indicate the rate at which the electrical impulses occur, with the counting rate usually being expressed in terms of counts per minute.

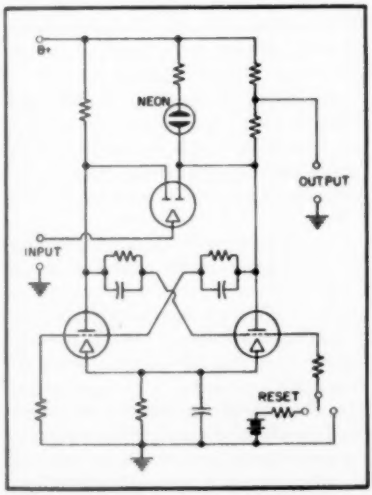

FIG. 1. Higinbotham scale-of-two circuit

The simplest counting-rate indicator is a loudspeaker, or a headphone, coupled to the Geiger tube through an amplifier. Such an aural system is quite useful for conveying an approximate idea of the counting rate. The accuracy obtainable with such a simple arrangement depends almost entirely on the "calibration" of the hearer's ear.

Various schemes have been devised to provide a more reliable means for determining the counting rate. The two most important methods are the counting-rate meter and the scaling circuit system. Both have many advantages. As so often happens, neither method supplies the ideal solution for all applications.

Scaling Circuits

The simplest scaling circuit is the scale-of-2 trigger circuit (*1*). A typical basic design is the Higinbotham (*2*) scaling circuit shown in Fig. 1. The scaler circuit arrangement allows two stable operating conditions. For every second pulse at the input terminals, the scale-of-2 delivers a single pulse at its output. Several scale-of-2 circuits in tandem provide net scaling factors of 4–8–16–32–64, etc. Other designs, utilizing "ring scalers" (*3*) or modified scale-of-16 scalers (*4*) yield decimal scaling ratios (10–100–1000). Whatever the method used, the purpose is to provide an impulse counting method which will not jam or skip counts at high counting rates.

The scaling-circuit system is usually preceded by a pulse-shaping circuit and is followed by an amplifier to drive the mechanical count-registering device.

A complete scaling-circuit system consists either of:

a. the pulse-counting device and a time-measuring device, or

b. a circuit which counts the pulses over a predetermined period of time, or

c. an electronically controlled method for measuring the time required to count a predetermined number of pulses (*5*).

A well-designed scaling system is capable of yielding high accuracy. The random nature of disintegrations, however, introduces an apparent error. If the counting rate of a radioactive sample is measured several consecutive times over equal periods of time, the several results will not agree. They cannot agree because the rate really is different over different counting periods. For a given rate, the longer the counting periods are, the less will be the discrepancies in any intercomparison. The probable magnitude of the discrepancies between the several measurements can be determined from the number of pulses counted during any one of the measurements. This probability has been expressed variously as the "average deviation," the "standard deviation" or the "probable error" (*6*). The average deviation is 1.183 times the probable error, and the standard deviation is 1.483 times the probable error. Any one of the three expressions can serve equally well as an index of the precision of any one measurement. The percent probable error in a measurement of the counting rate N of radioactive disintegration by the scaling method is

$$\% P.E. = \frac{67.45}{\sqrt{NT}} \qquad (1)$$

where T is the counting time. The dashed curve of Fig. 9 is a plot of the counting time required to obtain a given probable error at various counting rates with a scaling circuit.

The quantitative significance of the term "percent probable error" is as follows: if the counting rate is measured several times, each time over equal time periods, half of the measurements will yield results which agree to within the calculated probable error, and half of the measurements will yield results which are in excess of the calculated probable error.

Sources of Error

As with all equipment of this nature, there are more tangible errors that must be corrected, minimized, or at least recognized. Sources of error include high resolving time as evidenced by the inability of the equipment to respond to pulses at high rates. The resolving time of the Geiger tube is usually much greater than the resolving time of the rest of the equipment.

A source of error which the recording rate meter would show up immediately is an inadvertent shift in the geometry or positioning of the radioactive sample with respect to the counter tube.

Similarly, a change in the Geiger tube characteristic is immediately evident on a recording. In spite of improvements in Geiger tube design, this type of error must always be guarded against (*7*).

A serious disadvantage of the scaling-circuit system is the existence of the "blind spot" during the counting period. The apparent counting rate may change because of reasons outlined above, but the equipment cannot be aware of the change. The simultaneous use of an aural monitor is of some help to indicate abrupt and large shifts in apparent rate, but of course the aural monitor cannot give an adequate signal when the changes are of the order of 2 or 5%.

The Rate Meter

The recording type of counting-rate meter has a great advantage over the scaling method in that it has no blind spot. If the apparent rate deviates from the true rate, the recording will show it up.

Similarly, of course, if, by the very nature of the experiment, the short-term average rate varies with time, the scaling circuit is not well adapted to measure the change in rate, but the counting-rate meter method can be used advantageously. Examples include medical applications where the tracer technique requires a method that is both monitoring and quantitative. Oil-well survey methods, spectrometer techniques, Geiger counter development, health monitoring, thickness measurements, most industrial nuclear applications—in short, any nuclear measurement where the rate is liable to change should be made by the rate-meter method.

The major disadvantage of the rate meter is its accuracy limitation. For absolute measurements, its accuracy cannot be any greater than the full-scale accuracy of its indicating meter or of its recorder. As a consequence, the absolute accuracy at best is about 1 or 2% of full scale, and the precision of comparison to a radioactive sample of approximately equal activity is limited to about 0.5% of full scale.

In spite of this limitation, the counting-rate meter has a wide field of application, because it is not restricted to measuring unvarying rates.

The counting-rate meter (*8, 9, 10*) is essentially a specialized frequency meter. It is specialized because the pulses applied to its input terminals arrive in a random fashion, and the pulse rate must somehow be averaged to indicate the rate in a useful manner on the panel meter or the recorder. It is specialized too because of the accessory circuits which adapt it to its peculiar application. Thus, before the pulses from the Geiger counter tube are applied to the frequency meter they must first be modified by a pulse-shaping circuit to obtain pulses that are all identical in shape and magnitude.

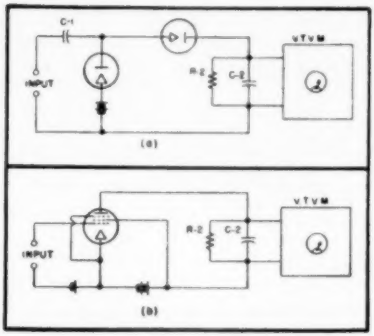

FIG. 2. Two forms of frequency-meter

Two typical frequency meter circuits are shown schematically in Fig. 2. In the method of Fig. 2*a*, an incoming positive pulse charges *C*-1 through one of the diodes. The capacitor then discharges through the other diode into the tank circuit (*R*-2, *C*-2). A vacuum-tube voltmeter across the tank circuit is calibrated in terms of the average counting rate.

In the method of Fig. 2*b*, the tube is biased beyond cutoff. An incoming positive pulse at the grid of the tube causes a pulse of plate current to flow through the plate resistor *R*-2 of the tank circuit. The resultant voltage built up across the tank circuit is a function of the pulse rate. A vacuum-tube voltmeter across the tank circuit is calibrated in terms of the average rate.

In both methods, most of the averaging of the random rate is accomplished by introducing damping in a tank circuit (*R*-2, *C*-2). If no damping is introduced, the result is as shown on the erratic portion of the chart recording of Fig. 3*b*. The stylus of the re-

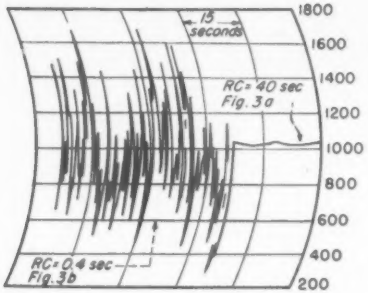

FIG. 3. Effect of *RC* time constant on fluctuations

corder responds to each individual pulse. When *C*-2 has been increased to provide proper damping, the result is as shown at the smooth-line end of the chart in Fig. 3*a*. To show these data to better advantage, the chart was operated at the high speed of three inches per minute.

A functional wiring diagram of the type 1500-A counting-rate meter is given in Fig. 4 and its mode of operation is as follows:

The pulses from the probe or from the external pulse generator are applied to the first amplifier which operates at zero bias; the input pulse must be of negative polarity. The amplifier is used to make sure that the equipment will respond to peak pulses as small as one volt. The time constants of the amplifier are selected to insure that the resultant pulse, which it applies to the pulse-shaping circuit, is sharp and will not cause the pulse shaper to produce spurious pulses.

The pulse-shaping circuit is of the "single shot" relaxation type. Regeneration allows it to generate its own single pulse each time a positive pulse is applied to the grid of its first tube. The single pulse it generates depends for its amplitude and general shape on its own circuit constants and in no way on the general shape of the applied pulse. As a consequence, it delivers to the frequency-metering circuits a series of pulses which depend on the Geiger counter pulses for their number and time distribution only. The critical components of the pulse-shaping circuit are the coupling capacitors (*C*-8, *C*-9) and the grid resistor, *R*-11, of the output tube.

The present design of the frequency-metering portion of the type 1500-A meter includes a significant improvement in so far as stability is concerned. Originally, the various ranges were obtained by changing the value of the

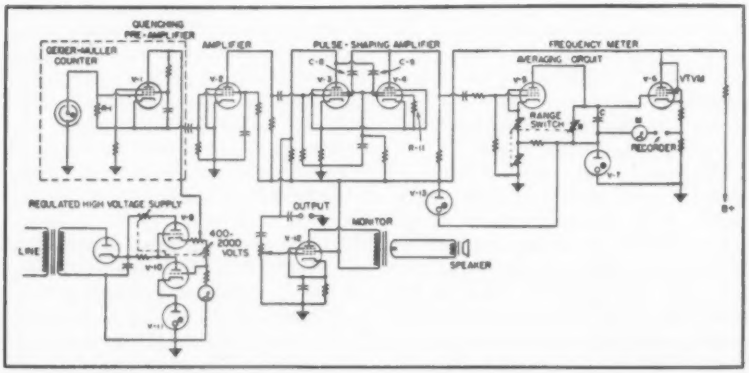

FIG. 4. Functional diagram of type 1500-A counting-rate meter

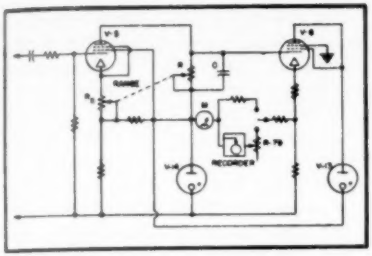

FIG. 5. Improved frequency meter and vacuum-tube voltmeter

resistance in the tank circuit and by changing the screen-grid voltage. As the line voltage was varied over a 20% range, on some ranges the indicated output changed as much as 9%. In the present design (Fig. 5) the screen-grid voltage is maintained at a constant value, and the ranges are selected by changing the value of the resistance in the tank circuit as before and by introducing selected amounts of degeneration, R_D, in the cathode circuit. As a result, the change in calibration is nil for most ranges and is about ¼% for the most sensitive (200 cpm) range, when the line voltage is changed over a 20% range.

The resistance values and the time constants chosen for the tank circuit are shown in the table below:

Range	Tank Circuit	
Counts per minute	*Resistance (megohms)*	*Time constant (minutes)*
200	30	1
600	30	1
2,000	20	⅔
6,000	20	⅔
20,000	10	⅓

Capacitor C is wound with a polystyrene dielectric to assure a low dielectric absorption; its capacitance is 2 μf for all ranges.

The RC tank circuit is at high d-c

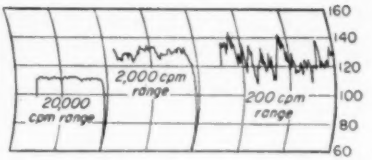

FIG. 6. Examples of recorder tracings

potential above ground. Dr. W. N. Tuttle devised an interesting method (*11*) for measuring the d-c potential appearing across the tank circuit in spite of its high constant potential. In Fig. 5, note that regulator tube V-14 supplies both the plate tank circuit and bucking-zero circuit of the vacuum-tube voltmeter. Since the vacuum-tube voltmeter is of the fully degenerated type, any fluctuations in the regulator-tube voltage are degenerated down to a negligible value, and the vacuum-tube voltmeter is highly stable and linear. A 5-ma pen-and-ink recorder may be plugged directly in series with the meter; the instrument resistance of the recorder may have any value within the range of the 700-ohm compensating rheostat (R-79). If a 1-ma recorder is used, it may be shunted down to operate as a 5-ma device. Though the shunt will overdamp the recorder, this will cause no trouble because the circuit is already damped to from 20 to 60 seconds by the RC tank circuit, so a parallel damping of 4 or 5 seconds in the recorder will have no noticeable effect on the results.

Examples of recordings at various counting rates with a 5-ma Esterline Angus graphic recorder are shown on the charts of Fig. 6. The average counting rate is determined by estimating the average stylus position. To obtain a high precision in estimating the correct average rate from the chart, a line may be drawn through the recorded data in such a manner that the area enclosed above the line equals the

area enclosed below the line. As will be seen later, the probable error is reduced by increasing the recording time. At the high counting rates, the fluctuations about the average rate are quite small. The relatively large fluctuations at the low rates could be reduced by increasing the capacitance of the tank circuit, but the equilibrium time, as discussed in a following section, would be increased.

The equalized pulses are also coupled to an aural monitor and to a pair of output terminals. The aural monitor consists of a power amplifier driving a small loudspeaker. The controllable volume from the speaker is sufficient for class-room demonstration purposes and for use as an alarm in monitoring service. The output terminals may be used to drive a scaling circuit if extreme accuracy in counting is desired. The equipment includes a carefully regulated high-voltage Geiger-counter anode supply, variable from 400 to 2,000 volts.

A major feature is pointed out here, since it could advantageously be incorporated in other designs. The output circuit of the regulated supply includes a chain of 200-kilohm wire-wound resistors in series with a 200-kilohm wire-wound voltage-divider; a current of one milliampere flows in the series network. The total voltage output is adjusted by shorting out an appropriate number of fixed resistors and switching in compensating resistors ahead of the series regulator tube, thus providing 200-volt increments, so that varying the voltage-divider provides a continuous adjustment of 200 volts between steps. The panel milliammeter may be switched in series with the chain of resistors. The voltage is always correctly indicated by the panel control settings as long as the meter indicates exactly one milliampere. Thus the accuracy of the system can be, for example, 2% of the *actual* value over the entire 400 to 2,000-volt range rather than 2% of *full scale* as is the usual accuracy when a single-range voltmeter is connected to the output of the power supply.

The calibration of the counting-rate meter can be checked at any time by setting a switch which connects pulses of power line frequency to the input. Any discrepancy can be quickly corrected by readjusting the vacuum-tube voltmeter sensitivity control.

Statistical Effects

When a calibration check is made, the absence of fluctuations is immediately evident, whereas during normal operation, the randomness of the radioactive disintegration causes the meter reading to fluctuate about the average value. The amount of fluctuation is a function of the counting rate and of the damping introduced in the tank circuit.

Because of the random nature of radioactive disintegration, the results obtained with scaling circuits and with rate meters require a statistical interpretation. Since the amount of the indicated fluctuation can be controlled by introducing damping in the rate meter, special statistical methods are used for the rate meter. The derivation of these methods has been thoroughly covered elsewhere (*10–12*). The results are reviewed here for the sake of completeness.

If, after the equipment has been operating long enough to have reached equilibrium conditions, a single meter-reading is taken, it may be the true average indication or it may just as likely be any indication which lies within the fluctuation range. Since the meter readings are due to a series of random events, the Poisson law of statistical distribution applies; when the average counting rate is 30 per minute or more, the normal law of statistics can also be used. As a

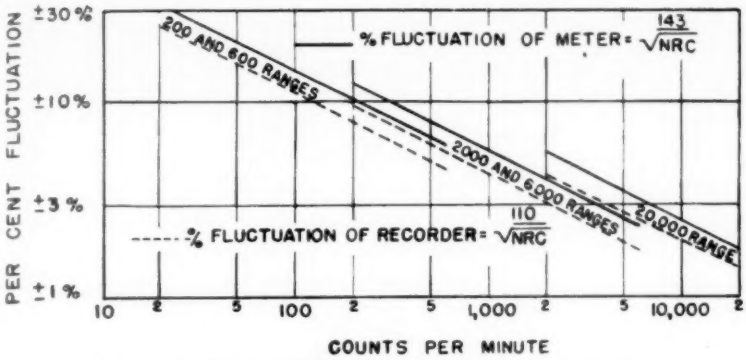

FIG. 7. Percent fluctuations due to random nature of disintegrations

result, it may be predicted that the maximum amount by which the meter reading can fluctuate about the average value is

$$\% \text{ fluctuation} = \frac{143.1}{\sqrt{NRC}}, \qquad (2)$$

where N is the average counting rate in counts per minute, and RC is the time constant of the tank circuit in minutes. Since a knowledge of the expected fluctuations can be useful in spotting spurious results due to multiple discharges in the Geiger counter or to any other cause, a plot of percent fluctuation as it applies to this particular meter is given in Fig. 7. Since the drag of the stylus of a pen-and-ink recorder will reduce the amount of fluctuation by about 78% (*10*), the data of Fig. 7 have been plotted to show the expected fluctuations for both meter reading and a pen-and-ink recording.

In accordance with the normal law of distribution the percent probable error of a *single* observation is

$$\% P.E'. = \frac{67.45}{\sqrt{2NRC}}. \qquad (3)$$

The data of Eq. 3 are shown in Fig. 8 where the RC time constants have the values tabulated on page 71. A comparison of the equation with Eq. 1 emphasizes the memory feature of the RC tank circuit in the rate meter and

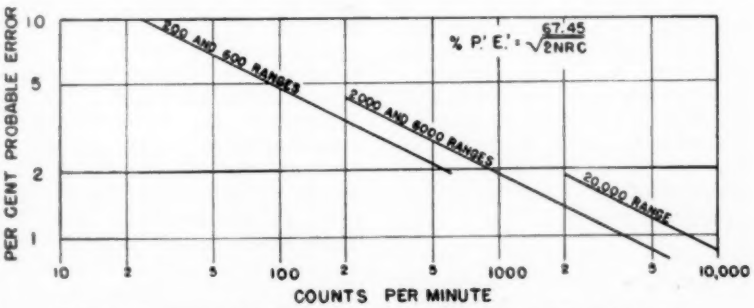

FIG. 8. Percent probable error of a single observation of the rate meter

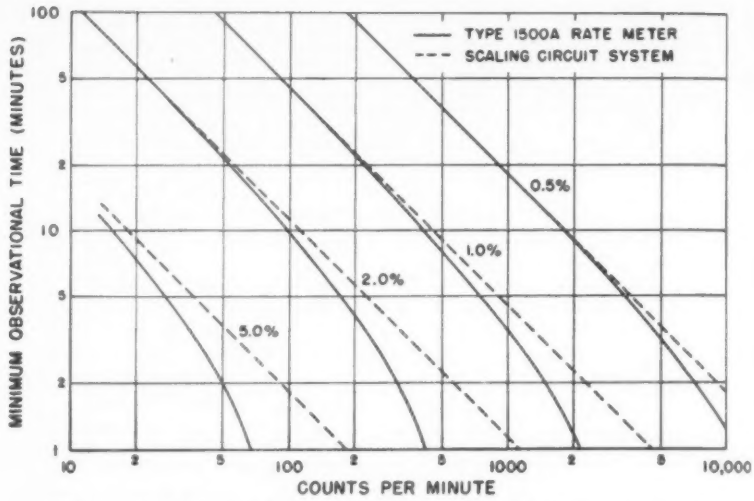

FIG. 9. Minimum counting time to obtain percent probable error indicated

the significant distinction between the scaler method and the rate meter method. After the charge in the tank circuit of the rate meter has reached equilibrium, the rate meter indicates the counting rate at a glance and within a reasonably small probable error. The probable error may of course be reduced either by observing the meter for a given time or by obtaining a pen-and-ink recording and determining with high precision the average rate by drawing a straight line through the recording so that the enclosed area above the line equals the enclosed area below the line. The recording or observational time enters into a determination of this new probable error. The percent probable error in the average rate N as obtained from data accumulated with a rate meter over a period of T minutes is

$$\% P.E. = \frac{\sqrt{1 + \frac{2T}{RC}}}{1 + \frac{T}{RC}} \frac{47.7}{\sqrt{NRC}} \quad (4)$$

where, again, RC is the time constant of the tank circuit.

The results obtained from Eq. 4 are presented graphically in Fig. 9 for the RC time constants and the counting-rate ranges that are used in the type 1500-A meter.

As shown by Eq. 1, the probable error of the results obtained with a scaling circuit is a function of the average pulse rate and the time required to gather the data. For comparison purposes, this result is plotted as a dashed line in Fig. 9. It is interesting to note that the recording time required of a counting-rate meter is always the same as or less than the counting time required of a scaling circuit, if one considers only the two equations, 1 and 2. Obviously, the story is not complete because no mathematical juggling can reduce the time required to determine within a given probable error an average rate from random information. The reason for the discrepancy is that the derivation of Eq. 4 assumes that

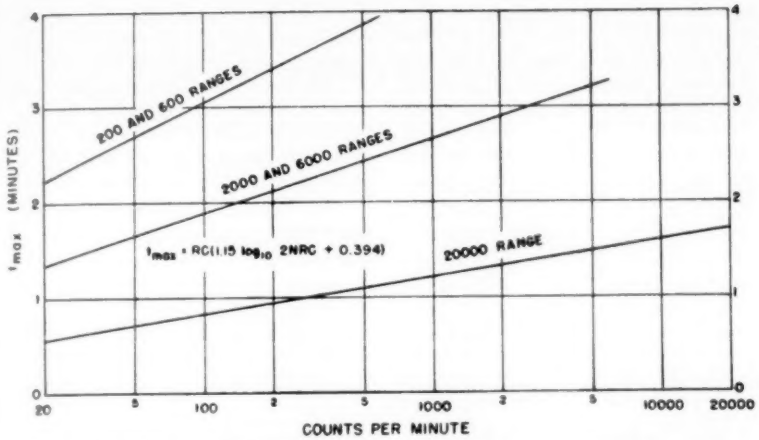

FIG. 10. Maximum equilibrium time. Can be reduced to a few seconds by technique described in text

equilibrium conditions exist, that is, that the capacitor of the tank circuit in the counting-rate meter has previously been charged to the value which corresponds to the true average counting rate. In all fairness, the charging time must be included in any comparison. This period of time is referred to as the equilibrium time, since it is the time required for the meter or recorder to reach a new equilibrium value whenever the counting rate has been changed.

Equilibrium Time

The equilibrium time will depend on the time constant of the tank circuit and on the change in average counting rate. It will also depend to a large extent on the technique followed to obtain the new equilibrium value.

The equilibrium time will usually be greatest when no special technique precautions are taken and when the change is from zero rate to a given rate, N. Under these conditions, the equilibrium time is

$$t_{max} = RC(1.15 \log_{10} 2NRC + 0.394) \quad (5)$$

Data showing this maximum equilibrium time are plotted in Fig. 10.

When a radioactive sample is changed, the equilibrium time may easily be reduced to a matter of seconds. The technique consists in watching the direction of the needle on the panel meter or the recorder and quickly charging or discharging the capacitor of the tank circuit approximately the correct amount by manipulating the range switch, the calibration switch or a shunt push-button switch.

It is evident from the probable error and equilibrium time equations that the one can be improved by changing the RC time constant, but always at the expense of the other. The time constant values selected for the type 1500-A meter represent what seemed to be the best compromise and in actual field practice have proved to be generally satisfactory. For special applications, however, different time constant values may be chosen. As an example, if the rate meter is being used to detect the passage of relatively fast-moving radioactive samples, the capacitance of the tank circuit may be

reduced to obtain rapid response. The calibration will not be affected, and the equilibrium time will be reduced; but the probable error and the fluctuations will be increased.

Applications where a change in rate must be detected and measured emphasize the distinction between the two major counting methods.

The scaling circuit performs but one function: it counts pulses, and it counts them well; the counting rate may be determined from the results.

The rate meter indicates the rate directly at moderate accuracy; it also shows up variations in rate, and when used with a recorder it provides a permanent record. As a consequence, the rate meter has a broader field of application.

BIBLIOGRAPHY

1. Don DeVault, *Rev. Sci. Instr.* **12,** 83 (1941). The references of this paper constitute a valuable historical bibliography of scaling circuits.
2. W. A. Higinbotham, James Gallagher, Matthew Sands, *Rev. Sci. Instr.* **18,** 706 (1947)
3. Leo Seren, *Rev. Sci. Instr.* **18,** 654 (1947); V. H. Regener, *Rev. Sci. Instr.* **17,** 375 (1946)
4. J. T. Potter, *Electronics* **17,** No. 6, 110 (1944)
5. Raymond P. Ghelardi, Cyril H. Brown, NUCLEONICS **1,** 50 (1947)
6. H. M. Goodwin, "Elements of the Precision of Measurements and Graphical Methods," (McGraw-Hill Book Co., New York, 1913); also H. Margenau and G. M. Murphy, "The Mathematics of Physics and Chemistry," (D. Van Nostrand Co., New York, 1943)
7. Sanborn C. Brown, NUCLEONICS **3,** No. 2, 50 (1948)
8. N. S. Gingrich, Robley D. Evans, Harold E. Edgerton, *Rev. Sci. Instr.* **7,** 450 (1936)
9. Robley D. Evans, Robert L. Adler, *Rev. Sci. Instr.* **10,** 332 (1939)
10. A. F. Kip, A. G. Bousquet, R. D. Evans and W. N. Tuttle, *Rev. Sci. Instr.* **17,** 323 (1946)
11. W. N. Tuttle, U. S. Patent 2,374,248, April 24, 1945
12. L. I. Schiff and Robley D. Evans, *Rev. Sci. Instr.* **7,** 456 (1936)

BOOKS

ADVANCES IN ELECTRONICS, edited by L. Marton (National Bureau of Standards), Academic Press, New York, 1948, 475 p., $9.00.

The first of what promises to be an annual review of certain phases of physical electronics (charged particle phenomena) and engineering electronics (applications of devices employing the charged particles).

Of nine divisions, each edited by an expert, two are of particular interest to readers of NUCLEONICS. These are the section on *Mass Spectroscopy* by Mark G. Inghram, Argonne National Laboratory, and the section covering *Particle Accelerators* by M. Stanley Livingston, Massachusetts Institute of Technology.

The other sections are devoted to *Oxide Coated Cathodes, Secondary Electron Emission, Television Pickup Tubes* and the *Problems of Vision, Deflection of Beams of Charged Particles, Ionospheric Research, Cosmic Radio Noise, Propagation in the FM Broadcast Band,* and *Electronic Aids to Navigation.*

The book is well illustrated, printed in type easy to read, and is obviously a solid contribution to the literature. Any one wanting a survey of present knowledge in the several fields will find the reviews most readable and instructive.

NUCLEONIC EVENTS

AEC INDUSTRIAL ADVISORY GROUP MAKES ITS REPORT

After a year combing through AEC policies and operations, the Commission's Industrial Advisory Group, made up of eight industrial executives, made its report on December 15. The AEC released the report on December 27 and held a press conference on the report on December 29, 1948.

According to this report greatly expanded participation by industry in the nation's atomic energy program is necessary not only to aid the Commission in solving its problems but to assure a high rate of technological advance in nuclear energy application. At the moment the only broad field open to industry generally is in the use of radioactive isotopes, but, the Group holds, there are other opportunities which await proper cultivation.

To secure such participation by industry generally, more knowledge must be available to technologists and executives of industry. At the present time "industry has no way of determining whether important opportunities in fact exist. . . . If industry is to help in atomic energy and benefit from it, industrialists must first be put in a position to find out enough about the subject."

To implement such participation by industry, the Group recommended that much more technical information be made available for publication in the technical press, that there must be opportunity for industrial personnel to have "broad personal contact with various phases of the enterprise," that a program be developed for bringing industry executives—many of whom commenced their careers as engineers or scientists—in close touch with developments, and that the methods by which the Commission makes contracts and the details of the patent policy be made clear to industry generally. The formation of industrial advisory committees was felt by the group to have important advantages in the direction of getting more active sharing of the atomic energy field by government and industry.

Throughout the report the necessity for secrecy was cited as a most important deterrent, but it was pointed out that the Group received the impression during its survey that a vast amount of non-secret information existed which, if dug out and made available, would help materially to push our research and speed the application of nuclear knowledge. On this score the committee report states:

"During our survey of the project, we observed, for example, interesting and valuable new metallurgical techniques, new chemical treatments to protect against corrosion, new plastics, instrumentation, and useful technical knowledge of many kinds. This information, although developed in research on atomic energy, is only incidentally related to atomic energy. It is still largely unknown except to those industrial organizations which actively participated in the research through which it was discovered.

"We have the impression that for reasons which are not at all clear, much of this knowledge is still buried in the files and activities of the Commission. We think the Commission should make a special effort to publish it—to the

extent that military security will permit —at the earliest possible date. The cost of secrecy is high. This is one of the many instances in which we have thought its value doubtful."

The report indicated that the Group felt that certain representative types of American industry stood to gain much from the development of atomic energy, notably the chemical, petroleum, power, heat transfer equipment, metallurgical and instrument industries. Highly technical information was only part of the AEC material which should be freed for industry use, the report stated.

"Scientific information appears to be made available by the Commission in a manner adequate to keep interested scientists informed. But the availability of additional material—in a form useful to industry—is indispensable to getting industrial participation in atomic energy.

Information Needed by Industry

"Industry requires information along two quite distinct lines. First, it needs much additional technical and semi-technical knowledge about the whole field of atomic energy. Such information will help in clarifying and identifying the opportunities which atomic energy potentially affords to industry.

"There is a second class of knowledge which must be made available to complement the first: information about the structure of the Commission, its administrative policies and its procedures. The better industry is informed about these matters, the better it will be able to deal with the Commission with assurance and understanding. The general atmosphere of secrecy which surrounds atomic energy has enveloped this kind of information—even though most of it is non-secret—almost as completely as technical matters."

The Group felt that "a simple but comprehensive report on the Commission's procedure in negotiating, awarding, and administering its numerous types of contracts would also be useful. At present there is considerable fragmentary information on this subject but no well-organized comprehensive report that gives a clear picture of Commission policies and procedure. Education in industry in these matters should help to give effect to the Commission's objective of interesting additional companies in taking part in Commission work. Another question on which industrialists need information is the Commission's labor policy. Unless potential contractors are satisfied that the Commission's policy can be accommodated to the policy which the contractor follows in his labor relations generally, there are sure to be difficulties and a hesitancy to engage in work for the Commission. An informational report by the Commission or under Commission sponsorship could go far to eliminate the misapprehension that now exists in industry on this subject."

Increasing Direct Contacts with Industry

As an indication of the techniques employed in the AEC's work, the Group cited an enlightening experience. "One of our number is at present in charge of an important specific industrial research and development project. Among the knotty unanswered questions in his project is one relating to the type of coolant to be used. During our survey, he observed, first hand, a unique process that was being worked on in one of the Commission's laboratories to solve a problem which also related to coolants. The Commission's work immediately suggested to him a new avenue of approach to his own special research problem. He remarked at the time that even had he read about the Commission's investigation in the technical journals the chances are that he would have missed the connection with his own

investigations. Direct personal contact with the work in the atomic energy laboratory gave him the concrete experience necessary to see a relationship that he would otherwise have missed."

Even if such knowledge is revealed by ordinary methods, *i.e.*, by publication, the report and the experiences noted above emphasize the fact that personal contact is still of great importance. Lectures for technologists and for technically trained executives were suggested.

Other recommendations were for a further strengthening, improvement and refinement of the AEC contract system; for the disparate abilities of the physicist and the engineer, for example, to be better employed and their respective responsibilities in the overall contract picture more clearly defined; and for certain changes in the actual AEC organization to be carried out.

In summary the report cites the following pre-conditions to increased industrial participation in the AEC programs: greater knowledge of the subject; development of a broad program for clearance of engineers, technologists and executives in industry; establishment of a General Advisory Committee; acquaintance of industry with AEC contract and patent systems; further reorganization of the Commission's internal setup.

James W. Parker, President and General Manager, Detroit Edison Co., was chairman of the Industrial Advisory Group, the other members being Isaac Harter, Sr., Chairman of Board, Babcock and Wilcox Tube Company; Gabriel O. Wessenauer, Manager of Power, Tennessee Valley Authority; Robert E. Wilson, Chairman of Board, Standard Oil Company of Indiana; Bruce K. Brown, Vice-President, Standard Oil Company of Indiana; Gustav Egloff, Director of Research, Universal Oil Products Company; Paul D. Foote, Executive Vice-President, Gulf Research and Development Company; and Jerome C. Hunsaker, Chairman, National Advisory Committee for Aeronautics.

WESTINGHOUSE TO BUILD REACTOR FOR NAVAL SHIPS

Construction of a nuclear reactor to be used in the propulsion of ships is to be undertaken by the Westinghouse Electric Corporation, according to an announcement by the Chicago Operations Office of the Atomic Energy Commission.

A. Tammaro, manager of AEC operations in Chicago, announced that work under the contract will be carried on in cooperation with the Argonne National Laboratory, major center of the commission's reactor development program. The objective of the developmental project is to meet requirements provided by the Navy Department Bureau of Ships for the propulsion of naval vessels.

The development of such specialized nuclear reactors was among the functions assigned to the Argonne National Laboratory in January, 1948, when this laboratory was made the major center of the AEC reactor development program. Under the terms of this allocation, the responsibility for the design, development and engineering of the new reactor rests with the Argonne Laboratory. Westinghouse has been delegated responsibility for the detailed engineering, construction and operation of the reactor, and will undertake such research and development activity as may be assigned to it by the commission.

HAFSTAD APPOINTED HEAD OF AEC REACTOR DIVISION

Lawrence R. Hafstad, executive secretary of the Joint Research and Development Board of the National Military Establishment, has been ap-

pointed director of the Reactor Development Division of the Atomic Energy Commission.

Dr. Hafstad is the first director of this new division which was created in August, 1948, to carry out the program of designing and developing nuclear reactors for the practical application of atomic energy for power, for propulsion of ships and aircraft, for production of isotopes and for research on reactors themselves. About $120,000,000 is in the President's budget for the coming fiscal year for the reactor development program.

Dr. Hafstad, with two colleagues, Richard Roberts and Merle Tuve, demonstrated uranium fission for the first time in the United States in 1939 in Washington following reports from abroad that German scientists had split atomic nuclei.

Dr. Hafstad has been on leave of absence from Johns Hopkins University where he holds the position of director of research of the Applied Physics Laboratory at Silver Spring, Md. It was in this laboratory that he helped perform much of the work leading to development of the proximity fuse and also took part in research and development work on guided missiles.

DU PONT TO STUDY CHEMISTRY OF PLUTONIUM

A survey of the total problem of research and engineering involved in improving the chemical processes used in the production of plutonium will be undertaken by E. I. duPont de Nemours and Company of Wilmington, Del., according to an announcement by the Atomic Energy Commission. Since it assumed direction of the atomic energy program in January, 1947, the AEC has had studies of the plutonium chemistry program made by several different institutions and industrial concerns.

The duPont Company was the builder and first operator of the Hanford Works at Richland, Wash., major center of U. S. production of plutonium. The General Electric Company succeeded duPont at Hanford when the latter withdrew at its own request at the end of the war.

NEW U-235 PLANT TO BE BUILT AT OAK RIDGE

Plans for the construction of a $70,000,000 plant for the production of U-235 at Oak Ridge have been outlined by David E. Lilienthal, chairman of the Atomic Energy Commission. These plans are in addition to ones for the building up of Oak Ridge National Laboratory as a permanent installation. Approximately $20,000,000 will be used for this purpose. Already under construction are radioisotope processing facilities which will cost $1,500,000.

The construction of the U-235 plant will begin in about five months. The job will take about two years and will employ about 3,500 construction workers.

WESTINGHOUSE NAMES HEADS OF ATOMIC POWER GROUP

William E. Shoupp has been named director of research and Robert A. Bowman has been appointed manager of engineering of the Westinghouse Electric Corporation's atomic power division, according to an announcement by Charles H. Weaver, division manager. Dr. Shoupp, a nuclear physicist, had previously been manager of electronics and nuclear physics research at the Westinghouse Research Laboratories. Mr. Bowman who is said to be especially familiar with heat transfer and ship propulsion problems, was previously manager of condenser engineering at the company's steam division in South Philadelphia, Pa.

Westinghouse was recently awarded a contract by the Atomic Energy Commission to construct and test an atomic power plant for the propulsion of naval

vessels. The nuclear reactor for this project will be engineered and built in the Pittsburgh area, but will be tested at a remote location.

NEW ROCHESTER CYCLOTRON OPERATES SUCCESSFULLY

Successful operation of the new 250-Mev cyclotron at the University of Rochester was announced last month. In the process of planning, construction and development for more than two and one-half years, the 130-inch machine is the first large post-war cyclotron to be put in operation and is at present second in size only to the 184-inch accelerator at the University of California.

Using protons on a carbon target, the machine is said to have already produced mesons.

The cyclotron project was initiated shortly after the war by Sidney W. Barnes, professor of physics, and Lee A. DuBridge. Its realization is said to have been due mainly to the active support and effective efforts of Dr. DuBridge in his last few weeks as chairman of the physics department at Rochester before leaving to become president of the California Institute of Technology in 1946. Dr. Barnes has been in charge of plans and development since its inception.

In accordance with original plans, the construction was divided into two buildings. One, housing the cyclotron, is located in a shallow gulley. The other, more than 100 feet away on higher ground and separated from the cyclotron building by an earth ramp, is the laboratory, which contains the control room from which the cyclotron is operated.

The group of physicists and engineers who have worked with Dr. Barnes on the project includes R. L. McCreary, S. N. Van Voorhis, J. B. Platt, A. L. Clar, and G. B. Collins, all of the university's physics faculty, T. Pearlman and R. Mortensen of its engineering staff, and W. Pierson, Berkeley, Calif., engineer.

CANADA TO AWARD 40 FELLOWSHIPS

Forty postdoctorate fellowships for research in pure chemistry and physics will be awarded by the National Research Council of Canada for 1949–50. The fellowships are for the NRC laboratories at Ottawa and for the Canadian Atomic Energy Project at Chalk River, Ontario.

Normally an applicant should possess a Ph.D. degree from a recognized university, but exceptions may be made in special cases. There are no restrictions as to the nationality of the applicant in the case of the Ottawa laboratories. Appointments at Chalk River are restricted to British subjects.

The awards are to be $2,820 per year, with a grant-in-aid of travelling expenses being made to persons coming from abroad. A similar grant will be made on termination of the fellowship if the holder is returning to his home abroad.

Applications, which should be received in Ottawa not later than March 1, should be made on a special form which may be secured from the secretary, Laboratories Awards Committe, National Research Council, Ottawa, Canada, or from the Chief Scientific Liaison Officer, National Research Council, Africa House, Kingsway, London, W. C. 2, England.

DU PONT ANNOUNCES RESEARCH FELLOWSHIPS

E. I. du Pont de Nemours and Co., Inc., has recently awarded 77 postgraduate and postdoctoral fellowships to 47 universities throughout the country for the 1949–50 academic year.

In continuing its 30-year-old plan to encourage graduate research in the fields of chemistry, physics, metallurgy, and

engineering, the company said it has authorized the expenditure of $226,800 for the 1949–50 awards.

This year's fellowship plan is little changed from that of 1948–49. Each postgraduate fellowship provides $1,200 for a single person or $1,800 for a married person, together with an award of $1,000 to the university. Each post-doctoral fellowship provides $3,000 for the recipient and is accompanied by a grant of $1,500 to the university. The selection of candidates for the fellowships and the choice of problems on which they are to work are, as in the past, left to the universities.

Of the post graduate fellowships, 45 are in chemistry, 4 in physics, 15 in chemical engineering, 5 in mechanical engineering, and 2 in metallurgy. The plan also provides for 6 post-doctoral fellowships in chemistry.

In addition, du Pont is instituting a program of grants-in-aid in the amount of $10,000 each to 10 universities for the 1949–50 academic year. They are intended for unrestricted use in the field of fundamental chemical research at the following universities: Cal. Tech., Cornell, Harvard, MIT, Ohio State, Princeton, Yale, Illinois, Minnesota, and Wisconsin.

The projects in which the grants will be employed are to be selected by the universities themselves, the only stipulation being that the research be free from any commercial implications at the time the work is initiated.

WEINBERG MADE OAK RIDGE ASSOCIATE DIRECTOR

Alvin M. Weinberg, formerly director of the Physics Division at Oak Ridge National Laboratory, has been appointed associate director of the laboratory in charge of research and development. A. H. Snell has succeeded Dr. Weinberg as director of the Physics Division.

NORWAY PRODUCING MATERIALS FOR PILE

Norwegian uranium and heavy water, sufficient to supply that country's first atomic pile, are now being mined and processed in Norway. A statement by Gunnar Randers (*Chemical Age*, Dec., 1948), research head of the Norwegian atomic project, says that uranium ore is now being mined at Evje in Setesdal, and is considered sufficient for Norway's preliminary experimental purposes.

Norsk Hydro, the Norwegian electrochemical firm whose facilities the Nazis seized for manufacture of heavy water during the past war, is cooperating with the government in this project, and sufficient quantities of the liquid are said to be assured. Norway's atomic center is now under construction at Kjeller, near Oslo.

WORLD POWER CONFERENCE TO DISCUSS ATOMIC ENERGY

It is expected that power from nuclear reactors will be one of the many subjects discussed at the fourth World Power Conference to be held in London in July, 1950.

A comprehensive survey of the progress made in the development of power will be composed from individual reports submitted by member countries, setting out their respective energy sources and the extent to which they, and the prime movers utilizing them, have been developed over the last quarter of a century. Papers will be presented on various processes for preparation and refining of solid, liquid and gaseous fuels to render them suitable as sources of power. The main interest will center, however, on the success attained in experiments with the hot-air engine, the potentialities of wind and tidal power, solar energy, terrestrial heat, thermal energy derived from the sea, in addition to the application of gas turbines, jet engines and atomic energy.

PRODUCTS and MATERIALS

CALCIUM TUNGSTATE CRYSTALS

Successful production of water-white single crystals of pure calcium tungstate in research quantities, has been announced by the **Linde Air Products Company,** unit of Union Carbide and Carbon Corporation, **30 E. 42 St., N. Y. 17, N. Y.** Among the applications indicated for this fluorescent material are its use in scintillation counters in the detection and measurement of radioactivity, and as screens in X-ray fluoroscopy.

Single crystals of pure calcium tungstate are at the present time being grown in rods, about ⅛ inch square section and up to 2 inches in length. Representative samples of these calcium tungstate crystals are colorless, and clarity varies from a transparent to a slightly cloudy crystal. Development work is being done on the growing of uniformly clear crystals and the production of other forms and sizes.

At the present time, Linde synthetic calcium tungstate is available in research quantities in rods about ⅛ inch in square section, in lengths of from ¼ inch to 2 inches in ¼ inch increments. Linde has facilities for the fabrication of special windows or mosaica from the rod presently available.

ISOTOPES AVAILABLE

Metal Hydrides, Inc., Beverly, Mass., is now synthesizing lithium deuteride and lithium aluminum deuteride. The deuterium gas used in this synthesis is approximately 99.8% H^2, and the isotopic purity of either compound is practically the same.

Abbott Laboratories, N. Chicago, Ill., has announced the availability of the following compounds: I^{131}-labeled diiodo fluorescein, Au^{199} in colloidal gold, Au^{198}-labeled gold sodium thiosulfate, S^{35}-labeled thiourea, P^{32} solution, and S^{35}-labeled pentothal.

Oak Ridge National Laboratory, Isotopes Division, has announced that the price of C^{14} has been changed from $50 to $36 per millicurie. This reduction in price was brought on by the fact that it was learned that the quantity of C^{14} which was previously being shipped as 1 mc contained more activity than it should. The amount of C^{14} now being shipped as 1 mc has been reduced 28%.

HEAVY ALLOY

General Electric Co., Ltd., Wembley, Middlesex, England, is now marketing an alloy of high density which is said to have a number of useful applications. It is known as Heavy Alloy and is composed of sintered tungsten with a trace of copper binder. The density is about 17 and the stopping power is about 1.5 times that of lead. The alloy is machineable, but it is recommended that fabrication be carried out by the manufacturer. It is available in standard-size blocks for approximately $4 per pound, or in special form for this price plus machining cost.—*From European Scientific Notes, Nov.* 15, 1948 (*Office of Naval Research, London Branch*)

DENSITOMETER

W. M. Welch Scientific Co., 1515 Sedgwick St., Chicago 10, Ill. The feature of the model 2150 Densichron densitometer and exposure meter is that it transforms light into a-c voltages within the phototube of the instrument by application

of an a-c magnetic field. The instrument provides density ranges of 0–1, 1–2, 2–3, and 3–4. The light-measuring ranges are 0.035, 0.05, 0.5 and 5 footcandles, with a maximum light sensitivity of 10 microlumens. The current consumption is 30 watts, with operation on 115 volt, 60 cycle a-c.

PHOTOGRAPHIC PLATES

Ward's Natural Science Establishment, Inc., 3000 Ridge Rd. E., Rochester 9, N. Y., has been appointed distributor for the special Eastman Kodak nuclear track emulsions. Shown below are the photographic plates which are available. Stripping film coated with NTB emulsion is also available. It is claimed to have the following special advantages for special autoradiographic problems: freedom from backscattering, emulsion staining, fogging and photographic developer damage; blood smear autoradiographs can be made; histological bodies above intense collection of grains can be identified, and grain counting for quantitation is permitted.

NEW COMPANY FORMED

Radioactive Products, Inc., 14 N. Huron St., Ypsilanti, Mich. This company has been formed in the Detroit area to design and manufacture instruments and equipment for the measurement and handling of radioactive materials. It also plans to establish facilities for purification, packaging and assay of radioisotopes and for the synthesis of tracer compounds. John R. Niles and Homer S. Myers, for-

Nuclear Track and Autoradiography Plates

Emulsion Type	*NTA*	*NTB*	*NTC*
Application	Alpha particles to 200 Mev Protons to 20 Mev Deuterons to 40 Mev	Autoradiography Alpha particles to 400 Mev Protons to 50 Mev Deuterons to 100 Mev Mesons to 5 Mev Electrons to 50 kev	Nuclear fission fragments of high ionizing power
Sensitivity to light, gamma and beta rays	Low	Moderate	Very low
Available emulsion thickness in microns	25, 50, 100, and 200	25 for autoradiography; 50, 100, and 200	25
Grain size in microns	0.2 to 0.4	0.2 to 0.3	0.1 to 0.4
% of weight of AgBr in dry emulsion	81	81	65
% of weight of gelatin	19	19	35
Density of emulsion	3.64 gm/cc	3.64 gm/cc	
Concentration of AgBr in emulsion	2.95 gm/cc	2.95 gm/cc	
Impregnated plates for bombardment and subsequent effect study	Li, Be, B	Li, Be, B	

merly with the Aeronautical Research Center, University of Michigan, are now director of engineering and director of sales, respectively.

G-M COUNTER

Electrotechnic Engineering Co., Lidcombe, New South Wales. A simplified Geiger-Müller counter is said to have been developed. The instrument is contained, complete with batteries, in a welded aluminum case, 11⅛ in. × 7½ in. × 8¾ in., and weighs 23½ pounds. For prospecting work a special attachment is provided which enables the tube to be carried close to the ground. It can also be lowered down boreholes and other inaccessible locations. The sensitivity of the tube contained in the case is reportedly such as to enable detection of ½ mc of radon at 20 ft. Higher counts can be read directly from a dial whereas an earphone is required for the lower counts.

DEMONSTRATOR

Tracerlab, Inc., 55 Oliver St., Boston 10, Mass. A radioactivity demonstrator has been developed for teaching the basic principles of radioactivity in high schools and colleges. Radiation is indicated by three different means: by loudspeaker, by a flashing neon light, and quantitatively with a counting-rate meter. Included with the demonstrator is a glass Geiger tube capable of detecting gamma and high-energy beta rays, and sources of beta and gamma activity.

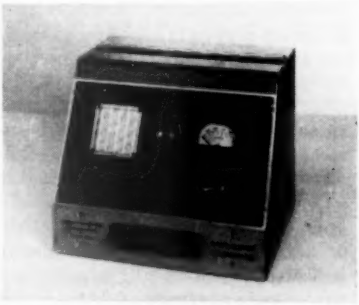

CHARGER-READER

Nuclear Instrument and Chemical Corp., 223 W. Erie St., Chicago, Ill. The model 2050 Charger-Reader has been designed for use in conjunction with pocket-type ionization chambers. The instrument charges the ion chamber to a known voltage, and measures the residual chamber charge after exposure to gamma or X-radiation. Operating on 110 volts a-c, the unit is claimed to have an accuracy of 2½% full scale.

NEUTRON COUNTERS

N. Wood Counter Laboratory, Box 76, Route 1, Chesterton, Ind. "Enriched" BF_3 neutron counters are available in diameters of 1 in., 1½ in. and 2 in., and varying lengths and pressures. Using 96% B^{10}, these counters are said to be four times as efficient as the unenriched counters. Long, flat plateaus are claimed.

TRACERLAB OPENS N. Y. OFFICE

Tracerlab, Inc., 55 Oliver St., Boston 10, Mass., has opened an office at 1775 Broadway, New York City, to serve

customers in Connecticut New York, New Jersey and Pennsylvania. In charge of the office is W. C. Nusbaum, New York sales manager of the company.

SURVEY METER

El-Tronics, Inc., 2647 N. Howard St., Philadelphia 33, Pa. The model SM-3 beta-gamma survey meter provides for direct reading on three full-scale ranges of 0.2, 2.0 and 20 mr per hour. The

meter has a sliding beta-ray shield in its probe and uses a battery which is said to have a life of 200 hours. The SM-3 is claimed to be waterproof and to have a weight of $8\frac{3}{4}$ pounds.

HAND ALPHA COUNTER

Radiation Counter Laboratories, Inc., 1844 W. 21st St., Chicago 8, Ill. This hand alpha counter for monitoring contamination of hands is a self-contained assembly which consists of two alpha-sensitive, ten-wire air proportional counters and a recording electronic circuit which is calibrated to read from 0–20,000 counts per minute. The

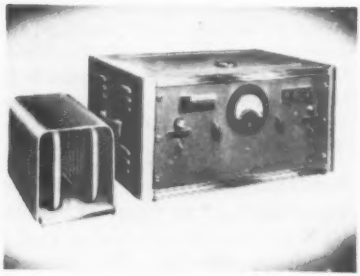

counters are arranged so that close proximity to the hand is assured. The electronic circuit consists of a linear amplifier, a multivibrator to equalize the incoming pulses, and RC tank circuit, a vacuum-tube voltmeter calibrated to read directly in cpm, and a regulated high-voltage power supply.

WIDE-BAND AMPLIFIER

Spencer-Kennedy Laboratories, Inc., 186 Massachusetts Ave., Cambridge 39, Mass. The model 200A chain amplifier is a traveling wave amplifier with a bandwidth of 200 megacycles and a gain of 10 db per stage. With a useful range from 100 kc to 220 Mc, at an impedance level of 200 ohms, the ampli-

fier has a transmission characteristic which is ± 1.5 db from 100 kc to 200 Mc, with a standing wave ratio of less than 1 db over this band.

ELECTRONIC COUNTER

Technitrol Engineering Co., Inc. 3212 Market St., Philadelphia, Pa. A basic decade electronic counter, which can be combined in multiple with electronic switching circuits to solve special counting and timing problems, has been developed. It is claimed that the instrument includes the following features: speed over 150,000 cps, elapsed time measured to less than 7 microseconds, decimal indication of counts, presetting switchable to any count, simultaneous inputs to two or more decades, positive or negative difference counts directly indicated, and automatic sequencing of two or more counters.

ABSTRACTS

CHEMICAL PUBLICATIONS

Radioactive determination of potassium in solids, A. M. Gaudin, J. H. Pannell (Massachusetts Inst. of Technology, Cambridge), *Anal. Chemi.* **20,** 1154–1156 (1948). A method is described for determining potassium in concentrations greater than 1% by measuring the beta activity of naturally occurring K^{40}. This is accomplished with a thin-walled Geiger-Müller counter mounted vertically in a lead shield and surrounded by a sample of infinite thickness (0.35 g per sq cm in potassium chloride). Good agreement was obtained between chemical and radioactive assays for potassium in sylvite ores and concentrations. Unless corrected for, large errors may occur when other naturally radioactive elements are present.

Chemistry of thorium, T. Moeller, G. K. Schweitzer (Univ. of Illinois, Urbana), *Anal. Chemi.* **20,** 1201–1204 (1948). A radiochemical method is described for estimating thorium in the presence of yttrium and the tripositive rare-earth elements. Thorium is precipitated from 0.3 *N* acid solutions with an excess of sodium pyrophosphate solution containing P^{32}, the precipitate is filtered off, and the filtrate is counted with a thin-walled Geiger-Müller counter having an annular sample holder. The difference in activity of the standard solution and the filtrate determines the quantity of unused pyrophosphate. Radiochemical studies showed that yttrium and the tripositive rare-earth elements are not precipitated as pyrophosphates from 0.3 *N* acid; however, to avoid coprecipitation of rare earths, a preliminary separation through carbonate precipitation is desirable. The method was applied successfully to synthetic mixtures of thorium, yttrium, and the rare-earth elements, as well as to monazite sand concentrates. Good agreement was obtained between results obtained with this method and with titrimetric iodate and gravimetric hexamine methods. The radiochemical method has the advantage of simpler manipulative techniques.

Radioactive electronic detector, I. Feuer (Seederer-Kohlbusch, Inc., Englewood, N. J.), *Anal. Chemi.* **20,** 1231–1237 (1948). A radioactive microbalance is described which has the advantages of high sensitivity (at least 1 microgram per mm deflection on a spotlight galvanometer), external control of sensitivity, constancy of sensitivity under increasing load, stability of sensitivity, very short weighing periods, external electrical recording device which can be read easily, large load capacity, and determination of balance errors quickly and directly. A sealed radium source, fixed on one balance arm, irradiates a three-plate ionization chamber which is mounted on a fine worm gear. The latter permits linear displacement of the chamber to better than 0.5 micron. Current in the ionization chamber is amplified and read by either a sensitive microammeter or a spotlight galvanometer. Displacements of the source relative to the chamber produce changes in the ionization current which are easily read and converted into micrograms after suitable calibration.

Some mechanism studies on the Fischer-Tropsch synthesis using C^{14}, J. T. Kummer, T. W. DeWitt, P. H. Emmett (Mellon Inst., Pittsburgh, Pa.), *J. Am. Chem. Soc.* **70,** 3632–3643 (1948). Studies made on the Fischer-Tropsch synthesis using C^{14} as a tracer show that the major fraction of the product is formed by some process other than by reduction of carbide on the catalyst. At or below 260° with iron catalysts, or at 200° for cobalt catalysts, only 10% of the hydrocarbon product is formed through the carbide. With an iron carbide surface at 250°, the exchange of the carbon in methane, butene-1, and acetylene, is very low. Carbon monoxide exchanges with the carbon in the carbide to the extent of 5% in 30 min at 250°, and 29% in 7 min at 322°. The mechanism of carbiding was investigated, but the process is complicated and no satisfactory mechanism was obtained.

The preparation of carbon-14-labeled methane and carbon tetrachloride, W. H. Beamer (Dow Chemical Co., Midland, Mich.), *J. Am. Chem. Soc.* **70,** 3900–3901 (1948). Methane-C^{14} and carbon tetrachloride-C^{14} were synthesized on a millimole scale from $BaC^{14}O_3$ in yields of 96% and 93%, respectively. The methane was prepared by reduction of carbon dioxide with hydrogen over a nickel-thorium oxide catalyst at 330°; the methane in turn was converted to carbon tetrachloride (better than 99% pure) by photochlorination. An all-glass vacuum line system was used.

Gamma-rays from proton bombardment of separated argon isotopes, K. J. Brostrøm, T. Huus, J. Koch (Inst. for Theoretical Physics, Univ. of Copenhagen, Denmark), *Nature* **162,** 695–696 (1948). Protons in the energy region from 0.5 to 1.8 Mev were used against four A^{40} targets and one A^{36} target to determine capture resonances in the two argon isotopes. The targets were prepared by bombarding silver disks with the separated beams of the argon isotopes in a mass spectrograph. Resonances for A^{40} were found at 900, 1050, 1080, 1100, and 1235 kev, and yields were calculated for each resonance; no gamma radiation was found in the case of A^{36}.

Short-range α-particles from the disintegration of sodium, aluminum, and fluorine by protons, J. M. Freeman, A. S. Baxter (Cambridge Univ., England), *Nature* **162,** 696–698 (1948). Emission of short-range α-particles was observed in the proton bombardment of sodium, fluorine, and aluminum. Disintegration particles emitted at 90° to the incident proton beam were allowed to pass through a 90°-focusing magnet. The resolved α-particles were focused onto a ZnS screen and the scintillations detected by a photomultiplier. For range measurements, an air-filled ionization chamber was used in place of the multiplier. The known excitation function for the reaction $F^{19}(p,\alpha)O^{16}\xrightarrow{\gamma}O^{16}$ was used to estimate the proton energy scale, and the ranges of α-particles from the aluminum and sodium reactions were compared with the α-particles emitted from this reaction. *Q*-values for the reactions studied were calculated from the range measurements with aid of the 1938 Cornell range-energy curve for α-particles.

Disintegration of nitrogen by fast neutrons, C. P. Sikkema (Rijks University, Groningen), *Nature* **162,** 698–699 (1948). The reactions $N^{14}(n,p)C^{14}$ and $N^{14}(n,\alpha)B^{11}$ were studied using monoenergetic $(D + D)$ neutrons. The combined cross sections so obtained were plotted as a function of the neutron energy. A resonance was observed at 2.23 Mev, corresponding to an excited state of the intermediate ${}_7N^{15}$ nucleus. The total cross section for resonance neutrons of dicyandiamide was found to be 2×10^{-24} cm² by means of absorption measurements.

A magnetic resonance accelerator for electrons, W. J. Henderson, H. Le Caine, R. Montalbetti (Natl. Research Council, Ottawa, Canada), *Nature* **162,** 699–700 (1948). A small electron accelerator, or microtron, was constructed and electrons were observed to be accelerated in the manner predicted by Veksler [*J. Phys. U.S.S.R.* **9,** 153 (1945)]. The radio-frequency voltage on the accelerating gap was between 500 and 600 kv, and the magnetic field was about 1000 oersteds. The final energy of the electrons after eight successive passages across the gap was 4.6 Mev. The orbits were found to be concentric circles, all passing through the accelerating gap.

Life-span of red and white blood corpuscles of the hen, J. Ottesen (Inst. for Theoretical Physics, Univ. of Copenhagen, Denmark), *Nature* **162,** 730–731 (1948). P^{32} was administered to a hen for one day only, and the activity of desoxyribosenucleic acid phosphorus isolated from erythrocytes was measured over a period of 40 days. It was found that the release of the labeled corpuscles into the circulation took place three days after injection of P^{32}. The mean life-span of erythrocytes was found to be 32 days. By means of similar experiments, it was found that not more than 10% of the white corpuscles have a life-span of more than eight days.

Introduction of radioactive tracers into antisera, F. D. S. Butement (Atomic Energy Research Estab., Harwell, Eng.) *Nature* **162,** 731 (1948). Radioiodine was introduced into the globulin molecule of an antiserum without seriously impairing the agglutinating power of the serum. This technique may be useful for the standardization of a variety of antisera.

Fast neutron-proton scattering and the law of interaction between nucleons, E. H. S. Burhop, H. N. Yadav (University College, London), *Nature* **162,** 738–739 (1948). Three types of *n-p* interaction were investigated using exchange properties of the symmetrical (I), charged (II), and neutral (III) meson theories, respectively, and the following interaction functions: spherical well, Yukawa potential, exponential potential, and Gaussian potential. The dependence of the total cross section and angular distribution on the range and shape of the assumed interaction were calculated using the Born approximation. The Yukawa potential of range 1.18×10^{-13} cm for type I interaction gives a value of the total cross section for 100 Mev neutrons of 9.1×10^{-26} cm²; the experimental value is $8.3 \pm 0.4 \times 10^{-26}$ cm². The experimental value of $\sigma_{180°}/\sigma_{90°}$ is approximately 3, which rules out any kind of type III

interaction. The Yukawa symmetrical case of range 1.18×10^{-13} cm gives about 6.2 for this ratio.

A high-pressure hydrogen-filled ionization chamber, G. H. Stafford (Cambridge Univ., Cambridge, Eng.) *Nature* **162,** 771–772 (1948). Electron collection was obtained with a cylindrical ionization chamber filled with pure hydrogen at various pressures up to 90 atm. The size of recoil proton pulses produced by neutron irradiation was found to decrease with increase in pressure. In spite of electron loss the pulses were still proportional to the initial ionization. With a pulse-size analyzer, the chamber may be useful for measuring neutron spectra up to approximately 13 Mev. At 90 atm the efficiency for detecting neutrons of 2.2 Mev is 17%.

Masses of meson, R. Fürth (Univ. of London, England), *Nature* **162,** 772–773 (1948). It is suggested that the decay of a π-meson into a μ-meson is the analog of the Compton effect. The collision of a π-meson with a nucleon gives rise to a μ-meson and emission of a neutral particle of small rest mass such as a neutrino. Applying the author's "hypothesis of elementary indeterminacy" to mesons, m_π/m_μ is found to be 1.32, in good agreement with recent experimental results. This analogy between mesons and photons leads one to expect a continuous spectrum of mesons over a wide range of masses above and below that of the π-meson. The hypothesis also gives the value of $293m_e$ for the π-meson mass.

Evolution of the universe, R. A. Alpher, R. Herman (Johns Hopkins Univ., Silver Spring, Maryland), *Nature* **162,** 774–775 (1948). Corrections are made to Gamow's recent article in *Nature* on the evolution of the universe. When these corrections are made it is found that the formation of condensations must have occurred when the expansion was linear with time. At the time of condensation the gas temperature was 600° K, while the present temperature in the universe is about 5° K.

Relative abundances of potassium and argon in the earth's surface materials, J. H. J. Poole (Trinity College, Dublin, Ireland), *Nature* **162,** 775–776 (1948). If one assumes that the total half-life of K^{40} is about 2.4×10^9 years, a calculation of the amount of A^{40} which should have been produced from the decay of K^{40} in the lifetime of the earth leads to a value that is about 430 times the known amount of argon in the atmosphere. The author concludes that either the assumed data for the decay of K^{40} and its abundance in the surface materials of the earth are incorrect, or that the present estimates of the age of the earth are too large by a factor of two.

Tracer phosphatase determination in tissue sections, J. B. Dalgaard (Univ. of Aarhus, Denmark), *Nature* **162,** 811 (1948). A quantitative determination of phosphatase in tissue sections was carried out using a modified Gomori technique. By means of a microscope and slide, a small region of the tissue containing radioactive calcium phosphate may be selected and exposed to a Geiger-Müller counter. Brass diaphragms of $\frac{1}{2}$–2 mm diameter limit the area of the tissue to be counted. When stained sections are used, the histological and radioactive surveys can be made on the same section.

Lead isotopes and the age of the earth, H. Jeffreys, *Nature* **162,** 822–823 (1948). The ratios of the abundances of isotopes of lead from 25 rock samples was treated statistically to derive an estimate of the age of the earth. Ahrens' value of 2,100 million years is not much less than the true age of the crust. Isotopic analyses of at least four times as many old ores as were used are necessary to improve the estimate appreciably.

. . . I. W. RUDERMAN

LIFE SCIENCE PUBLICATIONS

The permeability of the human placenta to water and the supply of water to the human fetus as determined with deuterium oxide, L. Hellman, L. Flexner, W. Wilde, G. Vosburgh, N. Proctor (Dept. of Obstetrics, Johns Hopkins Univ., Baltimore, Maryland), *Am. J. Obstet. Gynecol.* **56,** 861–868 (1948). There is about a fivefold increase in the transfer rate of water per unit weight of placenta from the fourteenth week of pregnancy until term. The placental transfer coefficient for water is five times as great as sodium at corresponding periods of gestation. At the fourteenth week of gestation, the human fetus receives 700 times as much water as is incorporated into the growing tissues. This increases to 3,800 times as much at the thirty-first week.

Calcium ion changes in some normal tissues and in epidermal carcinogenesis, A. Lansing, T. Rosenthal, M. Kamen (Mallinckrodt Inst. of Radiology and Dept. of Chemistry, Washington Univ., St. Louis, Mo.), *Arch. Biochem.* **19,** 177–183 (1948). Experiments indicate that normal epidermis actively exchanges calcium. There is a loss of storage capacity in the epidermis for calcium in early methylcholanthrene-induced hyperplasia. Transplantable squamous cell carcinoma and thirty-day hyperplastic epidermis are unable to exchange calcium ions.

16-C^{13}-Dehydroisoandrosterone acetate, E. Hershberg, E. Schwenk, E. Stahl (Chemical Research Div. of Schering Corp., Bloomfield, N. J.), *Arch. Biochem.* **19,** 300–310 (1948). 3-Hydroxyetiobilienic acid has been prepared by hypoiodite oxidation of dehydroisoandrosterone and a new intermediate iodine compound has been isolated. The preparation of diazomethane with C^{13} is described. 16-C^{13}-Dehydroisoandrosterone acetate has been synthesized.

The incorporation of carbon-labeled formic acid and carbon dioxide into hypoxanthine in pigeon liver homogenates, G. Greenberg (Department of Biochemistry, Western Reserve Univ., Cleveland, Ohio), *Arch. Biochem.* **19,** 337–339 (1948). The synthesis of a purine in essentially cell-free liver homogenates by incorporating labeled formate and bicarbonate into hypoxanthine is reported.

Thyroglobulin formation in the thyroid follicle visualized by the "coated autograph" technique, C. Leblond, J. Gross (Dept. of Anatomy, McGill Univ., Montreal, Can.), *Endocrinology* **43,** 306–324 (1948). Radioactive iodine uptake by the thyroid gland was observed using the autographic technique. Thyroids of rats on a low iodine intake, rats receiving about 22 μgrams of iodine daily, hypophysectomized rats on a low iodine intake, and guinea pigs receiving thyrotropic hormone were observed. The radioiodine was shown to be present as thyroglobulin in all cases. The thyroglobulin was deposited continuously in the colloid of the thyroid follicle.

Studies on nitrogen metabolism in tomato with use of isotopically labeled ammonium sulfate, R. MacVicar, R. Burris (Dept. of Biochemistry, Univ. of Wisconsin, Madison), *J. Biol. Chem.* **173,** 511–516 (1948). Labeled ammonium sulfate was supplied to tomato plants, and various nitrogenous fractions and amino acids were isolated and examined for isotope content. All nitrogenous fractions and amino acids isolated contained significant amounts of N^{15}. Of the amino acids isolated, glutamic had the highest concentration while histidine and lysine contained the lowest excess of isotope.

The nature of the circulating thyroid hormone, A. Taurog, I. Chaikoff (Div. of Physiology, Univ. of California Med. School, Berkeley), *J. Biol. Chem.* **176,** 639–656 (1948). Evidence is presented that the circulating hormone in the normal animal consists of thyroxine loosely attached to plasma protein.

The *in vitro* synthesis of cholesterol from acetate by surviving adrenal cortical tissue, P. Srere, I. Chaikoff, W. Dauben (Div. of Physiology, Univ. of California Med. School, Berkeley), *J. Biol. Chem.* **176,** 829–833 (1948). Doubly labeled C^{14}-acetate is converted to cholesterol by surviving slices of beef adrenal cortex.

Study of carbon dioxide fixation in the synthesis of citrulline, S. Grisolia, P. Cohen (Lab. of Physiological Chem., Univ. of Wisconsin, Madison), *J. Biol. Chem.* **176,** 929–933 (1948). A study of the synthesis of labeled citrulline from ornithine and C^{14}-labeled CO_2 has been made. Citrulline containing C^{14} in the carbonyl position is converted to urea of the same specific activity by liver homogenates. The effect of these findings on the role of citrulline in the Krebs-Henseleit cycle is discussed.

The conversion of formate and glycine to serine and glycogen in the intact rat, W. Sakami (Dept. of Biochemistry, School of Medicine, Western Reserve Univ., Cleveland, Ohio), *J. Biol. Chem.* **176,** 995–996 (1948). Using glycine labeled in the carboxyl group with C^{13} and formate labeled with C^{14}, evidence was obtained for converting glycine and formate to glycogen via serine.

Rate of flow of venous blood in the legs measured with radioactive sodium, H. Wright, S. Osborn, E. Edmonds (Univ. College Hospital and Med. School, London), *Lancet* 767–769 (Nov. 13, 1948). A method is described for measuring the rate of venous blood flow in the leg using radioactive sodium. The accuracy of the method is discussed and a comparison with other methods made.

Effect of amino acid deficiencies on incorporation of radioactive carbon-labeled

amino acids into animal tissue proteins, D. Sanadi, D. Greenberg (Div. of Biochemistry, Univ. of California Medical School, Berkeley), *Proc. Soc. Exptl. Biol. Med.* **69,** 162–163 (1948). A deficiency of either tryptophan or phenylalanine impairs the ability of animals to incorporate C^{14} from labeled amino acids into protein.

. . . BERNARD KANNER

PHYSICAL PUBLICATIONS

Energy diagrams for beta-disintegration, A. L. Hughes (Washington Univ., St. Louis, Mo.), *Am. J. Phys.* **16,** 415–420 (1948). The methods of presenting data on beta-disintegration in the form of energy level diagrams are discussed. The effect of using atomic masses in the cases of positron emission and *K*-capture is explained, where the binding energy is either omitted or included. Atomic binding energies may forbid *K*-capture while allowing *L*-capture.

The search for the neutrino through nuclear recoil experiments, J. S. Allen (Univ. of Illinois, Urbana), *Am. J. Phys.* **16,** 451–461 (1948). Summarized is experimental work with cloud chambers and particle detectors to find the recoils from beta disintegration of solid and gaseous sources in order to obtain the angular correlation between the recoil and electron. In particular the work of Jacobsen and Kofoed-Hansen (on Kr^{85}), Allen (on He^6), Sherwin (using thin sources of P^{32} and Y^{90}), and Lauritsen (Li^8 decay) is discussed.

Anomalous absorption of RaC gamma-rays, P. K. Sen Chaudhary (Tata Memorial Hospital, Bombay, India), *Indian J. Phys.* **22,** 341–346 (1948). The absorption coefficient of RaC gamma rays in lead as a function of lead thickness agrees with the accepted value for that between 19–20 cm (as measured with a Geiger counter). It falls far below the theoretical minimum as the thickness increases to 24.2 cm, but then rises again to 27 cm. The possible causes for the anomaly are discussed; they include multiple scattering in the forward direction and some meson type of radiation.

The interaction of high energy neutrons and heavy nuclei, M. L. Goldberger (Univ. of Chicago, Ill.), *Phys. Rev.* **74,** 1269–1277 (1948). The interaction is theoretically studied by considering individual collisions, between the incident nucleon and one in the target nucleus, in which small amounts of energy are transferred. The effects due to the presence of other nucleons are accounted for by use of the statistical model of the nucleus. The angular distribution of the scattered neutrons, the mean free path of scattered neutrons within the nucleus, the effective cross section for neutrons traversing matter, and the distribution of excitation energies in the bombarded nuclei (from which their subsequent behavior can be predicted by the evaporation model), are calculated and experimental results predicted for neutrons in the region of 100 Mev.

Depolarization of neutrons during diffusion, S. Borowitz, M. Hamermesh (New York University, New York), *Phys. Rev.* **74,** 1285–1293 (1948). A possibility for experimental determination of the spin dependence of the interaction between a neutron and a nucleus is the study of the depolarizing effect of a scattering process on a beam of polarized neutrons. The depolarizing factor for a single collision depends on the scattering amplitudes for both spin-orientations, and the depolarization is calculated for the normal incidence of a plane monochromatic polarized beam of thermal neutrons on a slab of finite thickness in which the neutrons are isotropically scattered with or without capture.

A direct determination of the energy of the He^3 nucleus from the D-D reaction, H. V. Argo (Univ. of Chicago, Ill.), *Phys. Rev.* **74,** 1293–1299 (1948). An electrostatic analyzer with an electron multiplier detector was used to determine the energy of He^3 ions coming off at 90° in the lab system from the reaction $D + D \rightarrow n + He^3 + Q$. The bombarding particles were deuterons of known energy from a voltage multiplier; the target was of D_2O ice laid down by a constant flow method so as to have a fresh surface at all times. Using corrections for energy losses by the deuterons and He^3 particles, the value of Q was calculated as 3.30 ± 0.01 Mev.

Neutral decay products of cosmic radiation at great depths, J. Barnothy, M. Forro (Inst. for Experimental Physics, Univ. of Budapest, Hungary), *Phys. Rev.* **74,** 1300–1310 (1948). Measurements of double and triple coincidences as a function of thickness of lead between Geiger-Müller counters at 700–1000 meters water equivalent below sea level were made over a period of seven years. The curves

indicate that the cosmic radiation at these depths consists largely of nonionizing or scarcely ionizing radiation. Various evidences (such as the temperature effect) indicate that this radiation (which was found to be isotropic over the hemisphere) is probably a neutral decay product of cosmic-ray mesons (possibly a neutral meson).

Radioactive isotopes of Ga and Ge, D. A. McCown, L. L. Woodward, M. L. Pool (Ohio State Univ., Columbus), *Phys. Rev.* **74,** 1311–1314 (1948). Alpha, deuteron, and neutron bombardments of ordinary and enriched isotopic mixtures of various targets produced activities of various lifetimes, which were assigned to germanium and gallium. Ge^{69}, decaying with a 1.65-day half-life through emission of positrons, X-rays, and gamma-rays, was produced by $Zn(\alpha,n)$, $Ga(d,2n)$, and $Ge(n,2n)$ reactions. Fast neutron bombardment of arsenic gave the 1.37 ± 0.02-hour Ge^{75}. Alpha-particle bombardment of zinc gave 3.26 ± 0.02-day Ga^{67}.

Radioactive arsenic isotopes, D. A. McCown, L. L. Woodward, M. L. Pool (Ohio State Univ., Columbus), *Phys. Rev.* **74,** 1315–1319 (1948). The arsenic activity of 76 ± 3-day half-life is established at mass number 73 by alpha-particle bombardment of ordinary germanium and enriched Ge^{70}. As^{74} has a 17.5 ± 0.1-day half-life. Deuteron bombardment of germanium produces 2.08-day As^{71}. Selenium enriched in mass numbers 74 and 76, respectively, was bombarded with deuterons, the results placing the 1.08-day activity at As^{72}. The methods of decay of these isotopes are described.

Further remarks on the magnetic moments of H^3 and He^3, R. Avery, R. G. Sachs (Univ. of Wisconsin, Madison), *Phys. Rev.* **74,** 1320–1322 (1948). Magnetic moments of H^3 and He^3 have been interpreted as indicating the presence of an "exchange moment" not due to either the spin or orbital moments. An alternative description without exchange moments is possible if the ground state of He^3 has ^2P and ^4P wave functions much larger than that of ^4D. Rough binding energy calculations indicate the best choice of wave functions is 96% ^2S and 4% ^4D; using this and the experimental H^3 magnetic moment, the calculated moment of He^3 agrees with the experimental value. This calculation indicates that the exchange moment hypothesis is to be preferred to the large admixture of the P state.

Inelastic scattering of protons from light nuclei, H. W. Fulbright, R. R. Bush (Princeton Univ., Princeton, N. J.), *Phys. Rev.* **74,** 1323–1329 (1948). The proton beam within a 35-in f-m cyclotron is incident on a scattering foil. Protons scattered downward describe helical paths of radius dependent on their energy, pass through a defining slit, and fall on a horizontal photographic plate at an angle of about 15°, so that their path lies entirely within the emulsion. An X-ray line due to the passage of the protons through the foil marks the direct line through the slit; proton groups of different energy appear on the plate in different positions. The highest energy group corresponds to inelastic scattering; the energies of the other groups can be calculated from their positions on the plate and the magnetic field of the cyclotron. The energy levels of the nuclei are calculated from the proton energies and energy-momentum relations. This was done for B, C^{12}, N^{14}, O^{16}, Al^{27}, Si^{28}, and Ni.

Delayed neutrons from U^{235} after short irradiation, F. de Hoffmann, B. T. Feld, P. R. Stein (Los Alamos Scientific Lab., N. Mex.), *Phys. Rev.* **74,** 1330–1337 (1948). A slug of active material falling through a core of active material produced a momentary chain reaction, giving a neutron burst of 10^{14} neutrons in 10 milliseconds. Two U^{235} fission chambers, filled with an argon and CO_2 mixture and using electron collection for rapid response, were used to detect the delayed neutrons from the slug after it had fallen into a catcher box. The decay curve was measured from 0.2 sec to 10 min. Five periods, ranging from 80 to 0.52 sec, were found; indications of a 6-millisecond delayed neutron period were also found.

The capture probability of negative mesons, H. K. Ticho (Univ. of Chicago, Ill.), *Phys. Rev.* **74,** 1337–1347 (1948). Disintegration curves of positive and negative mesons (separated by a magnetic field), giving relative numbers for which various times elapse between entrance of the meson into the absorber and detection of the decay electron, were taken for H_2O, NaF, Mg, Al, and S absorbers. Relative counting rates of positive and negative disintegration electrons support the idea that the change in the mean life of negative mesons is due to competition between processes of spontaneous decay and nuclear capture, which are of comparable probability. The positive mesons show the same mean

life (2.11 ± 0.10 μsec) in all absorbers. The capture probability for negative mesons near absorber nuclei is calculated from the mean life of the mesons in the various absorbers and the mean life of free mesons; the probability is proportional to Z^a where Z is the charge on the absorber nucleus and a is 3.7 ± 0.85.

Thick-target X-ray production in the range from 1250 to 2350 kilovolts, W. W. Buechner, R. J. Van de Graaff, E. A. Burrill, A. Sperduto (Massachusetts Inst. of Technology, Cambridge), *Phys. Rev.* **74,** 1348–1352 (1948). Thick-target production of X-rays by electrons from an electrostatic accelerator was investigated by using an ionization chamber at various angles to targets of Be, Al, Cu, Ag, W, and Au. The total radiation intensity integrated over all angles was found to be linear in nuclear charge in this energy range. The efficiency of X-ray production was also calculated and found to be in adequate agreement with theory.

Further calculations on the cascade theory, H. J. Bhabha (Tata Inst. of Fundamental Research, Bombay, India), S. K. Chakrabarty (Colaba Observatory, Bombay, India), *Phys. Rev.* **74,** 1352–1363 (1948). A summary is given of previous calculations on cascade theory. The solution is used to calculate the number of shower particles at various thicknesses (in characteristic units) for primary particles of various energies. The relative importance of the second term of the series solution is evaluated.

A search for delayed photons from stopped sea level cosmic-ray mesons, R. D. Sard, E. J. Althaus (Washington Univ., St. Louis, Mo.), *Phys. Rev.* **74,** 1364–1371 (1948). If a meson decays into an electron and photon, the photon should have an energy of 50 Mev. A circuit was set up to find delayed coincidences between the mesons (stopped in a brass absorber) and the photon. The latter is detected by being converted in a lead absorber into a positron-electron pair, from which at least one emerges to be detected. The coincidences were measured in adjacent time intervals covering the range 1.2 to 8.0 microseconds. The expected number of true delayed photon coincidences under this hypothesis (as computed on the basis of electron coincidences measured with the same geometry) was of the order of 100. Nine apparent coincidences were found, with five spurious ones expected from the inefficiency of the anticoincidence circuit. This presents an argument against decay into photon and electron, or decay into a neutral meson with subsequent decay into two photons with lifetime less than 10^{-10} sec.

Relation between apparent shapes of monoenergetic conversion lines and of continuous β-spectra in a magnetic spectrometer, G. E. Owen, H. Primakoff (Washington Univ., St. Louis, Mo.), *Phys. Rev.* **74,** 1406–1412 (1948). Internal conversion lines of Cs^{137} and Th(B + C), theoretically monoenergetic, are found to have finite width and, with 180° spectrometers, asymmetrical shape. Assuming that the distortion is due to the spectrometer and source, the approximate true shape of a continuous beta spectrum may be obtained from experimental data by application of a correction derived from the form of the conversion line. The Kurie plots for corrected continuous beta-ray spectra are more linear than the uncorrected ones, and the positron-electron ratio for Cu^{64} is found to agree better with Fermi theory after application of the correction.

The Geiger discharge, D. H. Wilkinson (Cavendish Lab., Cambridge, England), *Phys. Rev.* **74,** 1417–1429 (1948). A theory of the development of the positive ion sheath in Geiger counter operation is given and used to calculate the relation between starting potential and counter variables, the amount of charge generated in the discharge, the shape of the plateau curve, and the velocity of propagation of the discharge down the wire. The resulting conclusions are confirmed by experiment.

Excited level in Li^7 from the $Li^6(d,p)Li^7$ and $Be^9(d,\alpha)Li^7$ reactions, W. W. Buechner, E. N. Strait, C. G. Stergiopoulos, A. Sperduto (Massachusetts Inst. of Technology, Cambridge), *Phys. Rev.* **74,** 1569–1574 (1948). The reactions were studied by directing deuterons from an electrostatic accelerator onto the respective targets and analyzing the resulting charged particles in an annular magnet. In each case two groups were found to emerge and, from the difference in their energy, the energy of the excited state in Li^7 was calculated. Using the alpha particles from polonium to calibrate the magnet, the detector being a photographic plate in which the particle tracks could be counted, the level was found at 482 ± 3 and 483 ± 6 kev in the two experiments.

Use of enriched molybdenum in cross-section measurements of the $(p,n):(p,\gamma)$ and $(d,n):(d,2n)$ reactions, D. N. Kundu, M. L. Pool (Ohio State Univ., Columbus), *Phys. Rev.* **74,** 1574–1576 (1948). By bombarding ordinary and enriched isotopic mixtures with a monitored proton or deuteron beam and measuring the various radioactivities produced by means of a ionization chamber and electrometer, simultaneous equations were set up which allowed a measurement of the relative cross sections of various reactions in different isotopes. The cross section ratios found were for Mo^{95} $(p,\gamma):Mo^{95}$ $(p,\gamma):Mo^{95}(p,n):Mo^{96}(p,n)$, and for (d,n) and $(d\ 2n)$ reactions on the same isotopes.

A neutron-capture theory of the formation and relative abundance of the elements, R. A. Alpher (Johns Hopkins Univ., Silver Spring, Md.), *Phys. Rev.* **74,** 1577–1589 (1948). A theory is developed for the formation of the elements by neutron capture and beta decay from a primordial neutron gas. It is reasoned: (1) that the relative abundance of elements depends largely on the capture cross sections for various nuclides; (2) that large amounts of radiation must originally have been present, and (3) that the element-building process began several hundred seconds after the beginning of expansion of the gas, when the temperature was about 10^9 K and the density about 10^{-2} g/cm³. The observed relative abundances are successfully predicted by calculations on this basis.

The occurrence of He^3 in natural sources of helium, L. T. Aldrich, A. O. C. Nier (Univ. of Minnesota, Minneapolis), *Phys. Rev.* **74,** 1590–1594 (1948). The abundance ratio of He^3 to He^4 was investigated in a mass spectrometer for helium from the atmosphere, gas wells, and minerals. Explanations for the wide variations which are found are based on possible nuclear reactions in which He^3 may have been formed. There may have been several sources for He^3 production.

The angular distribution of 1 to 3.5 Mev deuterons scattered by deuterons, J. M. Blair, G. Freier, E. Lampi, W. Sleator, Jr., J. H. Williams (Univ. of Minnesota, Minneapolis), *Phys. Rev.* **74,** 1594–1598 (1948). A collimated deuteron beam from an electrostatic accelerator was passed through a chamber containing deuterium gas at 1 cm Hg, a monitor being placed at the other side. A fraction of the scattered deuterons from a well-defined volume of the chamber passed through a slit system and were counted by a proportional counter. Observed yields were corrected for particles produced in nuclear reactions and deuterons scattered by contaminants. The elastic scattering cross sections are given for 1 to 3.5 Mev, at angles from 10° to 45° (laboratory system), to an accuracy of 2.5%.

The angular distribution of the products of the D-D reaction: 1 to 3.5 Mev, J. M. Blair, G. Freier, E. Lampi, W. Sleator, Jr., J. H. Williams (Univ. of Minnesota, Minneapolis), *Phys. Rev.* **74,** 1599–1603 (1948). By the same process as that used in the determination of the elastic D-D cross section, with proper biasing and discrimination, the cross sections per unit solid angle for the $D(d,n)$ and $D(d,p)$ reaction were measured. The angular dependence of the cross section for both reactions is nearly the same, having a constant term plus terms in the square and fourth power of the angle of observation in the mass coordinate system. The coefficients of these terms are given. Total cross sections for both reactions in this energy region are approximately constant at 10^{-25} cm².

On the proposal for determining the thickness of a transition layer between ferromagnetic domains by a neutron polarization experiment, R. R. Newton, C. Kittel (Bell Telephone Lab., Murray Hill, N. J.), *Phys. Rev.* **74,** 1604–1605 (1948). A measurement, as a function of neutron velocity, of the polarization changes in a neutron beam in passing through the Bloch wall between ferromagnetic domains suffices to determine wall thickness. From this, wall energy can be computed. A calculation shows that the experiment can probably be done if grazing angles of incidence are used.

The disintegration scheme of I^{131}, F. Metzger, M. Deutsch (Massachusetts Inst. of Technology, Cambridge), *Phys. Rev.* **74,** 1640–1644 (1948). The beta spectrum of this isotope, as measured with a lens spectrometer, shows a number of conversion lines indicating four gamma rays and a beta spectrum of two groups. Experiments with various radiators to produce photoelectrons were performed, and beta-gamma and beta-conversion electron coincidences were measured (using a naphthalene counter for gammas). The results show gamma rays at 80, 283,

363, and 638 kev; their intensities and conversion coefficients are given. A disintegration scheme is proposed.

Angular dependence of coincidences between fission neutrons, S. DeBenedetti, J. E. Francis, W. M. Preston, T. W. Bonner (Oak Ridge Natl. Lab., Oak Ridge, Tenn.), *Phys. Rev.* **74,** 1645–1650 (1948). Fast neutron counters working on the principle of proton recoil were used to measure coincidences at angles from 30° to 180° among neutrons produced by neutron-induced fission of U^{235}. Corrections were made for a single neutron's registering as a coincidence by being scattered from one counter into another. The number of coincidences was about constant from 30° to 90°, then increased by a factor 2 from 90° to 180°. The results may be explained by assuming that the fission neutrons most probably come from opposite fragments, since they are most likely to go in the direction of the fragments from which they are emitted.

Converted gamma-radiation from silver, cadmium, indium, praseodymium, and rhenium, J. M. Cork, R. G. Shreffler, C. M. Fowler (Univ. of Michigan, Ann Arbor), *Phys. Rev.* **74,** 1657–1659 (1948). Using beta spectrometers and absorption methods, studies were made of the half-lives and energies of beta and gamma rays emitted by radioisotopes produced by neutron capture (using pile bombardment) in these elements.

The "thick-film chamber" method for the measurement of fast neutron flux, K. W. Allen, D. H. Wilkinson (Cavendish Laboratory, Cambridge, Eng.), *Proc. Cambridge Phil. Soc.* **44,** 581–587 (1948). The absolute value of a fast neutron flux is measured using proton recoils from a polythene layer whose thickness exceeds the range of the most energetic recoils. The protons are detected in an ionization chamber, the neutron flux being derived from their number and energy distribution. The method has a relatively high sensitivity, which is almost linear with neutron energy because of the increasing range of proton recoils. Only the area, stopping power, and hydrogen content of the layer material need be known. The angular distribution of the neutron flux from the D-D reaction was measured for a deuteron bombarding energy of 930 kev.

On Schwinger's theory of nuclear forces, W. H. Ramsey (Univ. of Manchester, Eng.), *Proc. Phys. Soc.* **346,** 297–299 (1948). The possibility of putting to use Schwinger's generalization of the Moller-Rosenfeld theory to give a consistent description of nuclear forces is examined. Results on proton-proton scattering below and above 2 Mev apparently demand meson masses of 325 and 270 electron masses, respectively. Furthermore, only about one third of the quadrupole moment of the deuteron is accounted for.

The delayed coincidence method in the study of radioactivity, with application to isomerism in Ta^{181}, D. E. Bunyan, A. Lundby, A. H. Ward, D. Walker (Univ. of Birmingham, Eng.) *Proc. Phys. Soc.* **346,** 300–306 (1948). If the random coincidence rate is not too large, delayed coincidence techniques may be used to measure the mean time interval between two events which are 10^{-2} to 10^{-7} sec apart. As an example, the metastable state in Ta^{181} resulting from beta decay of Hf^{181}, was examined and found to decay in two gammas of 0.2 and 0.5 Mev, with half-life of $(20.1 \pm 0.7) \times 10^{-6}$ sec. Probable relative parity and spin values for the ground and excited states are discussed.

The penetrating particles in cosmic-ray showers: I. Heavily ionizing particles, G. D. Rochester, C. C. Butler (Univ. of Manchester, Eng.), *Proc. Phys. Soc.* **346,** 307–312 (1948). Analysis of cloud chamber photographs of showers of various types indicates that while most of the heavily ionizing particles are protons, some are slow mesons (momentum 10^7–10^8 ev/c). The apparent mass of these mesons (about 200 electron masses) created in showers shows that μ-mesons may be directly created.

Analysis of spurious counts in Geiger counters, J. L. Putman (Atomic Energy Research Estab., Harwell, Eng.), *Proc. Phys. Soc.* **346,** 312–319 (1948). An apparatus is described which measures the rate of arrival of pulse intervals between t and $(t + dt)$, where t is a variable time and dt is a constant time that is small compared with t. Using a long-lived emitter, the distribution of pulse intervals for an argon-alcohol counter was compared with that expected from random laws, and the number and time distribution of spurious pulses were found as a function of voltage. The spurious counts all occurred within the recovery time, and were eliminated by a quenching circuit which lowered the counter voltage by about 300 volts for 400 microseconds.

ALFAX ELECTROSENSITIVE PAPER

Now available to laboratories, instrument manufacturers, and experimenters.

ALFAX ELECTROSENSITIVE PAPER—marks directly by electric impulse. Density varies directly with intensity of signal so recordings can be made self-calibrating by introducing standard signals of different intensities.

ALFAX ELECTROSENSITIVE PAPER—in helix type recorder will record signal the instant it occurs—without overshooting,—no need for compensation or damping. **IT IS INERTIA FREE.**

ALFAX ELECTROSENSITIVE PAPER is extremely sensitive, so that the paper can be fed slowly, yet extremely rapid variations will be recorded in the helix stroke at writing speeds 300″ or more per second.

ALFAX ELECTROSENSITIVE PAPER is ideal for recording a group of related signals without the problems of multiple pens and their maintenance. Recordings differentiate the transient or stray signals from the true signals. Sudden signals of unusual amplitude cannot damage the recorder nor result in false readings as in D'Arsonval movements and pen type movements.

ALFAX ENGINEERING includes making special papers or developing electronic circuits and electrode materials to emphasize any portion of wave form or signal. Recordings are easily interpreted even where noise to signal ratio is greater than one.

Recording Four Simultaneous Signals

Signals Can Overlap with No Difficulty

ALFAX PAPER & ENGINEERING CO.
41 Riverside Ave.
Brockton, Mass.

Alfax Paper & Engineering Co.
41 Riverside Avenue
Brockton, Mass.

Enclosed is one dollar for a roll of Alfax Electrosensitive paper for experimental purposes to be mailed postpaid with booklet, "Questions and Answers on Electro Sensitive Paper."

Name_____ Position_____

Address_____

Air proportional counters, J. A. Simpson (Argonne Natl. Lab., Chicago, Ill.), *Rev. Sci. Instr.* **19,** 733–743 (1948). Designs for proportional counters using air (with normal variations in pressure, temperature, and humidity) are given for use in such connections as detection of alpha-radioactive contamination. Under these conditions no windows or very thin ones may be used. The difficulties of very high operating potentials, low counting geometry, and erratic behavior have to some extent been overcome. Dependence of threshold potential on pressure and of counting rate on temperature is given.

The photo-multiplier radiation detector, F.-H. Marshall, J. W. Coltman, A. I. Bennett (Westinghouse Research Lab., East Pittsburgh, Pa.), *Rev. Sci. Instr.* **19,** 744–770 (1948). A detector has been designed consisting of a fluorescent screen that gives off scintillations produced by radiation; these are reflected in a mirror and enter a photo-multiplier. Alpha particles and other heavy ions give very large signal pulses; beta particles of high velocity, gamma, and X-rays give a much lower signal-to-noise ratio (the noise pulses being produced by thermal electron emission at the photo-cathode).

The design and construction of a double-focusing beta-ray spectrometer, F. N. D. Kurie, J. S. Osoba, L. Slack (Washington Univ., St. Louis, Mo.), *Rev. Sci. Instr.* **19,** 771–776 (1948). A double-focusing beta spectrometer giving high resolution and large solid angle is described. Its radius of curvature is 24.33 cm, the resolution ⅓ %, and transmission 0.2 %. Conversion lines of Cs^{137} and ThB were used to investigate the spectrometer, which was of simple construction. The magnet used allows the measurement of energies up to 5 Mev.

High energy neutron detector, C. Wiegand (Univ. of California, Berkeley), *Rev. Sci. Instr.* **19,** 790–792 (1948). The detector utilizes the collection of the ionization produced by the fission fragments of bismuth (the fission threshold of which is about 50 Mev). Plates coated with bismuth are connected to a collecting voltage and the neutron beam impinges on them. The efficiency is about 10^{-9}; this is suitable for monitoring a high-energy neutron beam and for beam attenuation measurements.

. . . HAROLD BROWN

UNIVERSITY OF MICHIGAN LIBRARIES